SYNTHESIS OF LEVAMISOLE DERIVATIVES FOR ANTI-CANCER ACTIVITY

Thesis submitted to

THE KLE ACADEMY OF HIGHER EDUCATION AND RESEARCH,

BELAGAVI

(KLE DEEMED UNIVERSITY)

[Declared as Deemed-to-be-University u/s 3 of the UGC Act, 1956 vide

Govt. of India Notification No.F.9-19/2000-U.3 (A)]

(Accredited 'A' Grade by NAAC) (2nd Cycle)

[Placed in Category 'A' by MHRD (GoI)]

For the award of the degree of

Doctor of Philosophy In the Faculty of

Pharmacy

by

CHUDAMANI B

(Registration No: KLEU/Ph.D./14-15/DO1214009)

Under the Guidance of

Dr. SUBHAS S KARKI, M. Pharm, Ph. D

Professor

JANUARY - 2022

UNDERTAKING

I, **CHUDAMANI.B** hereby declare that the information and the data mentioned in my thesis entitled **"Synthesis of Levamisole Derivatives for Anti-cancer activity"** belongs to me and is original.

I am aware of definition of plagiarism as detailed below:

- An act or instance of using or closely imitating the language and thoughts of another author without authorization and the representation of that author's work as one's own, as by not crediting the original author.
- A piece of writing or other work reflecting such unauthorized use or imitation.
- The deliberate or reckless representation of another's words, thoughts or ideas as one's own without attribution in connection with submission of academic work, whether graded or otherwise.

I hereby declare that the thesis prepared by me isoriginal-one and does not involve plagiarism anywhere. In case at a later stage it is found that I have indulged in plagiarism, then I am solely responsible for the same and the Institution is at liberty to take any disciplinary action against me including cancellation of dissertation or any other penalties imposed by the University.

Date:

Place: Bengaluru

Signature of the Research Scholar

Chudamani B, **M. Pharm**

KLE College of Pharmacy,

Bengaluru

KLE ACADEMY OF HIGHER EDUCATION AND RESEARCH
(Formerly known as KLE University)
(Deemed-to-be-University established u/s 3 of the UGC Act, 1956)
ಕೆ.ಎಲ್.ಇ. ಎಕ್ಯಾಡಮಿ ಆಫ್ ಹಾಯರ್ ಎಜ್ಯುಕೇಶನ ಆ್ಯಂಡ್ ರಿಸರ್ಚ್
(ಕೆ.ಎಲ್.ಇ. ವಿಶ್ವವಿದ್ಯಾಲಯವೆಂದು ಮುಂಚೆ ಗುರುತಿಸಿದ)
(ವಿ.ಧ.ಆ.ಕಲಂ 3ರಡಿ ಸ್ವಾಯತ್ತ ವಿಶ್ವವಿದ್ಯಾಲಯವೆಂದು ಸ್ಥಾಪಿಸಲ್ಪಟ್ಟಿದೆ)
KLE EMPOWERING PROFESSIONALS
Accredited 'A' Grade by NAAC (2nd Cycle) Placed in Category 'A' by MHRD (GoI)

Ref. No. KAHER/AA/21-22/D- 02122100I 2nd December 2021

Madam,

The soft copy of Ph.D. research thesis of **Ms. Chudamani, Faculty of Pharmacy** of KAHER, has been submitted for anti-plagiarism check at the office of the undersigned through "Turn-it-in" package. The scan has been carried out and the scanned output reveals a match percentage of **7%** which is within the acceptable limit of 10%.

To obtain the comprehensive report of the plagiarism test, research scholar can send a mail to **diracademic@kledeemeduniversity.edu.in** along with the Registration Number, Name of the Scholar, Name of Guide/Co-guide and title of the thesis.

DIRECTOR Deemed-to-be University ACADEMIC AFFAIRS

Dr.(Mrs.) Roopa M. Bellad
Director, Academic Affairs

To,

Ms. Choodamani B
Full-Time Ph.D. Scholar, 2014-15 Batch
Faculty of Pharmacy,
College of Pharmacy,
Bengaluru.

Cc to :
1. The Principal, College of Pharmacy, KAHER, Bengaluru
2. Dr. Subhas S. Karki, Professor of Pharmaceutical Chemistry, College of Pharmacy, Bengaluru– **Guide**

KLE ACADEMY OF HIGHER EDUCATION AND RESEARCH,

(KLE DEEMED UNIVERSITY)

[Declared as Deemed-to-be-University u/s 3 of the UGC Act, 1956 vide Govt. of India Notification No.F.9-19/2000-U.3 (A)]

(Accredited 'A' Grade by NAAC) (2nd Cycle)

[Placed in Category 'A' by MHRD (GoI)]

BELAGAVI

COPYRIGHT DECLARATION

We hereby declare that KLE **ACADEMY OF HIGHER EDUCATION AND RESEARCH, BELAGAVI, KARNATAKA,** *shall have the rights to preserve, use and disseminate this thesis in print or electronic format for academic/research purpose.*

Signature of Research Scholar
Chudamani B, **M. Pharm Pharm. Ph. D**
Date :

Signature of
Research Guide
Dr. Subhas S. Karki, **M.**

Place : Bengaluru

KLE ACADEMY OF HIGHER EDUCATION AND RESEARCH,

BELAGAVI

KLE ACADEMY OF HIGHER EDUCATION AND RESEARCH,

(KLE DEEMED UNIVERSITY)

[Declared as Deemed-to-be-University u/s 3 of the UGC Act, 1956 vide Govt. of India Notification No.F.9-19/2000-U.3 (A)]

(Accredited 'A' Grade by NAAC)

[Placed in Category 'A' by MHRD (GoI)]

BELAGAVI

DECLARATION

*I hereby declare that the thesis entitled "***Synthesis of Levamisole Derivatives for Anti-cancer activity***"* is a bonafide and original research carried out by me under the guidance of Dr.SUBHAS S KARKI Ph.D, Professor & Head Dept. of Pharmaceutical Chemistry KLE College of Pharmacy, Bengaluru. *The thesis or any part thereof has not formed the basis for the award of any degree/fellowship or similar title to any candidate of any University.*

Date :
Place : Bengaluru

Signature of the Research Scholar
Chudamani B, **M. Pharm**
KLE College of Pharmacy, Bengaluru

KLE ACADEMY OF HIGHER EDUCATION AND RESEARCH,

(KLE DEEMED UNIVERSITY)

[Declared as Deemed-to-be-University u/s 3 of the UGC Act, 1956 vide Govt. of India Notification No.F.9-19/2000-U.3 (A)]

(Accredited 'A' Grade by NAAC)

[Placed in Category 'A' by MHRD (GoI)]

BELAGAVI

CERTIFICATE

This is to certify that the thesis entitled **"Synthesis of Levamisole Derivatives for Anti-cancer activity"** is a bonafide and genuine research carried out by Chudamani B under the guidance of **Dr. Subhas S Karki,** PhD, Professor & Head Dept. of Pharmaceutical Chemistry KLE College of Pharmacy, Bengaluru.

Date :
Place : Belagavi

Signature
Dr. M.S Ganachari, Dean
Faculty of Pharmacy
KLE Academy Of Higher
Education & Research
Belagavi, Karnataka

KLE ACADEMY OF HIGHER EDUCATION AND RESEARCH,
(KLE DEEMED UNIVERSITY)

[Declared as Deemed-to-be-University u/s 3 of the UGC Act, 1956 vide Govt. of India Notification No.F.9-19/2000-U.3 (A)]

(Accredited 'A' Grade by NAAC)

[Placed in Category 'A' by MHRD (GoI)]

BELAGAVI

CERTIFICATE

This is to certify that the thesis entitled **"Synthesis of Levamisole Derivatives for Anticancer activity"** is a bonafide record of original research carried out by CHUDAMANI B for the award of degree of DOCTOR OF PHILOSOPHY IN FACULTY OF PHARMACY under my supervision and guidance.

Signature

Date :

Dr. Subhas S Karki, M.Pharm. Ph.D

Place : Bengaluru

Professor & Head

Department of Pharmaceutical Chemistry

KLE College of Pharmacy, Bengaluru

KLE ACADEMY OF HIGHER EDUCATION AND RESEARCH,

(KLE DEEMED UNIVERSITY)

[Declared as Deemed-to-be-University u/s 3 of the UGC Act, 1956 vide Govt. of India Notification No.F.9-19/2000-U.3 (A)]

(Accredited 'A' Grade by NAAC)

[Placed in Category 'A' by MHRD (GoI)]

BELAGAVI

KLE
EMPOWERING PROFESSIONALS

CERTIFICATE

This is to certify that the thesis entitled **"Synthesis of Levamisole Derivatives for Anticancer activity"'** is a bonafide record of original research carried out by CHUDAMANI B under the guidance of **Dr. SUBHAS S KARKI, Professor & Head Dept. of Pharmaceutical Chemistry, KLE College of Pharmacy, Bengaluru**.

Date :
Place : Bengaluru

Signature
Dr. Raman Dang, **M. Pharm. Ph. D**
Principal KLE College of Pharmacy
Bengaluru

ACKNOWLEDGMENT

This dissertation would not have been possible without the guidance and the help of several individuals in one way or another who contributed and extended their valuable assistance in the preparation and completion of this study. I would like to thank ***'Almighty God' for giving me strength throughout my entire study****.*

I would like to express my sincere gratitude to My parents ***Mr. Byrappa & Smt.Rathnamma****, my husband* ***Mr. Shashi Kumar S V & daughters Harshitha, Haasini, Nithya*** *whose whole hearted cooperation, love and moral support made this day possible in my life.*

Firstly, it is a genuine pleasure to express my deep sense of thanks and sincere gratitude to my advisor ***Prof. Dr. Subhas S Karki*** *Ph. D Professor and Head KLE College of Pharmacy Bengaluru for the continuous support of my Ph.D study and related research, for his patience, motivation, and immense knowledge. His guidance helped me in all the time of research and writing of this thesis. I could not have imagined having a better advisor and mentor for my Ph.D study.*

Besides my advisor, I would like to thank ***Dr. Sujit Kumar*** *for his insightful comments and encouragement, but also for the hard question which incented me to widen my research from various perspectives.*

My sincere thanks also goes to ***Dr. Raman Dang,*** *Principal,* ***Dr. H N Shivakumar,*** *Vice-Principal,* ***Dr. Hipparagi S.M*** *former Principal for their encouragement & throughout the research work.*

Without their precious support it would not be possible to conduct this research.

I would like to express my genuine gratitude to the Office ***of Director Academic Affair, KAHER, Belagavi.***

To the non-teaching staff: ***Mr.Biradar, Mr. Parusuram, Mr. Malgowda Patil*** *for their help and support.*

Last but not the least, I would like to thank ***my friends Poornima V, Radhika Kandoori & Munishama Gowda*** *for supporting me throughout my Ph.D program with their moral support and help throughout my research and my life in general.*

Date : **Signature of the Research Scholar**
Place: **Chudamani B**

TABLE OF CONTENTS

Sl. No.	Particulars	Page No.
1	**Introduction**	**1-8**
1.1	Background	**4, 5**
1.2	Justification	**6-8**
2	**Review of Literature**	**9-15**
3	**Materials and Methods**	**16-32**
3.1	Materials	**17**
3.2	Methodology	**18-32**
4	**Results**	**33-84**
5	**Discussion**	**85-92**
6	**Summary**	**93**
7	**Conclusion**	**94**
8	**Bibliography**	**95-103**
9	**Annexure** • List of Publications	**104**

ABBREVIATIONS

α:	Alpha
°C:	Degree Celsius
µ:	Micro
3D:	Three-dimensional
A°:	Angstrom
AChE:	Acetylcholine esterase
ADME:	Absorption, distribution, metabolism, excretion
ANOVA:	Analysis of variance
Asn:	Aspargine
CADD:	Computer aided drug discovery
CC:	Cytotoxic concentration
Cys:	Cysteine
DFT:	d.-functional theory
DMEM:	Dulbecco's modified eagle
DMF:	Dimethyl formamide
DNA:	Deoxyribose nucleic acid
DNS:	Differential nuclear staining
E.coli:	*Escherichia coli*
EGFR:	Epidermal growth factor
EtOH:	Ethanol
FAF:	Free ADME-Tox filtering tools
FBS:	Fetal bovine serum
FITC:	Fluorescein isothiocyanate
FTIR:	Fourier transform infrared
FU:	Fluorouracil

g:	Gram
h:	Hour
hCA:	Human carbonic anhydrase
L:	Liter
HeLa:	Henrietta Lacks
HRMS:	High-resolution mass spectrometry
MD:	Molecular dynamics
m:	Milli
MP:	Melting point
MTT:	3-(4,5-dimethylthiazol-2-yl)-2,5-diphenyltetrazolium bromide
NCE:	New chemical entity
NCI-60:	National cancer institute
NF-Kb:	Nuclear factor Kappa-B cells
NIM-DAPI: dihydrochloride	Nuclear isolation medium-4,6-diamino-2-phenylindole
NMR:	Nuclear magnetic resonance
n:	Nano
NSCL:	Non-small cell lung cancer
OPLS:	Optimized potential for liquid simulations
PET:	Positron emission tomography
PI:	Propidium iodide
RMSD:	Root mean square deviation
RPMI:	Roswell Park Memorial Institute
s:	Second
SCI:	Selective cytotoxicity index
SP:	Structure precision
TGF:	Transforming growth factor

Thr:	Threonine
TLC:	Thin layer chromatography
U:	Unit
USFDA:	United States Food Drug Administration
WHO:	World health organization
XP:	Extra precision

LIST OF TABLES

Sl. No.	Particulars	Page No.
3.1	List of reagents and solvents.	**17**
3.2	R_1 of α-bromoketones.	**19**
3.3	R of 2-amino-5-aralkyl-1,3,4-thiadiazoles.	**19**
3.4	R and R_1 of 2,6-disubstituted-imidazothiadiazoles.	**20**
3.5	R and R_1 of 5-bromo-imidazothiadiazoles.	**21**
3.6	R and R_1 of 5-formyl-imidazothiadiazoles.	**22**
3.7	R and R_1 of 5-thiocyanato-imidazothiadiazoles.	**23**
4.1	Structure and IUPAC name of α-bromoketones (2a-h).	**33**
4.2	Physicochemical properties of α-bromoketones (2a-h).	**34**
4.3	Structure and IUPAC name of 2-amino-5-aralkyl-1,3,4-thiadiazoles (5a,b).	**34**
4.4	Physicochemical properties of 2-amino-5-aralkyl-1,3,4-thiadiazoles (5a,b).	**34**
4.5	Structure and IUPAC name of imidazothiadiazoles (CH 1-15).	**35, 36**
4.6	Physicochemical properties of imidazothiadiazoles (CH 1-15).	**37**
4.7	Structure and IUPAC name of 5-bromo-imidazothiadiazoles (CH 16-27).	**38**
4.8	Physicochemical properties of 5-Br-imidazothiadiazoles (CH 16-27).	**39**
4.9	Structure and IUPAC name of 5-formyl-imidazothiadiazole (CH 28-36).	**40**
4.10	Physicochemical properties of 5-formyl-imidazothiadiazoles (CH 28-36).	**41**
4.11	Structure and IUPAC name of 5-thiocyanato-imidazothiadiazoles (CH 37-50).	**42-44**
4.12	Physicochemical properties of 5-thiocyanato-imidazothiadiazoles (CH 37-50).	**45**
4.13	FTIR spectral data of 2,6-disubstitued-imidazothiadiazoles.	**56**

4.14	FTIR spectral data of 5-bromo-imidazothiadiazoles.	**57**
4.15	FTIR spectral data of 5-formyl-imidazothiadiazoles.	**58**
4.16	FTIR spectral data of 5-thiocyanato-imidazothiadiazoles.	**59**
4.17	^{1}H-NMR spectral data of 2,6-disubstituted-imidazothiadiazoles.	**60**
4.18	^{1}H-NMR spectral data of 5-bromo-imidazothiadiazoles.	**61**
4.19	^{1}H-NMR spectral data of substituted imidazothiadiazole-5-carbaldehydes.	**62**
4.20	^{1}H-NMR spectral data of 5-thiocyanato-imidazothiadiazoles.	**63**
4.21	^{13}C NMR spectral data of substituted imidazothiadiazoles.	**64**
4.22	HRMS data of substituted imidazothiadiazoles.	**65**
4.23	Anti-proliferative effects of CH 1-8, 16-20, 28, 29 and 37-43.	**67**
4.24	Selectivity index of CH 43 (7g) and CH-29 (8b) towards cancer and non-cancer cells.	**68**
4.25	Nature and types of interaction between TGF β type I receptor kinase and the test molecule CH-43 (7g) and CH-29 (8b).	**70**
4.26	Anti-proliferative effects on L1210, CEM and HeLa cells.	**72, 73**
4.27	Pharmacological properties of virtual screening and rationally designed compounds.	**74-77**
4.28	Nature of interaction with 1m17 EGFR receptor.	**83, 84**

LIST OF FIGURES

Sl. No.	Particulars	Page No.
1.1	Pathophysiology of cancer.	**1**
1.2	Chemotherapeutic agents and their mechanism of action (MOA).	**2**
1.3	Role of heterocycles in anticancer drug discovery.	**3**
1.4	Year-wise contribution of heterocycles in anticancer drug discovery.	**4**
2.1	Tubulin protein interaction with paclitaxel	**9**
2.2	Tubulin protein interaction with paclitaxel	**9**
4.1	FTIR spectrum CH-43.	**46**
4.2	^{1}H-NMR spectrum of CH-43.	**47**
4.3	^{13}C-NMR spectrum of CH-43.	**48**
4.4	HRMS spectrum of CH-43.	**49**
4.5	FTIR spectrum of 5b.	**50**
4.6	^{1}H-NMR spectrum of 5b.	**51**
4.7	^{1}H-NMR spectrum of 5b.	**52**
4.8	FTIR spectrum of CH-50.	**53**
4.9	^{1}HNMR spectrum of CH-50.	**54**
4.10	^{1}HNMR spectrum of CH-50.	**55**
4.11	Annexin-V-FITC mitochondrial depolarization and caspase 3 activation assay.	**68**
4.12	Jurkatcells treated compound 7g.	**69**
4.13	Interactions between TGF beta kinase I, CH-43 /7g, Ligand and Melphalan.	**71**
4.14	3D interactions between the receptor 1m17, Co-ligand, CH-11/5c, CH-15/5g and CH-27/6g.	**78**
4.15	2D interactions between 1m17 receptor,Co-ligand, CH-11/5c, CH-15/5g and CH-27/6g.	**79**
4.16	RMSD plot obtained molecular dynamics simulation for protein backbone (blue) and ligand (red) CH 31/7b, CH 32/7c, CH 33/7e, CH 35/7f, CH 36/7g and CH 50/8g.	**80**

4.17	Protein ligand contact for the compounds CH 31 (7b), CH 32 (7c), CH 33 (7e), CH 35 (7f), CH 36 (7g) and CH 50 (8g).	**81**
4.18	Molecular dynamics simulation time line (in ns) for CH 31/7b, CH 32/7c, CH 33/7e, CH 35/7f, CH 36/7g and CH 50/8g.	**82**

ABSTRACT

Background:

Cancer is responsible for millions of death every year. The drugs used to treat cancer bear severe side-effects. Hence, there is always a need for effective and safer molecules against it. It can be achieved either by screening the NCE or repurposing the existing one. The bioisosteric replacement on a synthetically versatile scaffold often gives the molecule with desired biological properties. In-silico analysis of existing drugs is also in us

heterocyclic synthesis and CADD play vital role inthe process.

Objectives:

Objectives of the work is to design, synthesize and screen 2,6-substituted-imidazo[2,1-b] [1,3,4]thiadiazoles as levamisole derivativewith desired cytotoxic property and convert them to a potential lead against cancer.

Methodology:

Analytical grade reagents used in synthetic work (scheme 3.2.1-3.2.3).Thiosemicarbazide was treated with aromatic carboxylic acids to get 2-amino-5-aralkyl-1,3,4-thiadiazoles (5a,b). In subsequent reactionsdifferent 2,6-substituted-imidazo[2,1-b][1,3,4]thiadiazoles(CH 1-50) were obtained. Structures duly characterized and in-vivo cytotoxicity performed on cancerous and normal cell lines as well. ANOVA was used to measure inter-group data variation (expressed as mean ± SEM) using Graph Pad Prism 6.01. In-silico analysesweredone onTGF-beta 1kinase (PDB ID: 1RW8) and EGFR (pdbID: 1M17) receptors using Glide, AutoDock Vina and Desmond's Schrodinger tools. Molecular interactions, real time simulations, ADME and Lipinski Ro5 parameterspredicted during the study.

Results:

Analytical data summarized in table 4.13-4.22 and figure 4.1-4.10 confirm the structure of newly synthesized derivatives.CH-43/7g (IC_{50}: 0.78-1.6 µM) and CH-29/8b (IC_{50}: 0.94-1.3 µM) have exhibited improved cytotoxicity over melphalan (1.4-2.13 µM) against tested cell lines while,CH-15/5g was similar to melphalan in potency (IC_{50}: 2.1-4.0 µM). The selective cytotoxicity data find CH-43/7g less toxic against non-cancerous HS27 cells (CC_{50}: 31.45 µM), indicating high selective index. Apoptosis, caspase-3 activationand increased DNA fragmentation was observed in CH-43/7g treated cells. All molecules were better than levamisole in potency. Results were summarized in table4.23-4.28 and figure 4.11-4.18.

Conclusion:

Based on biological data it was observed that molecule CH-43/7g inhibits cancerous cell growth inducing apoptosis, Caspase-3 activation, and interfering DNA synthesis. Further, the improved potency of newly synthesized 2-aralkyl-6-aryl-imidazo[2,1-b][1,3,4]thiadiazole derivatives [CH 1-50] over levamisole make them a possible lead against cancer.

Keywords:

2-Aralkyl-6-aryl-imidazo[2,1-b][1,3,4]thiadiazole;Cytotoxicity;Apoptosis; Caspase-3; DNA fragmentation;Levamisole;Melplhalan.

1.0 INTRODUCTION

Cancer represents a group of disease characterized by uncontrolled cell division and, often recognized as a swollen mass or lump in body called *tumo*r. Eventhough a tumor may not be cancerous always, it is advisable to get it cured at initial stage. The ability to affect the neighbouring healthy cells and spreading to other parts through body fluids such as blood or lymph (metastasis) makes the cancer lethal and an uphill task for the medical practitioners to control or cure it.[1] World Health Organization (WHO) had reported 10 million deaths globally in 2020 alone due to cancer.[2] It (cancr) can affect all age groups and almost every parts of the body including, blood and lymph.[3]

Pathophysiology of cancer:

A cancerous growth is the manifestation of abnormality in genetic material of transformed cell. Either it may be due to the external factors called carcinogens such as harmful chemicals, irradiations or microbial infections or, due to defective deoxyribonucleic acid (DNA) replication process. It can be inherited too. The genetic abnormalities (mutation) leading deregulation of tumor suppressor genes cause uncontrolled growth and cancer.[2, 4]

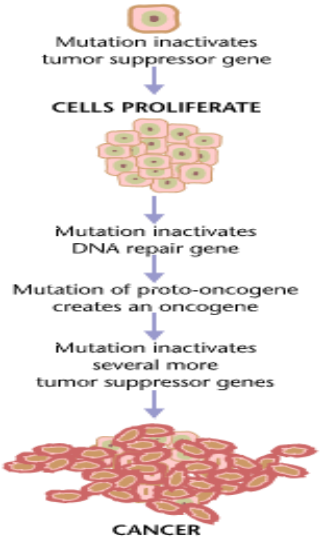

Fig. 1.1 Pathophysiology of cancer.[4]

Cancer therapy:

Early diagonosis is the first and foremost important step in cancer therapy. Majority of fatality in cancer are due to symptoms unawareness and lack of proper screening. Depending on severity, types and location the treatment methodology is selected. Pallaiative care, radiotherapy, chemotherapy and surgery are commonly employed, either alone or in combination (preferable) to cure the cancer and prolong patients' life.[2, 5]

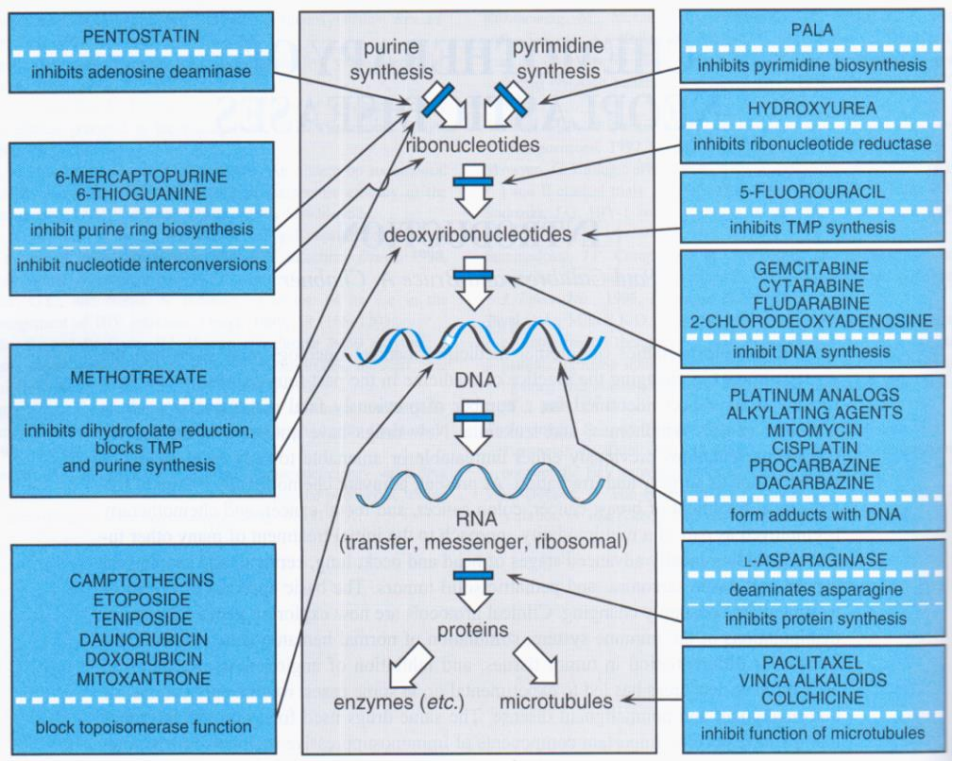

Fig. 1.2 Chemotherapeutic agents and their mechanism of action (MOA).[5]

Each method has its own limitations and none can be claimed to have 100% efficacy rate. Despite the severe toxic effects the chemotherapeutic agents are still preferred in combination with radiotherapy or after surgery in cancer treatment. Damage to surrounding tissues and inability to target certain types of cancer cells such as area near lymph nodes limits the radiotherapry application. Being an invasive technique and restricted applications, the surgery is not always a wise option in cancer therapy. Gene therapy[6] and peptide drugs[7] are another approach in terms of getting an effective

and safer anticancer molecule, however the cost may be a matter of concern with these class of drugs.

Heterocycles and anticancer drug discovery:

Since, majority of anticancer drugs (natural or synthetic) bear heterocyclic ring in their structure[8] it becomes prudent for researchers to explore or modify heterocyclic moieties for development of an effective anticancer lead.

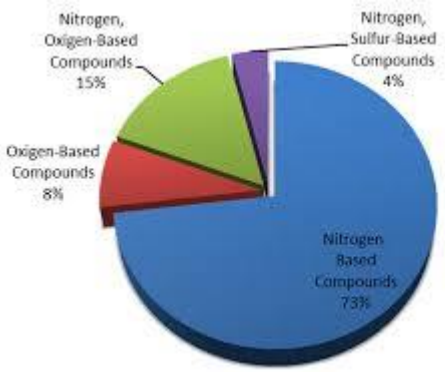

Fig. 1.3 Role of heterocycles in anticancer drug discovery.[8]

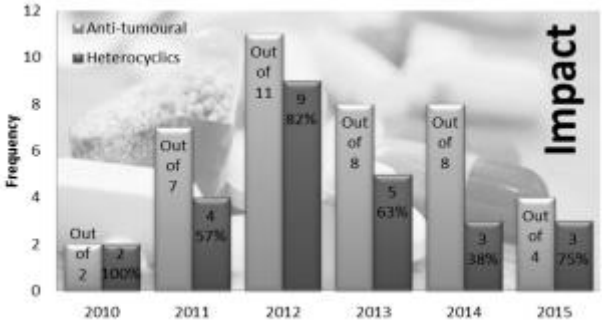

Fig. 1.4 Year-wise contribution of heterocycles in anticancer drug discovery.[8]

1.1 BACKGROUND

Development of an anticancer agent is a daunting task for medicinal chemists. As discussed in previous section the severe side effects, lack of specificity and metastasis make the cancer therapy complicated. Sometime the toxicity of an anticancer drug creates more trouble than the cancer itself. Hence, the race for an effective anticancer molecule is always on. Repurposing of existing drugs is another approach in novel drug discovery. It not only saves the time but also limits cost and makes the molecule affordable to large section of society. As far development of new chemical entity (NCE) is concerned, it can either be done by synthesizing a totally new scaffold or by modifying the existing candidates. Structural modification by isosteric replacement (biosisosterism) is another approach and had given several potent molecules differing in action than the parent moiety.[9]

In an attempt to get an effective NCE against cancer, the clinically obsolete levamisole (**1.1)** was modified isosterically to get new heterocyclic scaffold 2,6-disubstituted imidazo[2,1-*b*][1,3,4]thiadiazole **(1.2)**.

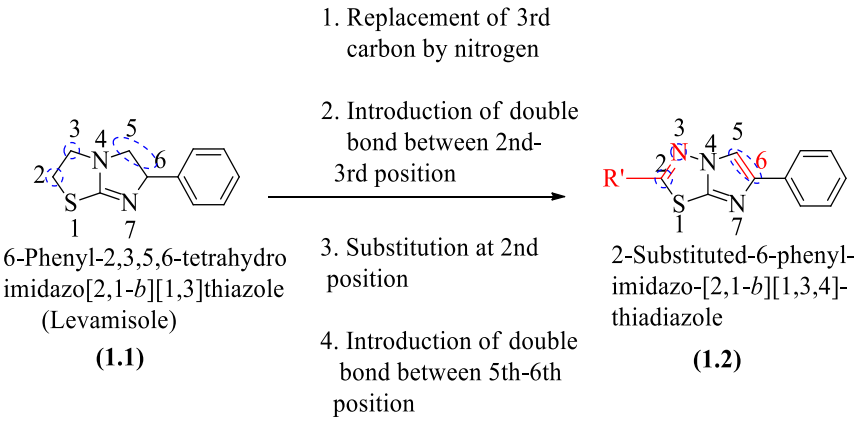

6-Phenyl-2,3,5,6-tetrahydro imidazo[2,1-*b*][1,3]thiazole (Levamisole)

(1.1)

2-Substituted-6-phenyl-imidazo-[2,1-*b*][1,3,4]-thiadiazole

(1.2)

Introduction of computer aided drug discovery (CADD) revolutionized the drug discovery process. It's not only rationale but also a time saving and cost effective process. Prediction of absorbtion, distribution, metabolism and excretion (ADME) parameters, docking study (molecular interaction) and real time simulation operations

were routinely performed by modern day's medicinal chemist to get a lead in stipulated time.[10, 11]

1.2 JUSTIFICATION

As briefed earlier, the heterocycles play vital role in drug discovery process. Nitorgenenous heterocycles contribute significantly in cancer research (fig. 1.3).[8] Let it be 6-mercaptopurine (1.3) or 5-F-uracil (FU) (1.4), all are nitrogenous with established anticancer property. Levamisole (1.1) is another example of it.[5]

Levamisole:

Chemically it is a thiazole derivative introduced in market by Janssen as deworming agent. It is levorotatory form of tetramisole (a racemic mixture). The drug got United States Food and Drug Administration (USFDA) approval in 1990 to treat colon cancer but soon (in 2003) withdrawn from US maket due to severe side effects (agranulocytosis). However, its anticancer property could not ruled out. It (levamisole) is still used by researchers round the globe as reference for anticancer screening of newly synthesized derivatives. The drug is also known for its immune modulatory property and still in practice to treat stage III colon cancer along with 5-FU in some countries.[12-14]

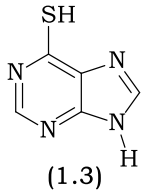

(1.3)

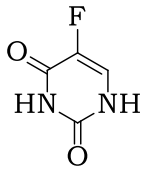

(1.4)

Considering importance of levamisole (1.1) in cancer research, the isosteric modification was done to get another synthetically versatile and biologically diversed heterocyclic scaffold imidazothiadiazole as levamisole analog in present study.

Imidazo[2,1-*b*][1,3,4]thiadiazole:

It is a fused ring structure containing bridged-head nitrogen at its 4th position (1.5 and 1.6). The molecule is known for its synthetic feasibility chemical versatility.

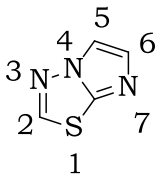

(1.5)

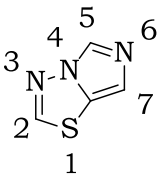

(1.6)

Methods of synthesis

Several synthetic methods were reported for synthesis of imidazothiadiazole nucleus (1.10) demonstrating its synthetic feasibility.[15-17] However, the method used commonly and in present work includes reaction between 2-amino-1,3,4-thiadiazole (1.7) and α-bromoketone (1.8).[18-20]

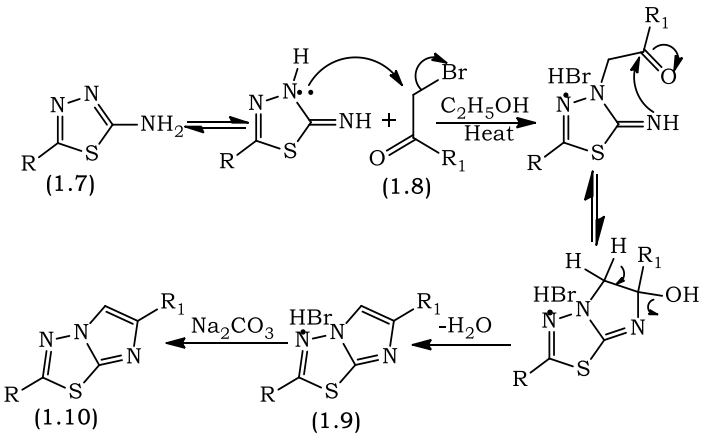

(1.7) (1.8) (1.9) (1.10)

(R= $-SO_2NH_2$, R_1=$-C_6H_5$, 4-Br-C_6H_4, 4-Cl-C_6H_4, 4-NO_2-C_6H_4, 4-Ph-C_6H_4, -COOEt, $-CH_2COOEt$, 3-coumarinyl, 2-furyl, 5-(4-NO_2-C_6H_4)-2-furyl).

Chemical reactivity

The molecule is highly reactive towards aromatic electrophilic substitution (1.11-1.14) at its 5th position.[20-22] However, depending on their nature the groups attached to 5th position can be further subjected to a variety of reactions such as Schiff and Mannich formation[23, 24], diazotization[25] and reduction.[26] Ring cleavage were also reported by few researchers.[27]

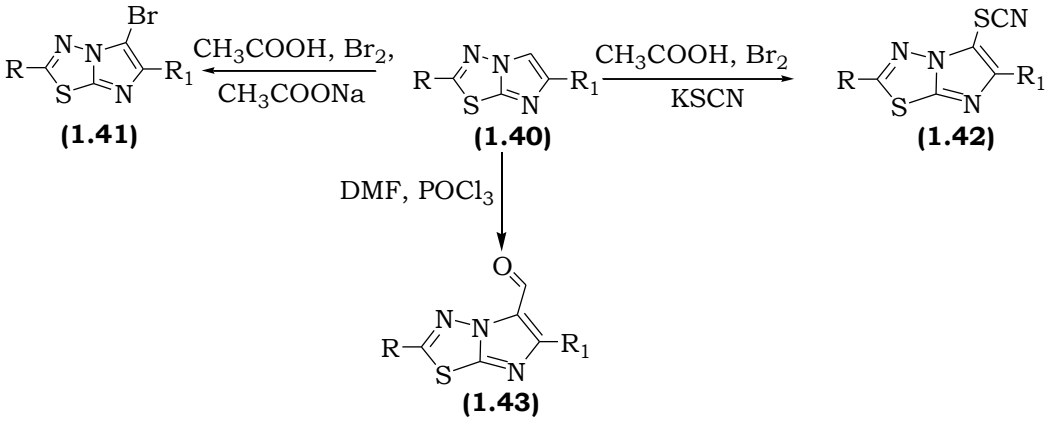

(1.41) **(1.40)** **(1.42)** **(1.43)**

(R= benzyl, 4-F-benzyl, 4-Cl-benzyl, 4-Br-benzyl, 4-CH_3-benzyl, R_1= 4-F-phenyl).

Apart from its versatile chemical nature, the imidazo[2,1-*b*][1,3,4]thiadiazole nucleus is well known for its promising anticancer property. Development of a novel BCL2 inhibitor by Iyer et al.[35] (2.14) and an imidazothiadiazole based tubulin inhibitor by Kamal et al.[39] (2.28-2.30) paved the way for selection of imidazothiadiazole moiety as levamisole analog for present work.

2.0 REVIEW OF LITERATURE

Below are the excerpts from literature reflecting imidazothiadiazoles as cytotoxic properties,

Askin et al.[28] had reported imidazothiadiazole derivatives (2.3) as human carbonic anhydrase (hCA) I/II and acetylcholine esterase (AChE) inhibitors. The synthesized derivatives had shown inhibitory activity against *h*CA I at 23.44–105.50 nano mole (nM), *h*CA II (10.32–104.70 nM) and AChE (K_Is20.52–54.06 nM). Cytotoxicity against L929 mouse fibroblast cells also obseved.

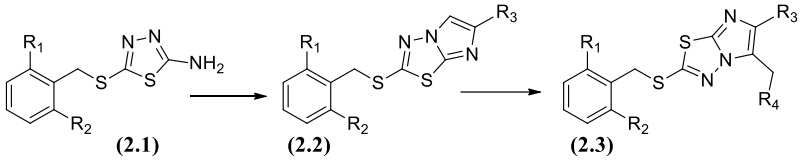

Reddy et al.[29] reported design, synthesis and cytotoxic property of some quinazolinone linked imidazothiadiazole derivatives against A549, Henrietta Lacks (HeLa) and MDA-MB-23 cells by 3-(4,5-dimethylthiazol-2-yl)-2,5-diphenyl tetrazolium bromide (MTT) method taking paclitaxel and doxorubicin as reference. The molecule 2.4 was active aginst A549 with 50 % growth inhibition (GI_{50}) at 0.25 micro mole (μM) while, 2.5 against MDA-MB-231 (GI_{50}; 0.23 μM). Docking study finds significant binding with tubulin protein like reference paclitaxel (fig. 2.1 and 2.2 respectively).

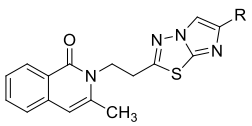

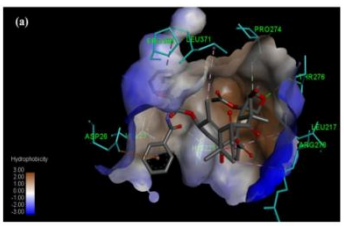

Fig. 2.1

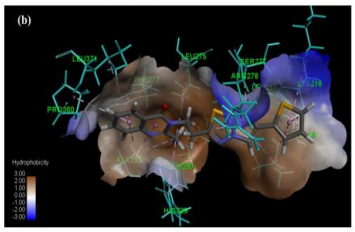

Fig. 2.2

(Tubulin protein interaction with paclitaxel)

Nakashima et al.[30] developed ^{68}Ga-labeled imidazothiadiazole derivatives as positron emission tomography (PET) probes targeting CA-IX. The monovalent DO3AIS1 (2.6) and divalent DO2AIS2 (2.7) derivatives had shown *in-vitro* affinity for high expressed CA-IX cells.

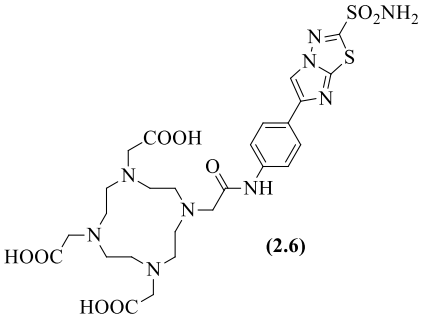

(2.6)

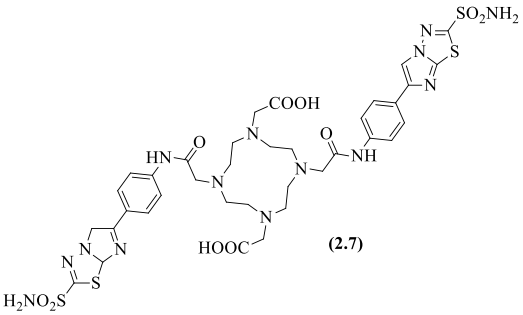

(2.7)

Cascioferro et al.[31] had reported series of imidazothiadiazole derivatives as antiproliferative agent against National Cancer Institute-60 (NCI-60) pannel. Structure 2.8 with 50% inhibitory concentration (IC_{50}) at 0.23-11.4 milli mole (mM) and 2.9 (0.29-12.2 mM) exhibited significant cytotoxic property. Further, 2.8 and 2.9 showed *in-vitro* antiproliferative activity against pancreatic carcinoma cell.

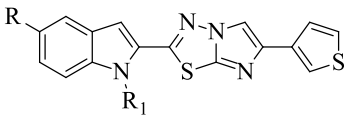

R=R_1=H **(2.8),** R=F,R_1=H **(2.9)**

Iikuni et al.[32] had synthesized imidazothiadiazole-sulfonamide base organometallic conjugate [^{99m}Tc]ISB2 as CA-IX imaging probe with greater enzyme affinity and faster renal clearance.

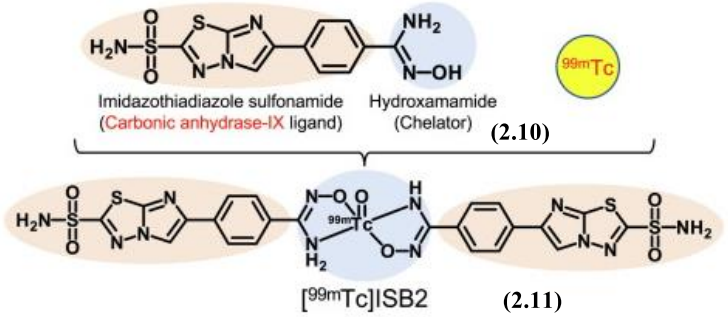

(2.10)

(2.11)

Beta Cell Lymphoma-2 (BCL-2) is a mitochondrial protein whose overexpression leads to cancer. Its inhibiton is an ideal approach in getting anticancer *lead*. Vartak et al.[33] had reported a specific BCL2 inhibitor *Disari*b (2.14) inhibiting BCL2-BAK interaction (*ki* 12.76 nM) sparing other pro-apoptotic proteins.

Series of benzenesulfonamide linked imidazothiadiazole (2.12) and thiazolotriazoles (2.13) were reported by Kumar et al.[34] as hCA I, II, IX & XII inhibitor. Against hCA I 2.12 and 2.13 had shown better inhibitory property than standard acetazolamide (k_i < 100, nM) while, against hCA-II and Hcaix moderate inhibition was observed.

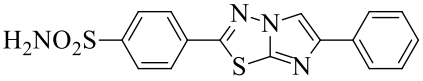

(2.12)

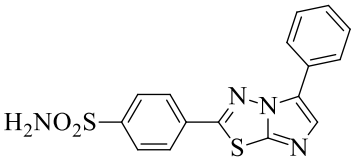

(2.13)

2-Oxindole linked imidazothiadiazole (2.14) [disarib] was reported as BCL2 inhibitor by Iyer et al.[35] Later, Vartak et al.[33] proposed it as an inhibitor of intrinsic pathway of apoptosis. The molecule found to be synergistic with paclitaxel (2.16).

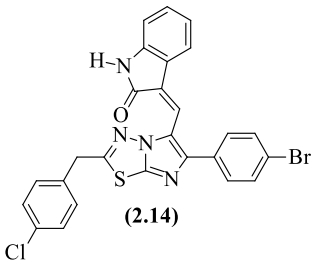

(2.14)

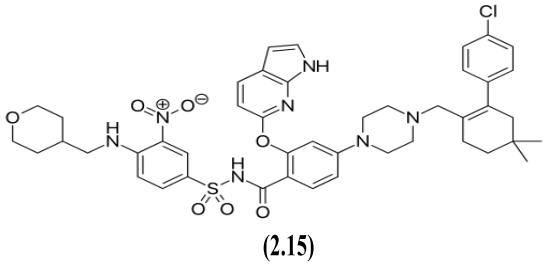

(2.15)

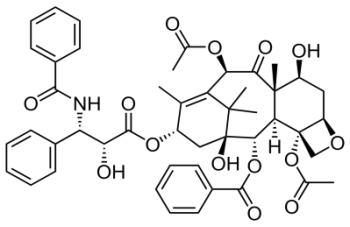

(2.16)

Katiyar et al.[36] screened series of imidazothiadiazoles for cytotoxicity against, cancerous cell CEM, HeLa, and L1210. Molecule 2.17, 2.18 and 2.20 were active

against HeLa at 49-63 μM while 2.22 was cytotoxic to L1210 and CEM cell at 23 μM. In addition, mild anti-influenza (A and B) property observed for 2.19 and 2.22.

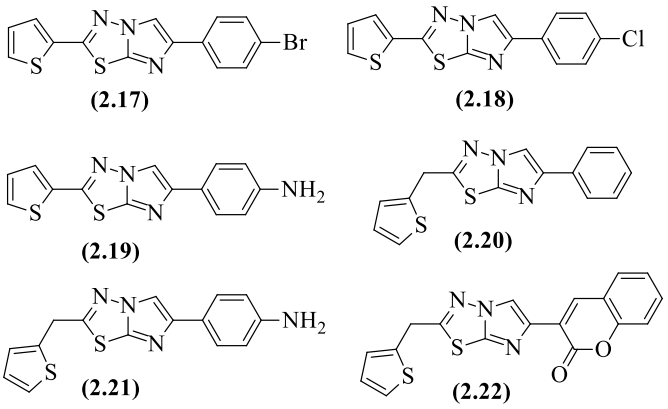

The antiproliferative property of imidazothiazoles/thiadiazoles (2.23-2.26) reported by Romagnoli et al.[37] find apoptosis induction by release of cytochrome-*C* and caspase cleavage. Melphalan, brostacillin, etoposide and staurosporine used as reference during the study.

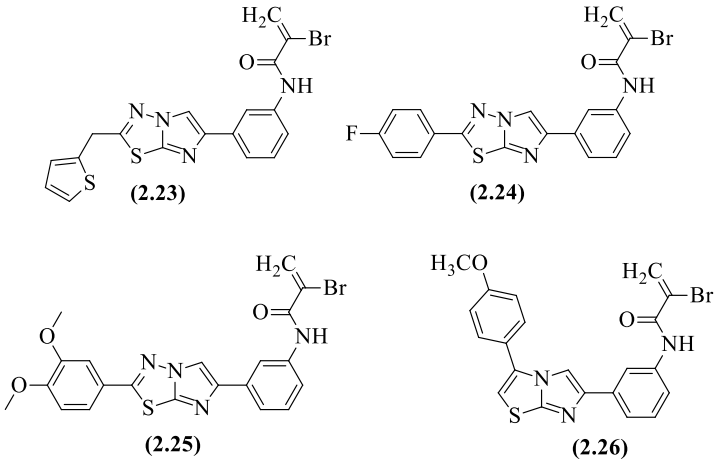

Imidazothiadiazole chalcones reported by Kamal et al.[38] reveal promising cytotoxicity with log GI_{50} -7.51 to -4.00. Cell cycle arrest was observed at G(0)/G(1)-phase alongwith enhanced p53, p21, and p27, suppressed Nuclear Factor Kappa-B cells (NF-Kb) and up-regulated caspase-9. The 3,4,5-*tri*-methoxy substituted derivative (2.27) had shown better cytotoxic property hence slected for further study.

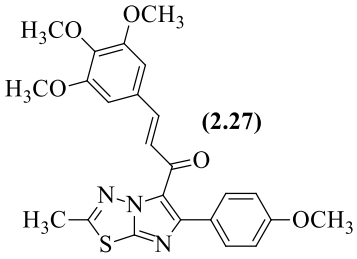

(2.27)

The tubulin inhibitory property of 2-oxindole substituted imidazothiadiazoles was reported by Kamal et al.[39] Study finds 2.28 as cytotoxic (IC_{50}: 1.1–1.6 μM) while, the tubulin inhibition was observed at 0.15 μM. *In-silico* study shows significant interaction by 2.28 and 2.29 with Asparagine (α-Asn101), Threonine (β-Thr 179), and Cysteine (β-Cys 241) at colchicine binding site in tubulin.

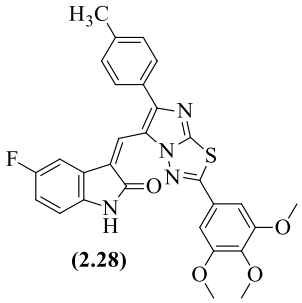

(2.28)

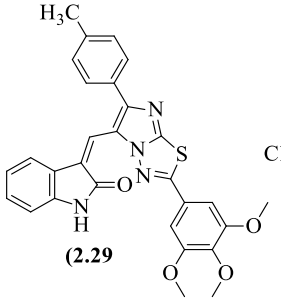

(2.29)

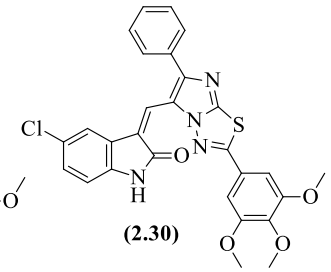

(2.30)

Sydnones of imidazothiadiazole were reported by Tegginamath et al.[40] as antibacterial against *Escherichia coli* (*E. coli*) AB1157DNA and DNA cleaving agent. Molecule 2.32 found to cleave DNA completely at 1 mg/mL

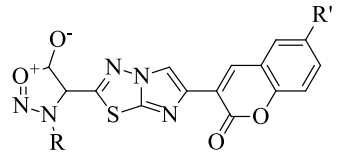

Where, R= Phenyl, 4-CH_3-phenyl, 4-OCH_3-phenyl

4-Cl-phenyl, R'= H, Cl, Br.

(2.31)

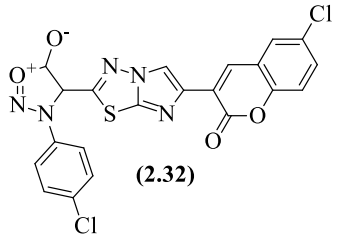

(2.32)

Gohil et al.[41] synthesized and screened phenyl substituted imidazothiadiazoles as anticancer agent against breast cancer cells. 73.70 and 52.56% inhibition was observed with structure 2.33 and 2.34.

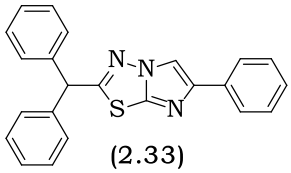

(2.33)

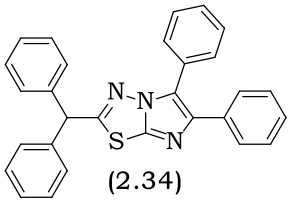

(2.34)

Levamisole derivatives inducing apoptosis was reported by Hegde et al.[42] Molecule 2.35 being the most active in group produced cytotoxic effect against CEM cells at 5 μM (IC_{50}) and was more potent than levamisole (1.1).

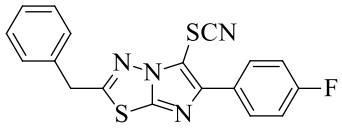

(2.35)

2,6-*Di*-substituted-imidazothiadiazole derivatives were screened by Noolvi et al.[43] against NCI-60 cell line panels. Structure 2.36 found to bear remarkable *in-vitro* cytotoxic property against non-small cell lung cancer (NSCL) HOP-92 cells (GI_{50}:0.114 μM). The molecule was also effective against cyclin-dependent activating kinase-1 (CAKI-1) renal cancer cells (GI_{50}:0.743 μM).

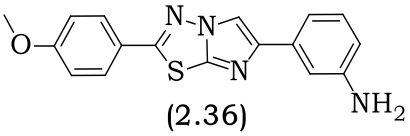

(2.36)

Synthesis and anticancer property of 2-phenyl-imidazothiadiazoles against NCI 60 cell line panel was reported by Taher et al.[44] Structure 2.37 and 2.38 were potent than 5-FU, GI_{50};6.0, TGI; 17.4 and LC_{50}; 55.1 μM.

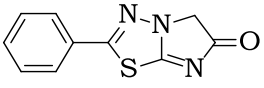

(2.37)

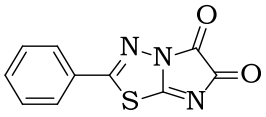

(2.38)

Synthesis and anticancer property of some 2-cycloalkyl linked 6-phenyl imidazothiadiazoles (2.39) was reported by Noolvi et al.[45] Molecule 2.40 found most active at 10^{-5} M against leukemic cells.

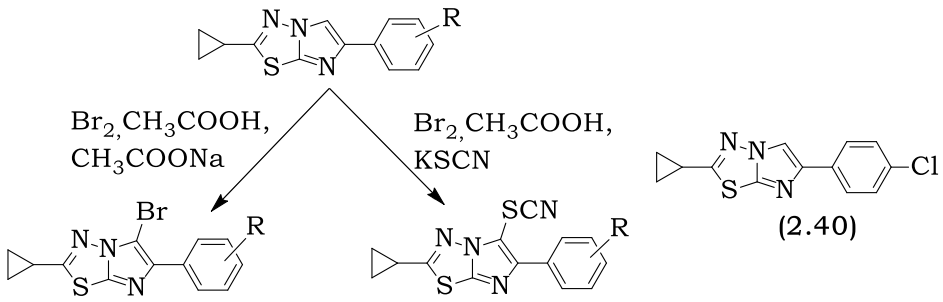

(R= H, 4-F, 4-Cl, 4-Br, 4-NO_2, 4-NH_2, 2,4-di-Cl, 2,4-di-OH, 3-NH_2, 3-OH, 2-OH).

(2.39)

Cytotoxic property of 2-aralkyl-6-aryl-imidazothiadiazoles (2.41-2.43) against different leukemic cell lines was reported by Karki et al.[20] The newly synthesized derivatives were more active than reference 5-FU (1.6).

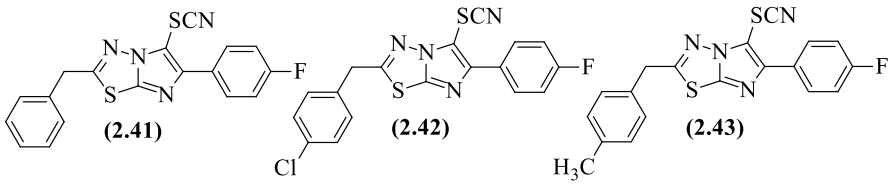

The carbohydrazides of imidazothiadiazole was synthesized and screened for *in-vitro* cytotoxicity. Terzioglu et al.[46] reported molecule 2.44 and 2.45 as potent cytotoxic agent better than reference chlorambucil and 5-FU (1.6) at 10^{-4}M.

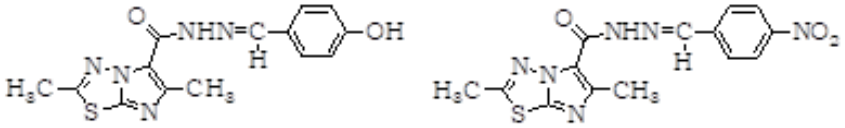

Apart from anticancer property the imidazothiadiazole nucleus are known to have antimicrobial[47], antioxidant[48], anti-viral[49], anti-inflammatory[50] and antidiabetic[51] properties, showing its diversed biological nature.

3.0 MATERIALS AND METHODS

Reagents and solvents mentioned in table-3.1 were used without further purification. Section 3.2.1-3.2.3 explain the synthetic routes while the procedures adopted to synthesize different substituted imidazothiadiazoles (CH 1-50) summarized in 1-6. Structure and purity of synthesized derivatives were confirmed by,

- Melting point (MP): By open capillary tube method.
- Thin layer chromatography (TLC): On pre-coated silica gel plates.
- Fourier transform infra-red (FTIR) spectroscopy: On Jasco FTIR 460+.
- Nuclear magnetic resonance (NMR) spectroscopy: On Bruker Ultraspec AMX-400 spectrometer/JeolJNM-ECZ400S.
- High resolution mass specctrometry (HRMS): On XEVO G2-XS QTOF mass spectrometer.

3.1 MATERIALS

Chemistry:

Table 3.1: List of reagents and solvents.

Sl. No.	Name	Source
1.	Acetic acid glacial	s d fine Chem. Ltd.
2.	Acetophenone	Spectrochem Pvt. Ltd.
3.	Sodium carbonate (anhydrous)	s d fine Chem. Ltd.
4.	Bromine (Br_2)	Spectrochem Pvt. Ltd.
5.	*p*-Bromoacetophenone	Spectrochem Pvt. Ltd.
6.	*p*-Chloroacetophenone	s d fine Chem. Ltd.
7.	Chloroform	s d fine Chem. Ltd.
8.	Concentrated sulphuric acid	s d fine Chem. Ltd.
9.	Dimethyl formamide	s d fine Chem Ltd.
10.	Ethylacetate	s d fine Chem. Ltd.
11.	Ethylacetoacetate	Spectrochem Pvt.Ltd.
12.	*p*-Fluoroacetophenone	Spectrochem Pvt. Ltd.
13.	n-Hexane	s d fine Chem. Ltd.
14.	*p*-Methoxyacetophenone	Spectrochem Pvt. Ltd.
15.	*p*-Methoxyphenylacetic acid	s d fine Chem. Ltd.
16.	*p*-Methylacetophenone	Spectrochem Pvt. Ltd.
17.	2-(Naphthalen-5-*yl*)acetic acid	s d fine Chem. Ltd.
18.	*p*-Nitroacetophenone	Spectrochem Pvt. Ltd.
19.	Piperidine	s d fine Chem. Ltd.
20.	Potassium thiocyanate	s d fine Chem. Ltd.
21.	Salicyladehyde	Spectrochem Pvt. Ltd.
22.	Sodium acetate (anhydrous)	s d fine Chem. Ltd.
23.	Sulphuric acid	s d fine Chem. Ltd.
24.	Thiosemicarbazide	s d fine Chem. Ltd.

3.2 METHODOLOGY

Chemistry:

Scheme

3.2.1 Synthesis of α-bromoketones (2a-h).

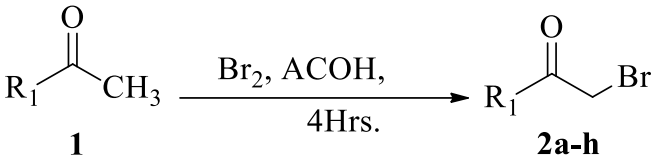

1 **2a-h**

3.2.2 Synthesis of 2-amino-5-aralkyl-1,3,4-thiadiazoles (5a,b)

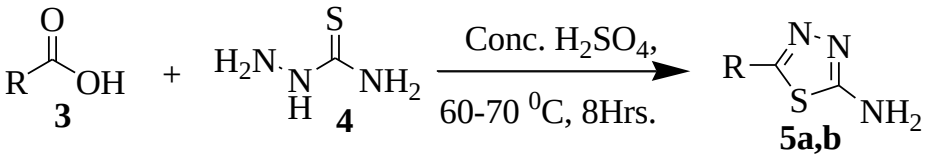

3 **4** **5a,b**

3.2.3: Synthesis of 2-aralkyl-6-arylimidazo[2,1-*b*][1,3,4]thiadiazoles (CH: 1-50)

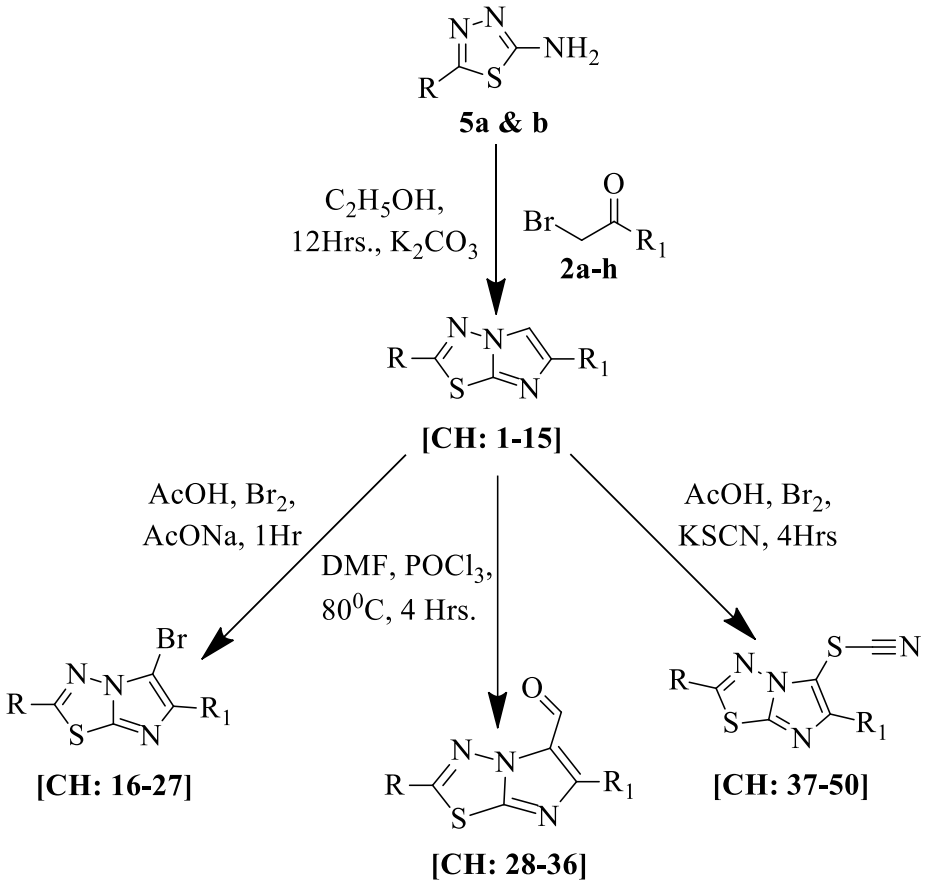

(R and R_1=table 3.2 - 3.7)

Table 3.2: R_1 of α-bromoketones.

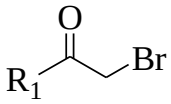

2a-h

Code	R_1	Code	R_1
2a		2e	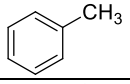
2b	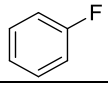	2f	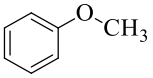
2c	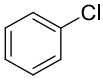	2g	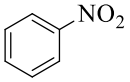
2d	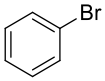	2h	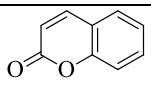

Table 3.3: R of 2-amino-5-aralkyl-1,3,4-thiadiazoles.

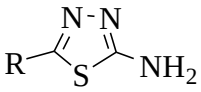

5a,b

Code	R	Code	R
5a	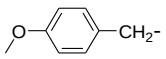	5b	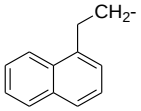

Table 3.4:-R and R_1 of 2,6-disubstituted-imidazothiadiazoles.

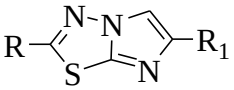

[CH: 1-15]

Code	R	R_1	Code	R	R_1
CH 1	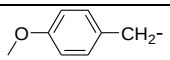		CH 9	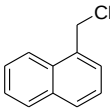	
CH 2	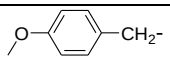	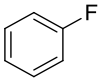	CH 10	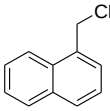	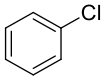
CH 3	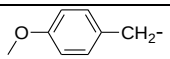	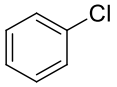	CH 11	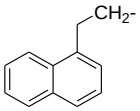	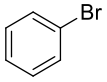
CH 4	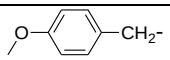	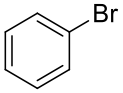	CH 12	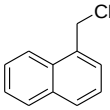	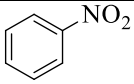
CH 5	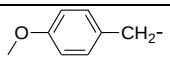	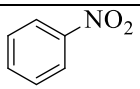	CH 13	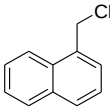	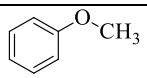
CH 6	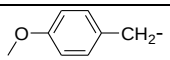	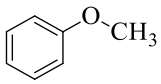	CH 14	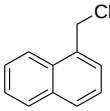	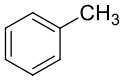
CH 7	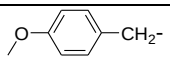	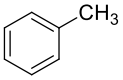	CH 15	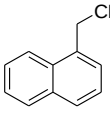	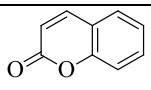
CH 8	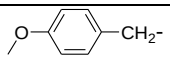	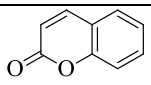	--	--	--

Table 3.5: R and R_1 of 5-bromo-imidazothiadiazoles.

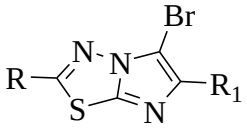

[CH: 16-27]

Code	R	R_1	Code	R	R_1
CH 16	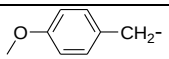		CH 22	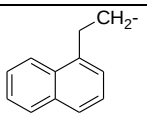	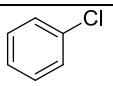
CH 17	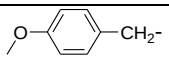	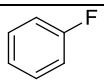	CH 23	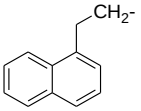	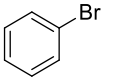
CH 18	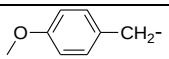	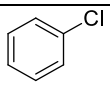	CH 24	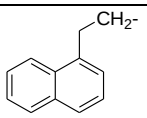	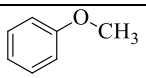
CH 19	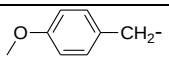	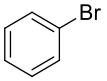	CH 25	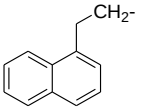	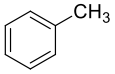
CH 20	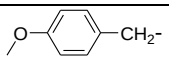	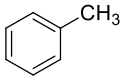	CH 26	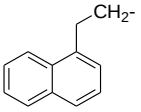	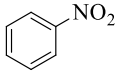
CH 21	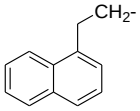		CH 27	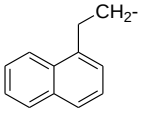	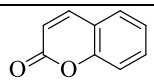

Table 3.6: R and R_1 of 5-formyl-imidazothiadiazoles.

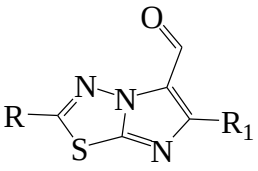

[CH: 28-36]

Code	R	R_1	Code	R	R_1
CH 28	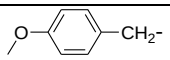		CH 33	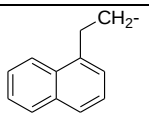	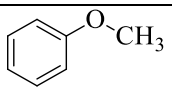
CH 29	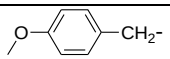	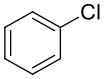	CH 34	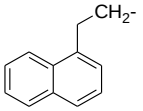	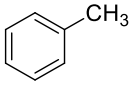
CH 30	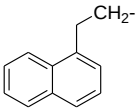		CH 35	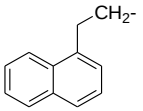	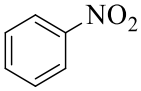
CH 31	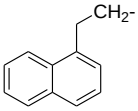	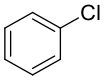	CH 36	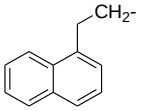	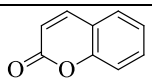
CH 32	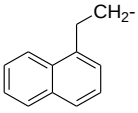	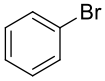	--	--	--

Table 3.7: R and R_1 of 5-thiocyanato-imidazothiadiazoles.

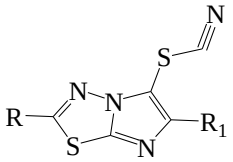

[CH: 37-50]

Code	R	R_1	Code	R	R_1
CH 37	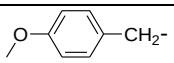		CH 44	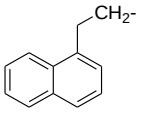	
CH 38	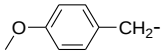	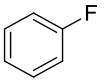	CH 45	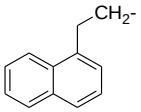	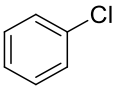
CH 39	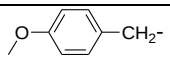	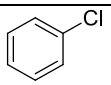	CH 46	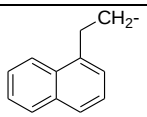	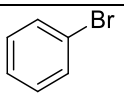
CH 40	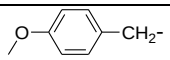	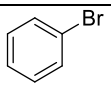	CH 47	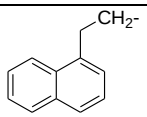	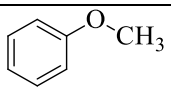
CH 41	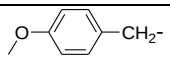	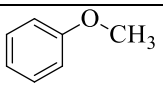	CH 48	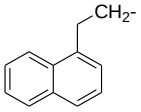	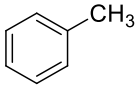
CH 42	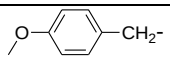	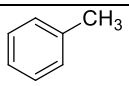	CH 49	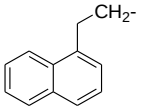	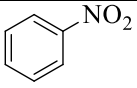
CH 43	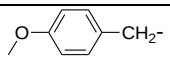	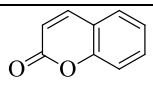	CH 50	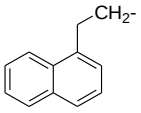	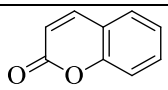

Chemistry: Procedure[18-20]

The experimental works comprise synthesis of,

1. α-Bromoketones (2a-h).

2. 2-Amino-5-aralkyl-1,3,4-thiadiazoles (5a and b).

3. 2,6-Disubstituted-imidazothiadiazoles (CH: 1-15).

4. 5-Bromo-imidazothiadiazoles (CH: 16-27).

5. 5-Formyl-imidazothiadiazoles (CH: 28-36).

6. 5-Thiocyanato-imidazothiadiazoles (CH: 37-50).

1. α-Bromoketones (2a-h):

0.1 mole (M) Br_2 in 20 millilitre (mL) CH_3COOH glacial added slowly to equimolar aromatic ketone (1) (in 25 mL CH_3COOH) at 5 degree Celsius (°C). Continued the stirring for 4 hours (h) at 28 °C and poured to 50 mL water. Filtered solid mass and purified from EtOH.

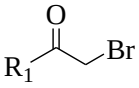

2a-h

(Table-3.2, 4.1 and 4.2)

2. 2-Amino-5-aralkyl-1,3,4-thiadiazoles (5a and 5b)

0.1 M carboxylic acids (2) and 0.15M thiosemicarbazide (3) were mixed and added slowly with stirring to 31.5 mL concentrated H_2SO_4 at 5 °C. Continued the reaction for 7 h at 80 °C. Cooled and poured the content into 200 gm crushed ice and made basic with dilute NH_4OH. Filtered the solid mass and purified from 6:4 dimethyl formamide-ethanol (DMF-EtOH) mixture.

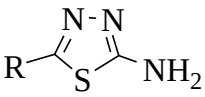

5a,b

(Table-3.3, 4.3 and 4.4)

3. 2,6-Disubstituted-imidazothiadiazoles (CH 1-15)

0.04 M of 5-substituted-2-amino-thiadiazoles (5a, b) and α-bromoketones (2a-h) were refluxed for 12 h in 100 mL EtOH. Filtered off the respective HBr salts and

suspended in 100 mL cold water. Neutralized the aqueous mixture with Na_2CO_3 to pH-7.0. Purified the obtained solid with EtOH-$CHCl_3$.

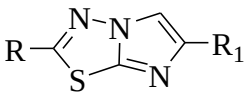

CH 1-15
(Table-3.4, 4.5 and 4.6)

4. 5-Bromo-imidazothiadiazoles (CH 16-27)

0.004 M Br_2 in CH_3COOH (glacial) added to 0.002 M mixture of CH_3COONa (anhydrous) and 2,6-disubstituted-imidazothiadiazole (CH 1-15) in 20 mL CH_3COOH (glacial). Continued the stirring for 2h and poured into cold water. Filetred the solid mass and purified from EtOH-$CHCl_3$ mixture.

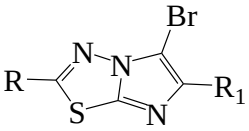

(CH 16-27)
(Table-3.5, 4.7 and 4.8)

5. 5-Formyl-imidazothiadiazoles (CH 28-36)

1.5 mL $POCl_3$ added slowly to 10 mL DMF at 5°C (Vilsmeier reagent). To the resulting solution 0.004 M 2,6-disubstituted-imidazothiadiazole (CH 1-15) was added and stirred for 4 h at 80°C. After cooling, adjust pH to 7.0 with sodium carbonate slution. Precipitaed mass was filetred, washed with water and re-crystallized using EtOH.

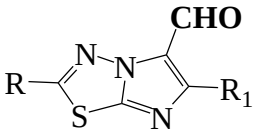

(Table-3.6, 4.9, 4.10)

6. 5-Thiocyanato-imidazothiadiazoles (CH 37-50)

0.004 M 2,6-disubstituted-imidazothiadiazole (CH 1-15) and 0.008M KSCN mixed together in 25 mL CH_3COOH (glacial). To the resulting suspension, 0.004 M Br_2 in

CH_3COOH (glacial) added in drop at 5 °C. Stirring continued at 30 °C for 2 h. Transfered the rsulting solution into 50 mL water. Filtered the solid and purified from EtOH-$CHCl_3$.

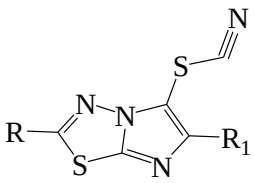

CH 37-50

[Table-3.7, 4.11, 4.12]

Biology:

A total of 50 derivatives of substituted imidazothiadiazoles' were prepared and subjected to *in-vitro* cytotoxic evaluation against different cancerous and non-cancerous cell lines. The mechanism of action was established and *In-silico* analysis were performed on the most active molecules from the seires. ADME properties were calculated and docking was performed to understand molecular basis of ligand-receptor interaction.

4-Methoxybenzyl substituted-imidazothiadiazoles (CH 1-8, 16-20, 28, 29 and 37-43):

Cell lines used

Jurkat

CCRF-CEM

Hs-27

Culture conditions

The Jurkat and CCRF-CEM cells were grown in RPMI-1640 medium containing 25 µg/mL amphotericin B, 1000 unit (U)/mL penicillin, 1000 µg/ml streptomycin, and 10% thermally deactivated FBS. The Dulbecco's Modified Eagle (DMEM) media

with similar antibiotics and Fetal Bovine Serum (FBS) as in Roswell Park Memorial Institute (RPMI) 1640 was used to culture the Hs-27 cells.

Cytotoxicity study (in human and murine tumor cell lines)

By adopting the procedure used for naphthyl substuted derivatives as mentioned in part of this section.

Cytotoxic activity (in human tumor cell lines)

The cytotoxicity study performed as per literature. Each experiment was repeated three times (n=3) and the IC_{50} values were expressed in μM. In brief, 5×10^3 HeLa cells were added to 96 micro-titer plates and, allowed to grow for 24 h. Culture medium with known concentration of test molecules were poured thereafter to each well. After 3days of incubation at 37 °C total cell count was done using Coulter counter. The CC_{50} value (μM) was calculated for treated and untreated (control) cells plotting a graph between the % of control and the concentration. The cytotoxicity was expressed as MCC.[52]

Differential nuclear staining assay (DNS)

The DNS assay was performed to analyze the potency of cytotoxic property of test compounds. Due to difference in permeation ability, the combination of PI and Hoechst dye was used in study. The Hoechst dye (blue) stains normal and dead cells nuclei while propidium iodide (PI) in red penetrates only through the structurally compromised membranes (dead cells) and stains the nuclei. The dead cells show blue and red stained nuclei. Cells with 95% viability was used for the study as determined by PI staining and flow cytometry. In brief, the cells were added to 96-well micro-titer plate (10,000 cells/well) containing 100 μL culture media. Incubation was done for 2 and 24 h for adherent and non-adherent cells respectively. Compounds in concentration of 0.1-10 μM (in gradient manner) was added to each well. Untreated

cells, 1%v/v dimethylsulfoxide (DMSO) and 1 mM H_2O_2 was used as control. All experiments were performed in triplicate. Further, 48 and 72 h incubation was done for non-adherent and adherent cells respectively. Mixture of Hoechst and PI 5 microgram (μg)/mL was added to each well before 2 h of the incubation period and continued for remaining 2 h. After incubation, the images were captured using the IN Cell Analyzer 2000. IN Cell Analyzer Workstation 3.2 software was used to separate and analyze live and dead cells.[53]

Mitochondrial depolarization assay

Cells were grown (200,000 cells/well) in 24-well plate. After 5 h of treatment with test molecules 2 μM JC-1 reagent (MitoProbe; Life Technologies; M34152) was added to each well. Flow cytometry analysis (Gallios; Beckman Coulter) performed. The appearance of green fluorescence represent a compromised/depolarized mitochondrial membrane.[54]

Cytotoxic concentration 50% (CC_{50}) and selective cytotoxicity index (SCI) values

CC_{50} represent amount required to kill 50% cell population. The dead cell % in DMSO (vehicle) was substracted from test sample and the CC_{50} value was calculated using linear interpolation equation. Cells were exposed to double concentration of test compound, due to short exposure time. The SCI values calculated separating CC_{50} of non-cancer cells from CC_{50} of the cancer cells.[55-56]

Annexin V- fluorescein isothiocyanate (FITC/PI) assay

100,000 cells/well were seeded in 1mL culture media into a 24-plate plates and treated for 24h with CC_{50} concentration of test compound **CH 43** (**7g)**. The cells were treated with PI and annexin V-FITC as per the user manual from supplier

(Beckman Coulter; IM3546) and subjected to flow cytometry analysis (Cytomics FC 500; Beckman Coulter) using the CXP software.[57]

Caspase-activation assay

To a 24-plate plate containing 1 mL RPMI medium, Jurkat cells added in concentration of 100,000 cells/well. To each well the CC_{50} of test compound was added and incubated for 7 h. After the incubation period, the caspase-3 activation was analyzed using fluorogenic NucView 488 kit. The green fluorescence after flow cytometry analysis represent apoptotic cells with caspase 3 activation.[58]

Cell cycle analysis

As mentioned above, the Jurkat cells treated with CC_{25} and CC_{50} concentration of test compound for 72 h. After completion of incubation, the cells were collected and centrifuged for 5 minutes at 262 *g* and regenerated into 100 µL fresh media to which, 200 µL nuclear isolation medium-4,6-diamidino-2-phenylindole dihydrochloride (NIM-DAPI) reagent was added. Flow cytometry analysis was done using Kaluza Flow Cytometry Software.[59, 60]

***In-silico* study:**

Protein preparation

The transforming growth factor (TGF)-beta receptor 1kinase (PDB ID: 1RW8, resolution: 2.4 Å) complexed with 5,6-dihydro-4*H*pyrrolo [1,2-b]pyrazole co-ligand prepared on protein preparation wizard (Schrödinger, LLC, New York, 2017). Three dimensional structure of 1RW8 was obtained assigning bond orders and adding H atoms and viewed in PyMol. Free (unbound) water molecules were removed and the structural geometry was optimized using optimized potentials for liquid simulations-2005 (OPLS) software.[61]

Ligand preparation

Structure of compound 7g and 8b were prepared and minimized on ChemBioDraw Ultra 11.0. The three dimensional structure of standard drug Melphalan was obtained from DrugBank. LigPrep module was used to prepare 3D structure of ligands 7g, 8b and melphalan. OPLS 2005 force field was used to optimize the three dimensional (3D) structure. Chirality of molecules were preserved during the structural optimization process.[63, 64]

Receptor Grid Generation

A receptor grid (20 Å×20 Å×20 Å) was prepared using Glide program (Schrödinger) to facilitate ligand binding within active site. Van der Waals scaling factor (1.00) and charge cut-off (0.25) were considered during the process.[65]

Molecular Docking

It involved two types, the shape precision (SP) and the extra precision (XP) docking. H-bonding and hydrophobic interactions were viewed by Discovery Studio v19 and PyMol. The ΔG (binding free energy) value was calculated in kJ/mole using following formula[66],

$$\text{Glide score} = E_{coul} + E_{vdW} + E_{bind} + E_{penalty}$$

E_{coul}: Electrostatic potential energy, E_{vdW}: Van der Waals energy.

E_{bind}: Binding interaction energy, $E_{penalty}$: Strain energy

2-Naphthalenmethyl substituted-imidazothiadiazoles (CH 9-15, 21-27, 30-35 and 44-50)

Cell lines used

HeLa.

CEM.

L1210.

Cytotoxic study

Synthesized molecules screened for cytostatic property in 96-well micro-titer plates. To each well 5-7.5 x 10^4 tumor cells were added followed by known concentration of test compounds. The L1210 cells were incubated at 37 °C in CO_2 controlled condition for 48 h while, 72 h incubation was done for CEM and HeLa cells. After incubation live cells were counted using Coulter counter and IC_{50} value was calculated.[19]

Statistical analysis

Values were expressed in mean ±standard error of the mean (SEM). One-way analysis of variance (ANOVA) was used to measure inter-group data variation using Graph Pad Prism 6.01. Any value with *$p<0.05$ was considered statistically significant

***In-silico* study:**

Theoretical calculations

Structural optimization (energy minimization) was done on 6-311G(d) and d.-functional theory (DFT)/B3LYP (Gaussian 09). Docking was performed using AutoDock Vina in PyRx software. The molecular descriptors for ADME calculated using free ADME-Tox filtering tools (FAF-Drugs4).[67-72]

Molecular dynamics simulation studies

Docking study was performed on epidermal growth factor receptor (EGFR) pdbID: 1M17 (residues: 684-951) using Desmond's Schrodinger tool. The molecular dynamics (MD) was performed for 20 nano seconds (ns) setting temperature 300 Kelvin (K) and pressure 1.013 bar. TIP4PEW was the solvent model used during study. The orthorhombic grid boundary of 8 Angstrom (A˚) was set for docking. To simulate the physiological condition, 0.15 M NaCl and Cl-counter ions were added.

After every 25 ps 1000 frames captured. Root mean square deviation (RMSD) was calculated for all ligand protein interactions.[73-74]

4.0 RESULTS

Chemistry

Table 4.1: Structure and IUPAC name of α-bromoketones (2a-h).

Code	Structure and IUPAC name	Code	Structure and IUPAC name
2a	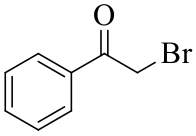 2-Bromo-1-pheny lethanone	**2b**	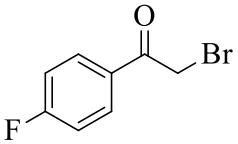 2-Bromo-1-(4-fluorophenyl) ethanone
2c	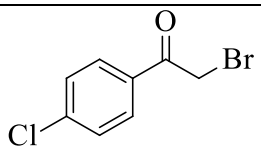 2-Bromo-1-(4-chlorophenyl) ethanone	**2d**	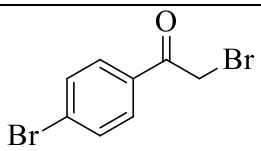 2-Bromo-1-(4-bromophenyl) ethanone
2e	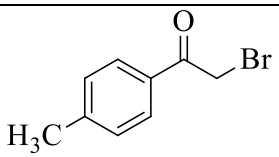 2-Bromo-1-(*p*-tolyl) ethanone	**2f**	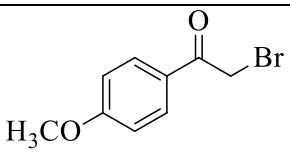 2-Bromo-1-(4-methoxyphenyl) ethanone
2g	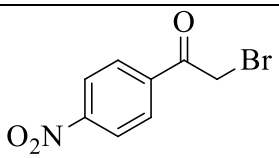 2-Bromo-1-(4-nitrophenyl) ethanone	**2h**	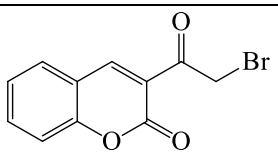 3-(2-Bromoacetyl)-2*H*-chromen-2-one

Table 4.2: Physicochemical properties of α-bromoketones (2a-h).

Code	Physical Appearance	M.F	M.W	M.P (°C)		Yield (%)
				Observed Value	Literature value[75-78]	
2a	White needles	C_8H_7BrO	199.04	50-51	48-50	85
2b	Coluorless crystals	C_8H_6BrF	217.04	45-48	47-49	80
2c	White crystals	C_8H_6BrClO	233.49	96-98	93-96	85
2d	White crystals	$C_8H_6Br_2O$	277.94	102-04	108-10	75
2e	Pale yellow crystals	C_9H_9BrO	213.07	50-52	46-48	70
2f	Pale yellow crystals	$C_9H_9BrO_2$	229.07	72-74	69-71	75
2g	Yellow crystals	$C_8H_6BrNO_3$	244.04	98-9	97-98	60
2h	Creamy Flakes	$C_{11}H_7BrO_3$	267.08	162-63	162-64	85

Table 4.3: Structure and IUPAC name of 2-amino-5-aralkyl-1,3,4-thiadiazoles (5a,b).

Code	R	Code	IUPAC name
5a	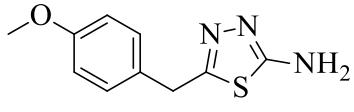 5-(4-Methoxybenzyl)-1,3,4-thiadiazol-2-amine	5b	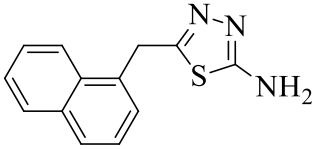 5-(Naphthalen-1-ylmethyl)-1,3,4-thiadiazol-2-amine

Table 4.4: Physicochemical properties of 2-amino-5-aralkyl-1,3,4-thiadiazoles (5a, b).

Code	Physical Appearance	M.F	M.W	M.P (°C)	Yield (%)
5a	White crystalline powder	$C_{10}H_{11}N_3OS$	221.06	196-98 (195-97)	85
5b	Off-white crystalline powder	$C_{13}H_{11}N_3S$	241.07	268-70	70

Table 4.5: Structure and IUPAC name of limidazothiadiazoles (CH 1-15).

Code	Structure and IUPAC name	Code	IUPAC name
CH 1	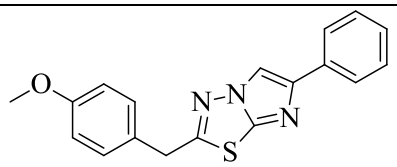 2-(4-Methoxybenzyl)-6-phenylimidazo [2,1-*b*][1,3,4]thiadiazole	CH 2	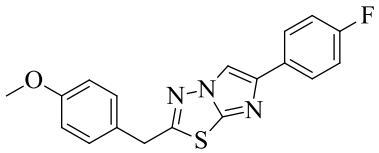 6-(4-Fluorophenyl)-2-(4-methoxybenzyl)imidazo [2,1-*b*][1,3,4]thiadiazole
CH 3	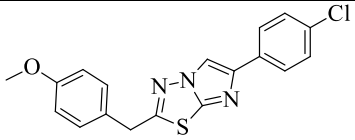 6-(4-Chlorophenyl)-2-(4-methoxybenzyl)imidazo [2,1-*b*][1,3,4]thiadiazole	CH 4	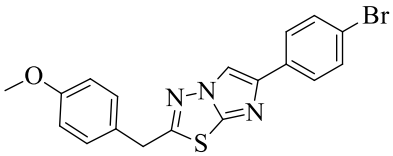 6-(4-Bromophenyl)-2-(4-methoxybenzyl)imidazo [2,1-*b*][1,3,4]thiadiazole
CH 5	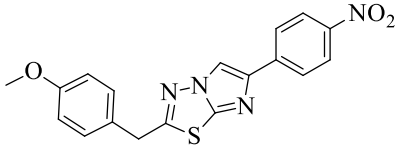 2-(4-Methoxybenzyl)-6-(4-nitrophenyl)imidazo [2,1-*b*][1,3,4]thiadiazole	CH 6	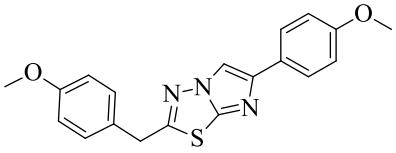 2-(4-Methoxybenzyl)-6-(4-methoxyphenyl)imidazo [2,1-*b*][1,3,4]thiadiazole
CH 7	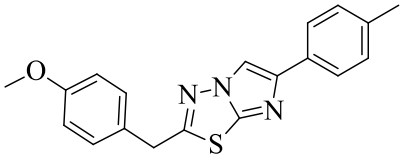 2-(4-Methoxybenzyl)-6-(*p*-tolyl)imidazo [2,1-*b*][1,3,4]thiadiazole	CH 8	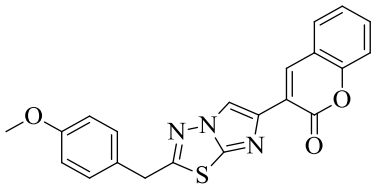 3-(2-(4-Methoxybenzyl)imidazo[2,1-*b*][1,3,4] thiadiazol-6-yl)-2*H*-chromen-2-one

CH 9	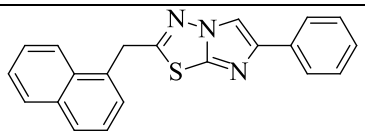 2-(Naphthalen-1-ylmethyl)-6-phenylimidazo[2,1-*b*][1,3,4]thiadiazole	CH 10	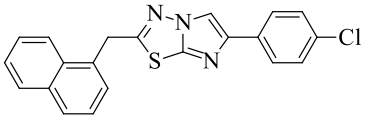 6-(4-Chlorophenyl)-2-(naphthalen-1-ylmethyl)imidazo[2,1-*b*][1,3,4]thiadiazole
CH 11	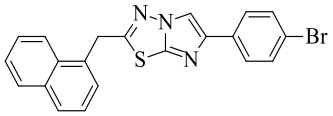 6-(4-Bromophenyl)-2-(naphthalen-1-ylmethyl)imidazo[2,1-*b*][1,3,4]thiadiazole	CH 12	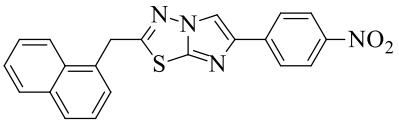 2-(Naphthalen-1-ylmethyl)-6-(4-nitrophenyl)imidazo[2,1-*b*][1,3,4]thiadiazole
CH 13	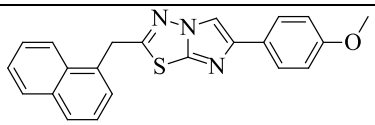 6-(4-Methoxyphenyl)-2-(naphthalen-1-ylmethyl)imidazo[2,1-*b*][1,3,4]thiadiazole	CH 14	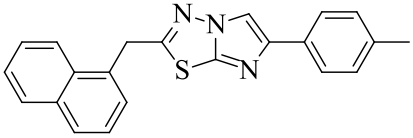 2-(Naphthalen-1-ylmethyl)-6-(*p*-tolyl)imidazo[2,1-*b*][1,3,4]thiadiazole
CH 15	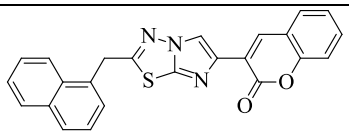 3-(2-(Naphthalen-1-ylmethyl)imidazo[2,1-*b*][1,3,4]thiadiazol-6-yl)-2*H*-chromen-2-one	--	--

Table 4.6: Physicochemical properties of imidazothiadiazoles (CH 1-15).

Code	Physical Appearance	M.F	M.W	M.P (°C)	Yield (%)	R_f*
CH 1	Colourless crystals	$C_{18}H_{15}N_3OS$	321.40	192-94 (196)	65	0.65
CH 2	Creamy amorphous powder	$C_{18}H_{14}FN_3OS$	339.39	130-32	55	0.55
CH 3	Colourless amorphous powder	$C_{18}H_{14}ClN_3OS$	355.84	148-50 (141-42)	80	0.68
CH 4	Colourless amorphous powder	$C_{18}H_{14}BrN_3OS$	400.29	168-70 (158-60)	77	0.70
CH 5	Brown amorphous powder	$C_{18}H_{14}N_4O_3S$	366.39	175-78 (183)	82	0.50
CH 6	Pale yellow crystals	$C_{19}H_{17}N_3O_2S$	351.42	201-03 (210)	75	0.55
CH 7	Light yellow amorphous powder	$C_{19}H_{17}N_3OS$	335.42	168-70 (163)	72	0.60
CH 8	White amorphous powder	$C_{21}H_{15}N_3O_3S$	389.43	120-22	64	0.75
CH 9	White amorphous poder	$C_{21}H_{15}N_3S$	341.43	196-98	58	0.60
CH 10	Creamy crystals	$C_{21}H_{14}ClN_3S$	375.87	198-200	61	0.55
CH 11	Creamy crystals	$C_{21}H_{14}BrN_3S$	420.32	198-202	64	0.70

CH 12	Light yellow crystals	$C_{21}H_{14}N_4O_2S$	386.43	268-270	55	0.50
CH 13	Colourless crystals	$C_{22}H_{17}N_3OS$	371.45	194-96	58	0.70
CH 14	Creamy crystals	$C_{22}H_{17}N_3S$	355.46	180-82	60	0.65
CH 15	Light yellow amorphous powder	$C_{24}H_{15}N_3O_2S$	409.46	220-22	62	0.55

*** Mobile Phase: Ethylacetate: Hexane (7:3) for all series.**

Table 4.7: Structure and IUPAC name of 5-bromo-limidazothiadiazoles (CH 16-27).

Code	Structure		IUPAC Name
CH16	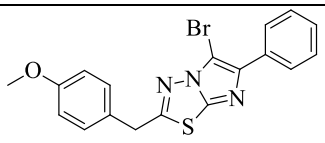 5-Bromo-2-(4-methoxybenzyl)-6-phenylimidazo [2,1-*b*][1,3,4]thiadiazole	**CH 17**	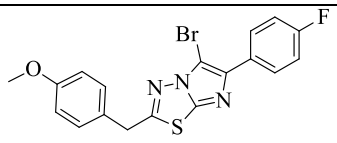 5-Bromo-6-(4-fluorophenyl)-2-(4-methoxybenzyl) imidazo[2,1-*b*][1,3,4]thiadiazole
CH 18	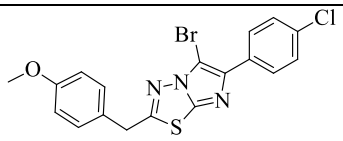 5-Bromo-6-(4-chlorophenyl)-2-(4-methoxybenzyl) imidazo[2,1-*b*][1,3,4]thiadiazole	**CH 19**	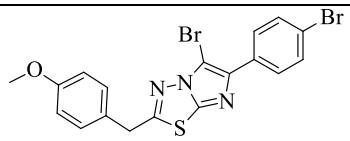 5-Bromo-6-(4-bromophenyl)-2-(4-methoxybenzyl) imidazo[2,1-*b*][1,3,4]thiadiazole
CH 20	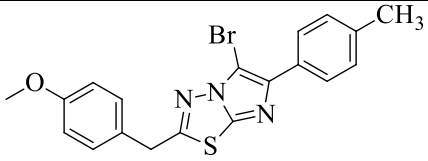 5-Bromo-2-(4-methoxybenzyl)-6-(*p*-tolyl) imidazo[2,1-*b*][1,3,4]thiadiazole	**CH 21**	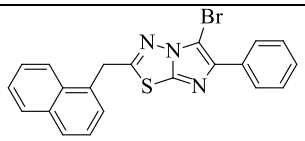 5-Bromo-2-(naphthalen-1-ylmethyl)-6-phenylimidazo[2,1-*b*][1,3,4]thiadiazole
CH 22	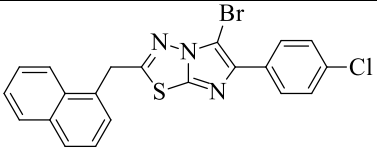 5-Bromo-6-(4-chlorophenyl)-2-(naphthalen-1-ylmethyl)imidazo[2,1-*b*][1,3,4]thiadiazole	**CH 23**	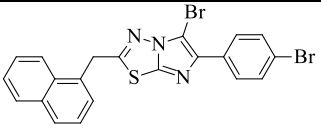 5-Bromo-6-(4-bromophenyl)-2-(naphthalen-1-ylmethyl) imidazo[2,1-*b*][1,3,4]thiadiazole

CH 24	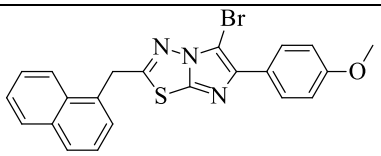 5-Bromo-6-(4-methoxyphenyl)-2-(naphthalen-1-ylmethyl)imidazo[2,1-*b*][1,3,4]thiadiazole	**CH 25**	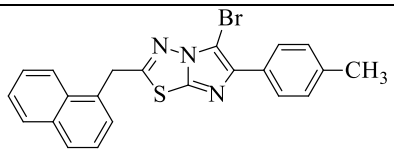 5-Bromo-2-(naphthalen-1-ylmethyl)-6-(*p*-tolyl) imidazo[2,1-*b*][1,3,4]thiadiazole
CH 26	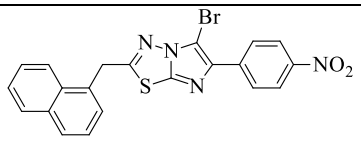 5-Bromo-2-(naphthalen-1-ylmethyl)-6-(4-nitrophenyl) imidazo[2,1-*b*][1,3,4]thiadiazole	**CH 27**	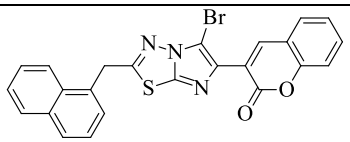 3-(5-Bromo-2-(naphthalen-1-ylmethyl)imidazo[2,1-*b*][1,3,4]thiadiazol-6-yl)-2*H*-chromen-2-one

Table 4.8: Physicochemical properties of 5-Br-imidazothiadiazoles (CH 16-27).

Code	Physical Appearance	M.F	M.W	M.P (°C)	Yield (%)	R_f *
CH 16	Light yellow crystals	$C_{18}H_{14}BrN_3OS$	400.29	135-38	60	0.65
CH 17	Light brown crystals	$C_{18}H_{13}BrFN_3OS$	418.28	123-25	58	0.60
CH 18	Creamy Crystals	$C_{18}H_{13}BrClN_3OS$	434.74	98-100	63	0.70
CH 19	Light yellow amorphous powder	$C_{18}H_{13}Br_2N_3OS$	479.19	100-102	55	0.58
CH 20	Creamy amorphous powder	$C_{19}H_{16}BrN_3OS$	414.32	138-40	58	0.50
CH 21	Creamy Crystals	$C_{21}H_{14}BrN_3S$	420.32	128-30	63	0.62
CH 22	Light yellow amorphous powder	$C_{21}H_{13}BrClN_3S$	454.77	154-56	67	0.50
CH 23	Light yellow crystals	$C_{21}H_{13}Br_2N_3S$	499.22	168-70	62	0.66
CH 24	Light yellow amorphous powder	$C_{22}H_{16}BrN_3OS$	450.35	138-40	65	0.70
CH 25	Creamy amorphous powder	$C_{22}H_{16}BrN_3S$	434.35	152-54	61	0.50

CH 26	Light yellow crystals	$C_{21}H_{13}BrN_4O_2S$	465.32	184-86	67	0.60
CH 27	White amorphous powder	$C_{24}H_{14}BrN_3O_2S$	488.36	226-28	58	0.40

*** Mobile Phase: Ethylacetate: Hexane (7:3) for all series.**

Table 4.9: Structure and IUPAC name of 5-formyl-imidazothiadiazole (CH 28-36).

Code	Structure	Code	IUPAC name
CH 28	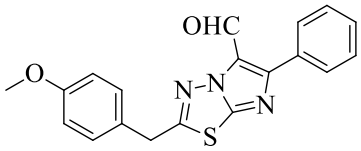 2-(4-Methoxybenzyl)-6-phenylimidazo [2,1-*b*][1,3,4]thiadiazole-5-carbaldehyde	CH 29	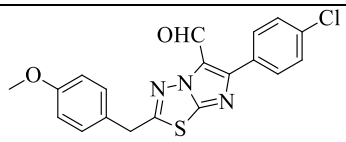 6-(4-Chlorophenyl)-2-(4-methoxybenzyl)imidazo [2,1-*b*][1,3,4]thiadiazole-5-carbaldehyde
CH 30	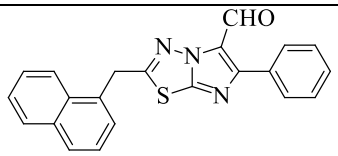 2-(Naphthalen-1-ylmethyl)-6-phenylimidazo [2,1-*b*][1,3,4]thiadiazole-5-carbaldehyde	CH 31	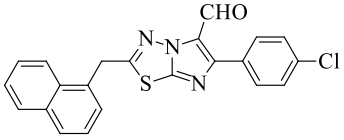 6-(4-Chlorophenyl)-2-(naphthalen-1-ylmethyl) imidazo[2,1-*b*][1,3,4]thiadiazole-5-carbaldehyde
CH 32	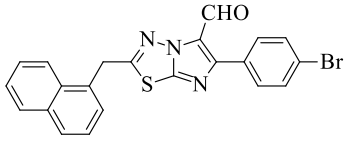 6-(4-Bromophenyl)-2-(naphthalen-1-ylmethyl) imidazo[2,1-*b*][1,3,4]thiadiazole-5-carbaldehyde	CH 33	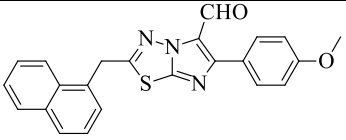 6-(4-Methoxyphenyl)-2-(naphthalen-1-ylmethyl) imidazo[2,1-*b*][1,3,4]thiadiazole-5-carbaldehyde

CH 34	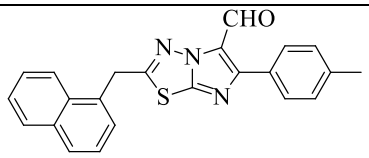 2-(Naphthalen-1-ylmethyl)-6-(*p*-tolyl)imidazo [2,1-*b*][1,3,4]thiadiazole-5-carbaldehyde	CH 35	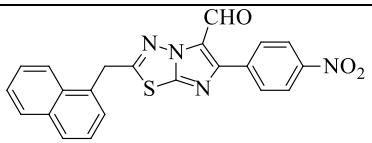 2-(Naphthalen-1-ylmethyl)-6-(4-nitrophenyl) imidazo[2,1-*b*][1,3,4]thiadiazole-5-carbaldehyde
CH 36	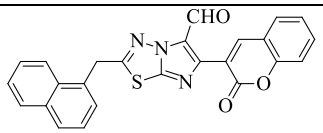 2-(Naphthalen-1-ylmethyl)-6-(2-oxo-2*H*-chromen-3-yl) imidazo[2,1-*b*][1,3,4]thiadiazole-5-carbaldehyde	--	--

Table 4.10: Physicochemical properties of 5-formyl-imidazothiadiazoles (CH 28-36).

Code	Physical Appearance	M.F	M.W	M.P (ºC)	Yield (%)	R_f *
CH 28	Creamy amorphous powder	$C_{19}H_{15}N_3O_2S$	349.41	118-20	55	0.75
CH 29	White amorphous Solid	$C_{19}H_{14}ClN_3O_2S$	383.85	125-28 (122)	60	0.62
CH 30	White flakes	$C_{22}H_{15}N_3OS$	369.44	154-56	52	0.65
CH 31	Light yellow Crystals	$C_{22}H_{14}ClN_3OS$	403.88	172-74	51	0.70
CH 32	Yellow crystals	$C_{22}H_{14}BrN_3OS$	448.34	138-40	48	0.65
CH 33	White flakes	$C_{23}H_{17}N_3O_2S$	399.46	90-92	52	0.45
CH 34	White crystals	$C_{23}H_{17}N_3OS$	383.47	102-04	50	0.55
CH 35	Yellow crystals	$C_{22}H_{14}N_4O_3S$	414.44	170-72	53	0.68
CH 36	Light brown amorphous powder	$C_{25}H_{15}N_3O_3S$	437.47	98-101	48	0.62

*** Mobile Phase: Ethylacetate: Hexane (6:4) for all series.**

Table 4.11: Structure and IUPAC name of 5-thiocyanato-imidazothiadiazoles (CH: 37-50).

Code	Structure and IUPAC Name
CH 37	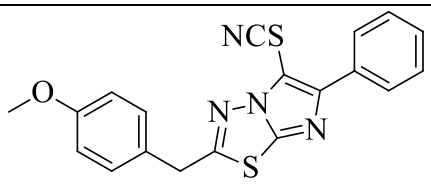 2-(4-Methoxybenzyl)-6-phenyl-5-thiocyanato imidazo[2,1-*b*][1,3,4]thiadiazole
CH 38	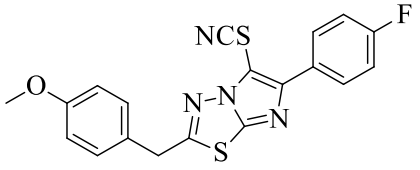 6-(4-Fluorophenyl)-2-(4-methoxybenzyl)-5-thiocyanato imidazo[2,1-*b*][1,3,4]thiadiazole
CH 39	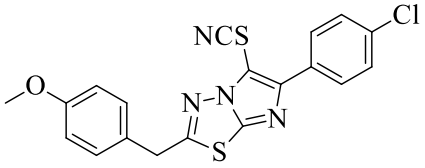 6-(4-Chlorophenyl)-2-(4-methoxybenzyl)-5-thiocyanato imidazo[2,1-*b*][1,3,4]thiadiazole

CH 40	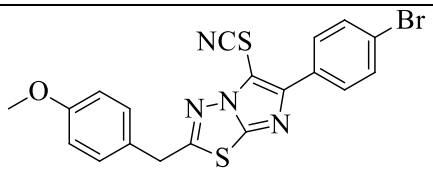 6-(4-Bromophenyl)-2-(4-methoxybenzyl)-5-thiocyanato imidazo[2,1-*b*][1,3,4]thiadiazole
CH 41	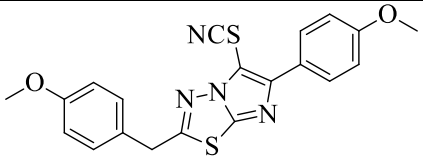 2-(4-Methoxybenzyl)-6-(4-methoxyphenyl)-5-thiocyanato imidazo[2,1-*b*][1,3,4]thiadiazole
CH 42	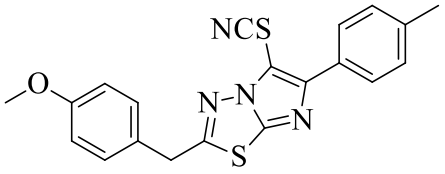 2-(4-Methoxybenzyl)-5-thiocyanato-6-(*p*-tolyl)imidazo[2,1-*b*][1,3,4]thiadiazole
CH 43	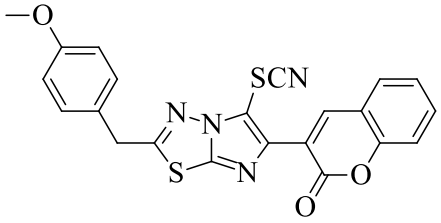 3-(2-(4-Methoxybenzyl)-5-thiocyanatoimidazo [2,1-*b*][1,3,4]thiadiazol-6-yl)-2*H*-chromen-2-one
CH 44	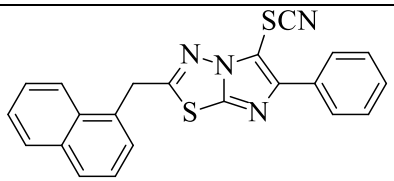 2-(naphthalen-1-ylmethyl)-6-phenyl-5-thiocyanato imidazo[2,1-*b*][1,3,4]thiadiazole
CH 45	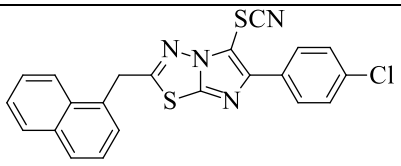 6-(4-Chlorophenyl)-2-(naphthalen-1-ylmethyl)-5-thiocyanato imidazo[2,1-*b*][1,3,4]thiadiazole

CH 46	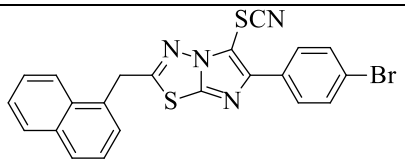 6-(4-Bromophenyl)-2-(naphthalen-1-ylmethyl)-5-thiocyanato imidazo[2,1-*b*][1,3,4]thiadiazole
CH 47	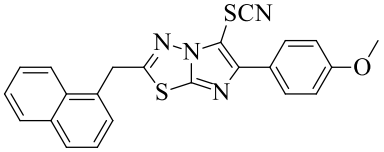 6-(4-Methoxyphenyl)-2-(naphthalen-1-ylmethyl)-5-thiocyanato imidazo[2,1-*b*][1,3,4]thiadiazole
CH 48	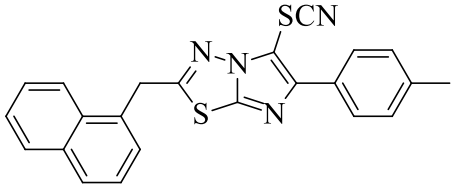 2-(Naphthalen-1-ylmethyl)-5-thiocyanato -6-(*p*-tolyl)imidazo[2,1-*b*][1,3,4]thiadiazole
CH 49	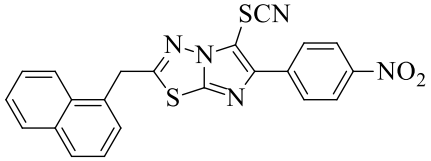 2-(Naphthalen-1-ylmethyl)-6-(4-nitrophenyl)-5-thiocyanato imidazo[2,1-*b*][1,3,4]thiadiazole
CH 50	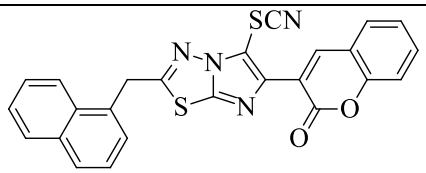 3-(2-(Naphthalen-1-ylmethyl)-5-thiocyanatoimidazo [2,1-*b*][1,3,4]thiadiazol-6-yl)-2*H*-chromen-2-one

Table 4.12: Physicochemical properties of 5-thiocyanato-imidazothiadiazoles (CH 37-50).

Code	Physical Appearance	M.F	M.W	M.P (°C)	Yield %	R_f*
CH 37	Creamy amorphous Powder	$C_{19}H_{14}N_4OS_2$	378.47	148-50	70	0.65
CH 38	Buff coloured amorphous powder	$C_{19}H_{13}FN_4OS_2$	396.46	118-20	65	0.55
CH 39	Creamy amorphous Powder	$C_{19}H_{13}ClN_4OS_2$	412.92	160-62	60	0.62
CH 40	Yellow amorphous powder	$C_{19}H_{13}BrN_4OS_2$	457.37	158-60	75	0.45
CH 41	Brown amorphous Powder	$C_{20}H_{16}N_4O_2S_2$	408.5	178-80	65	0.58
CH 42	Reddish brown amorphous powder	$C_{20}H_{16}N_4OS_2$	392.5	118-20	74	0.62
CH 43	Light yellow amorphous powder	$C_{22}H_{14}N_4O_3S_2$	446.5	188-90	66	0.52

CH 44	Colourless crystals	$C_{22}H_{14}N_4S_2$	398.5	148-50	58	0.70
CH 45	Creamy Crystals	$C_{22}H_{13}ClN_4S_2$	432.95	144-46	61	0.62
CH 46	Light yellow amorphous powder	$C_{22}H_{13}BrN_4S_2$	477.4	146-48	60	0.65
CH 47	Light brown Crystals	$C_{23}H_{16}N_4OS_2$	428.52	160-62	61	0.54
CH 48	Light brown Crystals	$C_{23}H_{16}N_4S_2$	412.53	102-04	60	0.50
CH 49	Light yellow Crystals	$C_{22}H_{13}N_5O_2S_2$	443.5	264-66	60	0.55
CH 50	Creamy crystals	$C_{25}H_{14}N_4O_2S_2$	466.53	258-60	57	0.65

*** Mobile Phase: Ethylacetate-Hexane (8:2).**

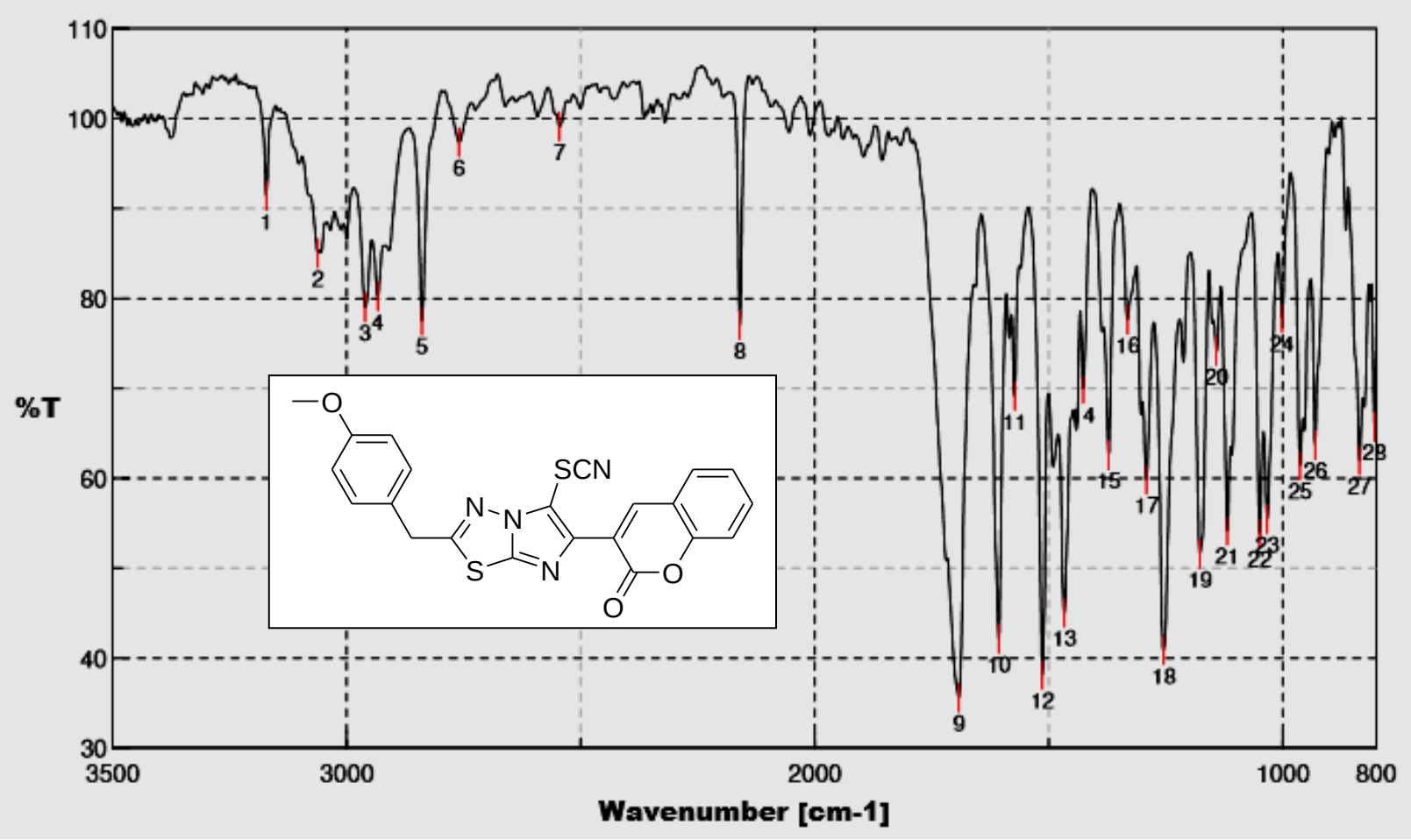

Fig. 4.1: FTIR spectrum CH-43.

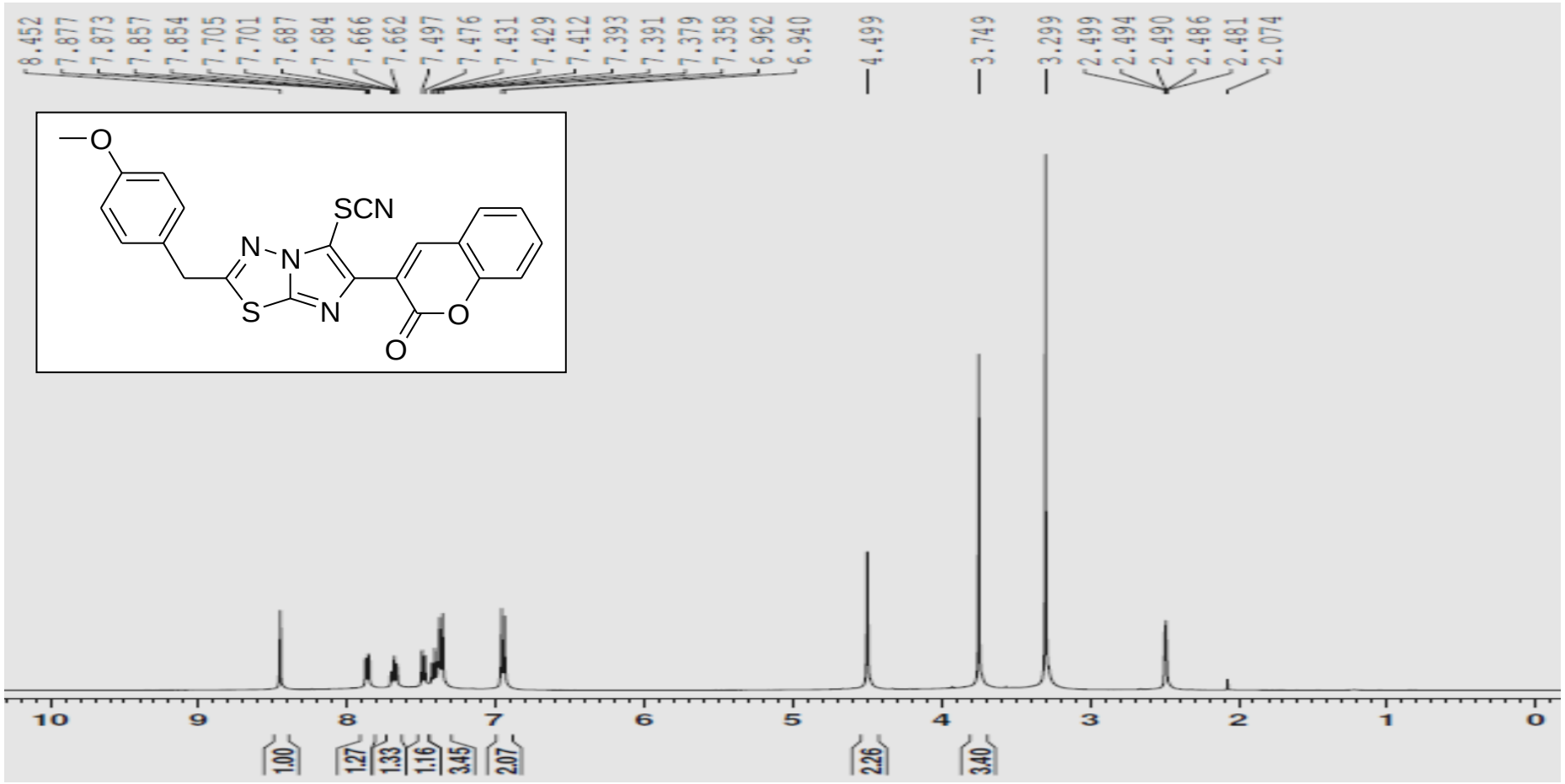

Fig. 4.2: 1H-NMR spectrum of CH-43.

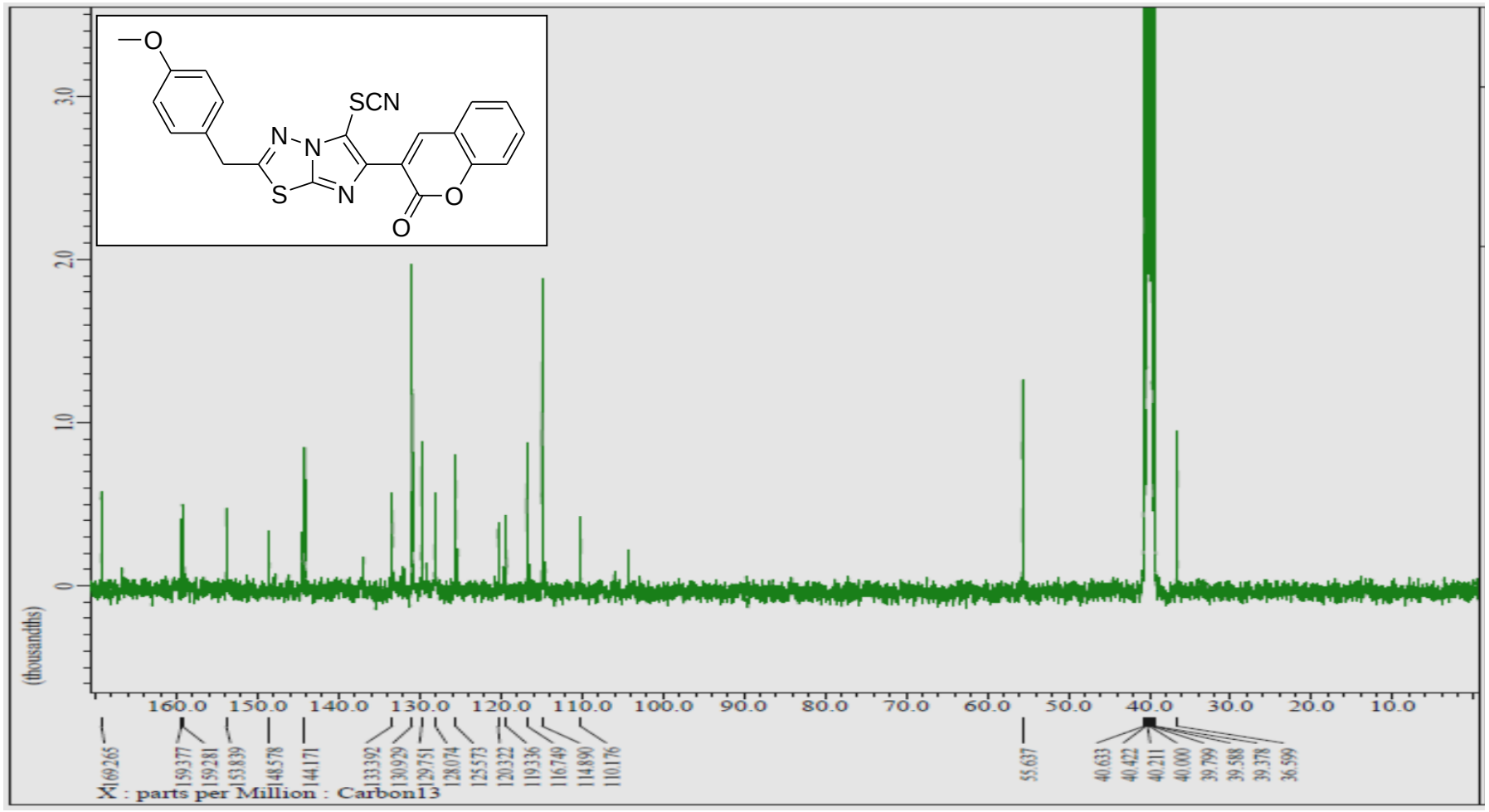

Fig. 4.3: ^{13}C-NMR spectrum of CH-43.

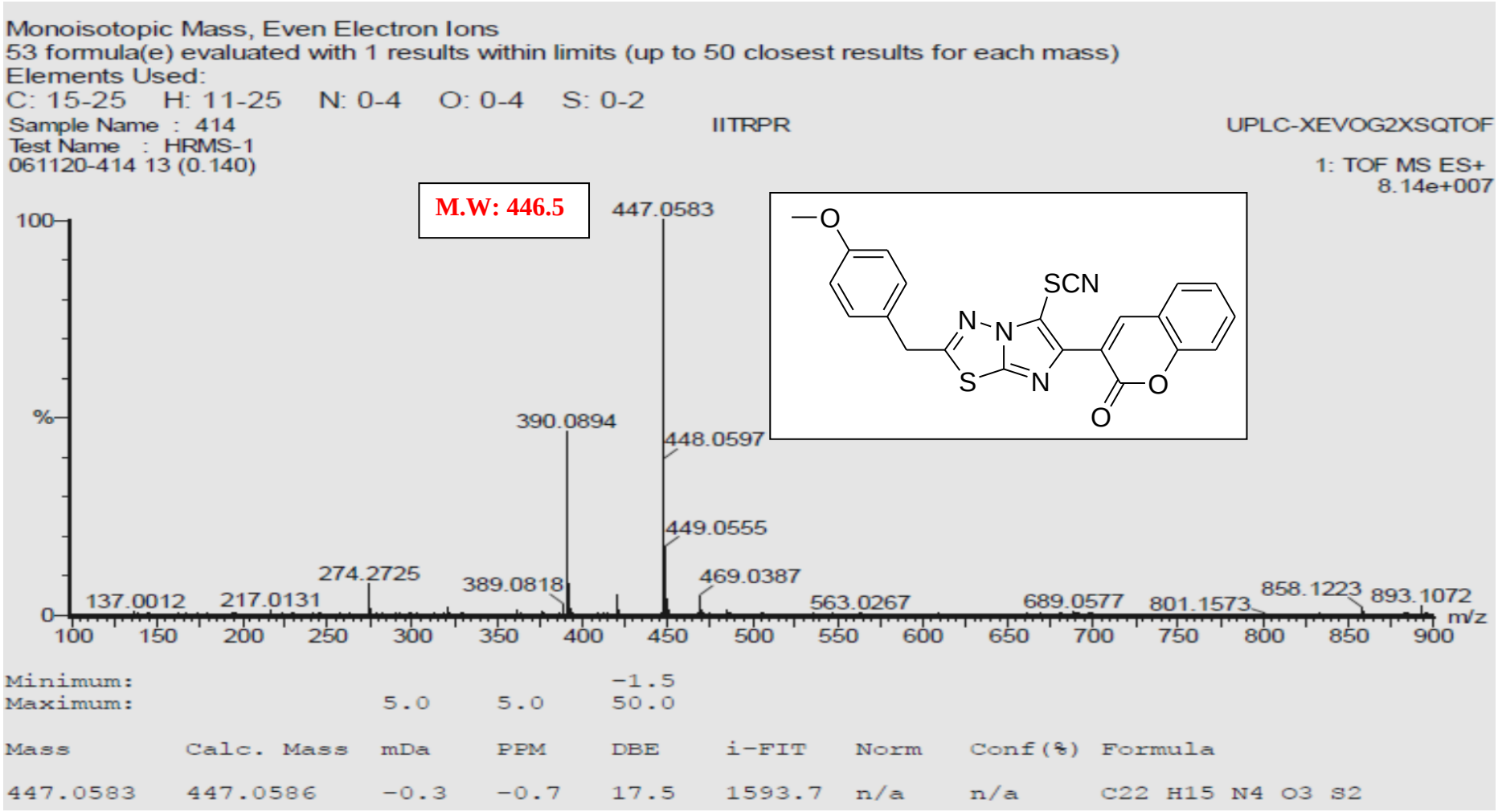

Minimum:				-1.5				
Maximum:		5.0	5.0	50.0				
Mass	Calc. Mass	mDa	PPM	DBE	i-FIT	Norm	Conf(%)	Formula
447.0583	447.0586	-0.3	-0.7	17.5	1593.7	n/a	n/a	C22 H15 N4 O3 S2

Fig. 4.4: HRMS spectrum of CH-43.

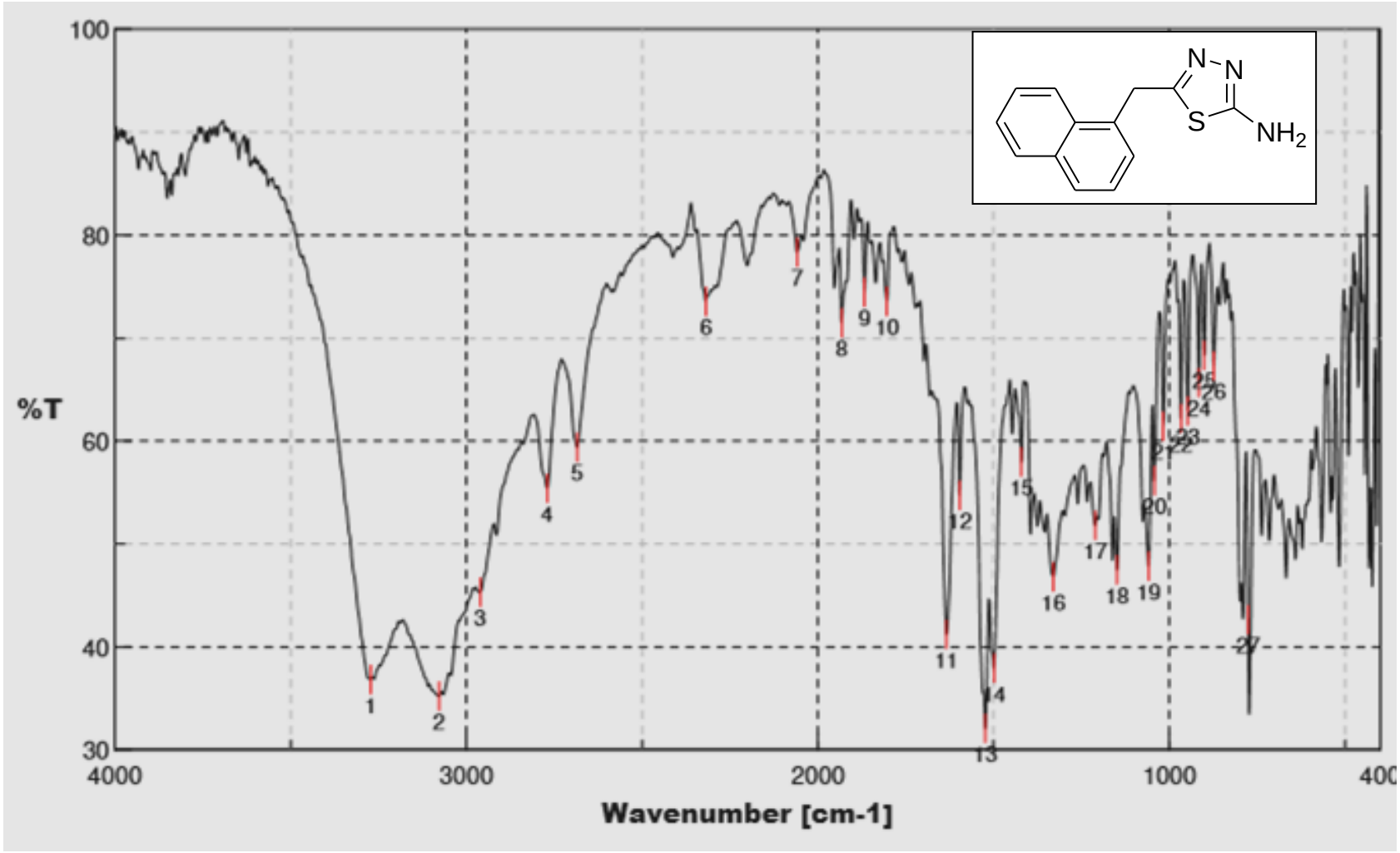

Fig. 4.5: FTIR spectrum of 5b.

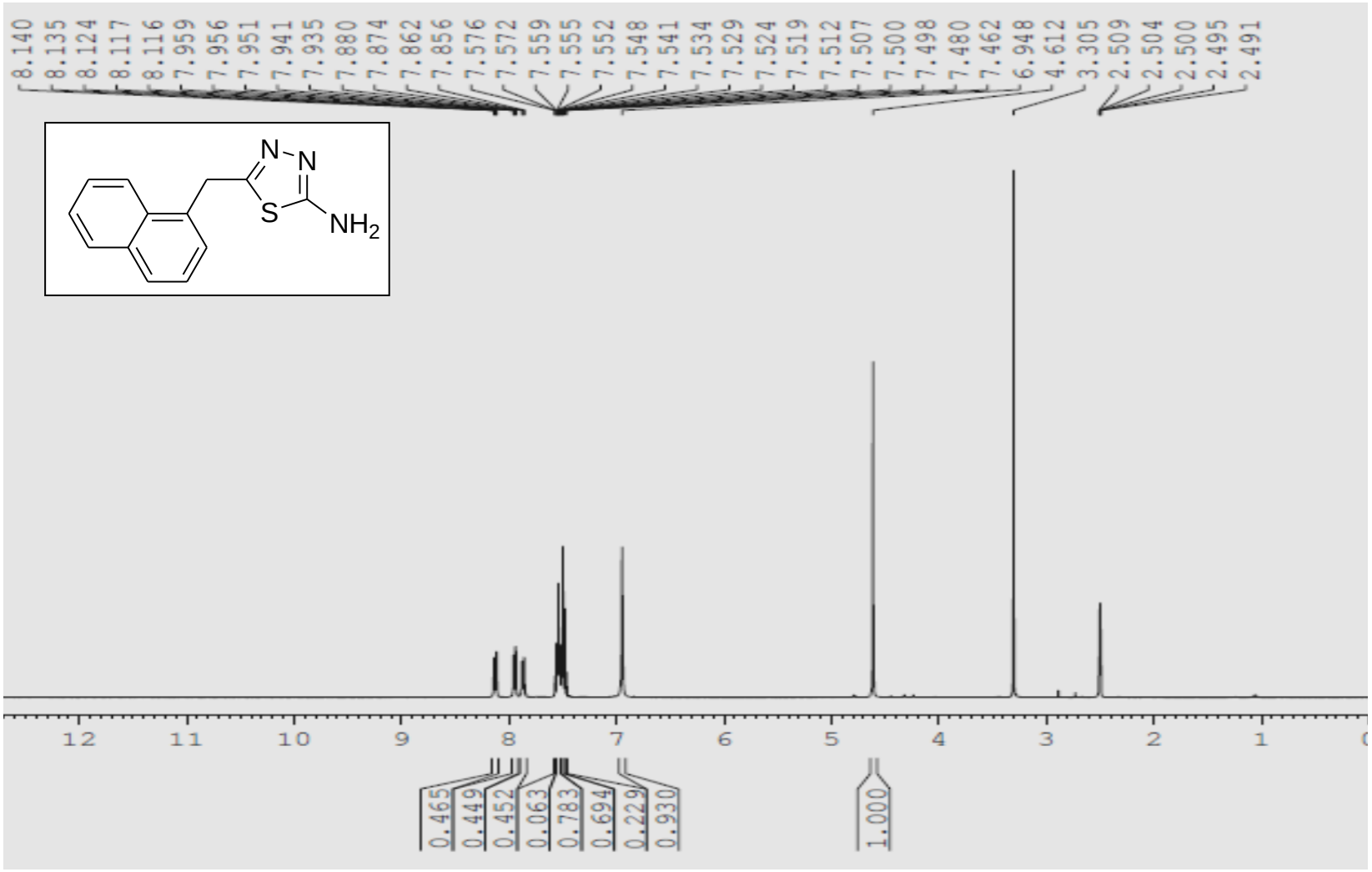

Fig. 4.6: ^{1}H-NMR spectrum of 5b.

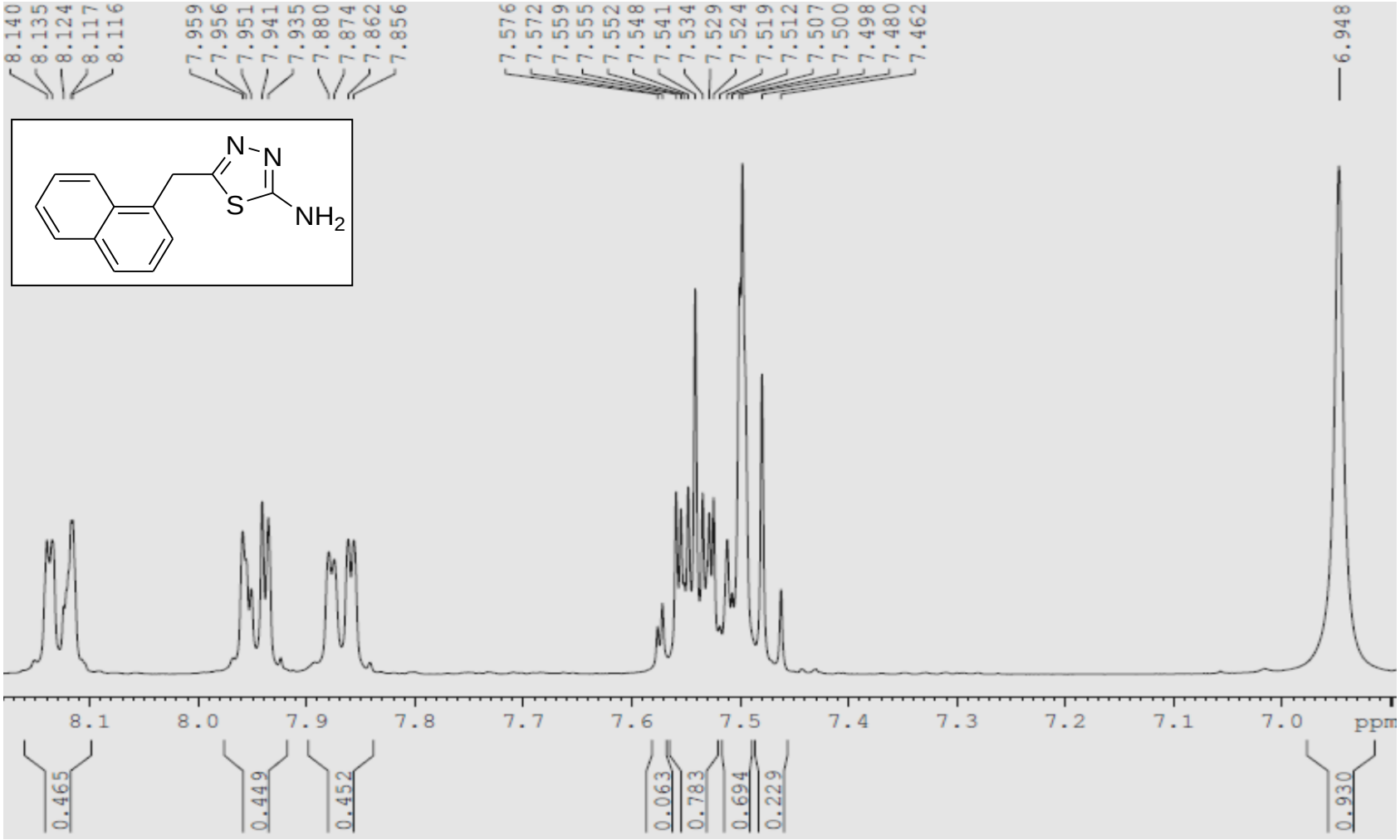

Fig. 4.7: ^{1}H-NMR spectrum of CH-50.

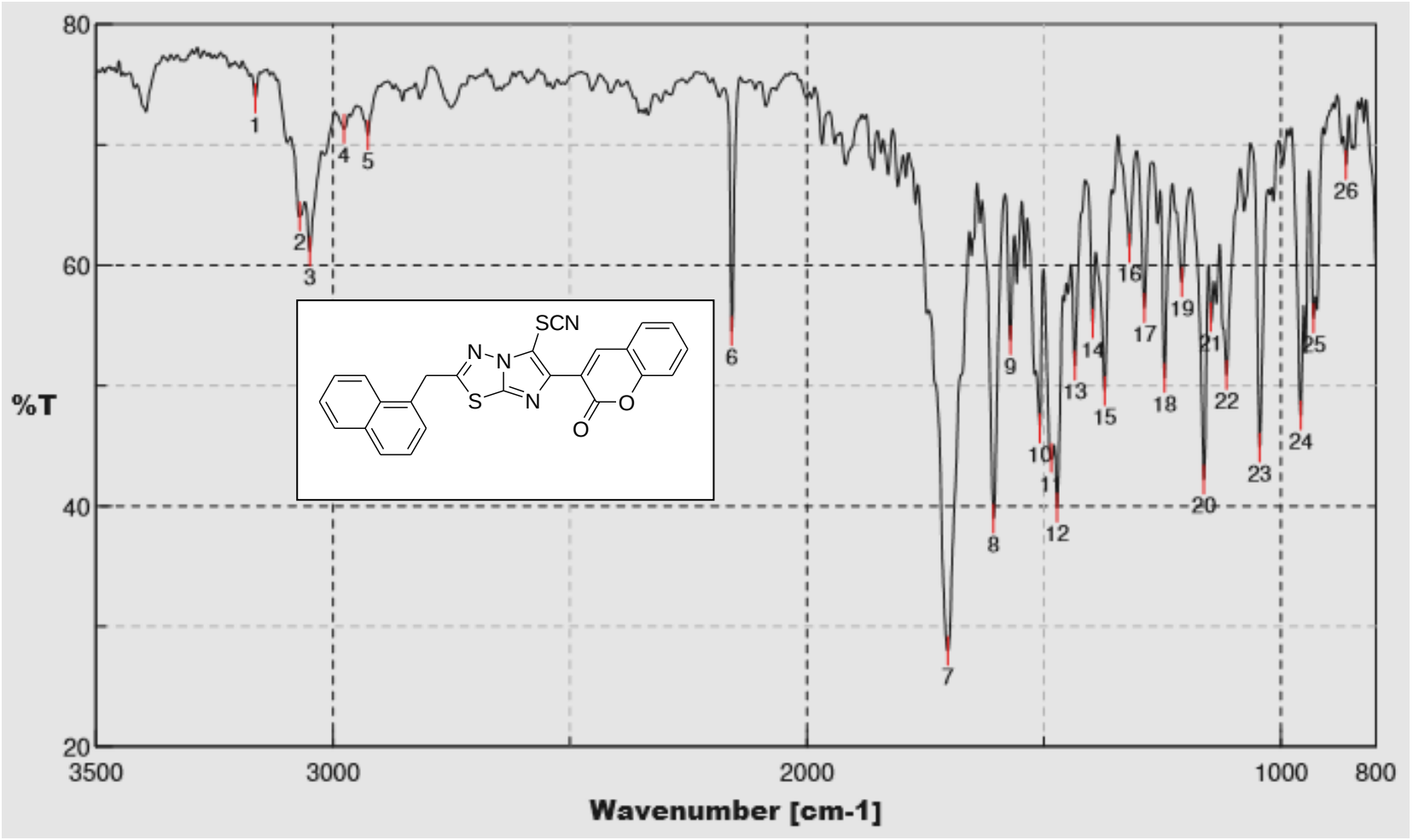

Fig. 4.8: FTIR spectrum of CH-50.

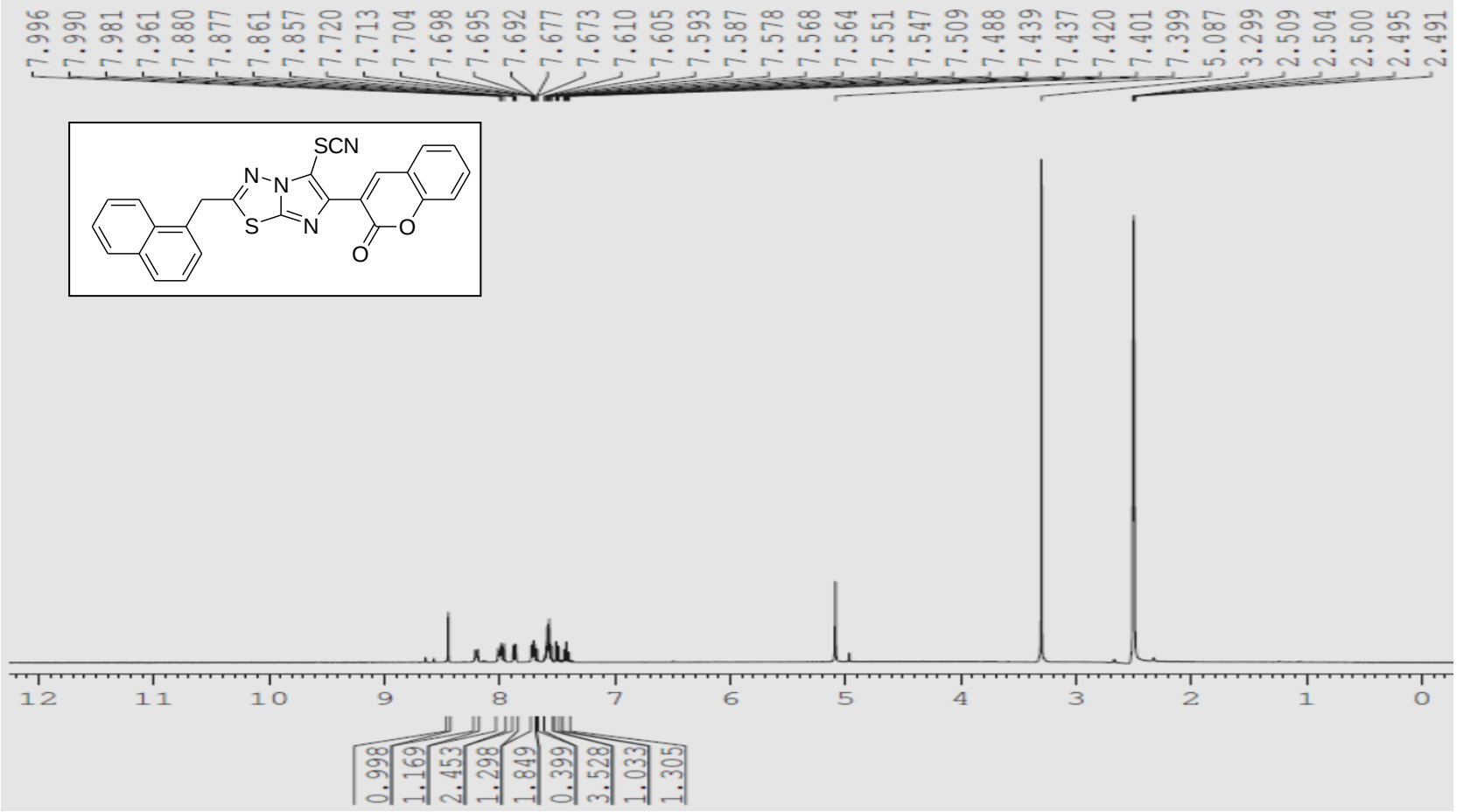

Fig. 4.9: ^{1}HNMR spectrum of CH-50.

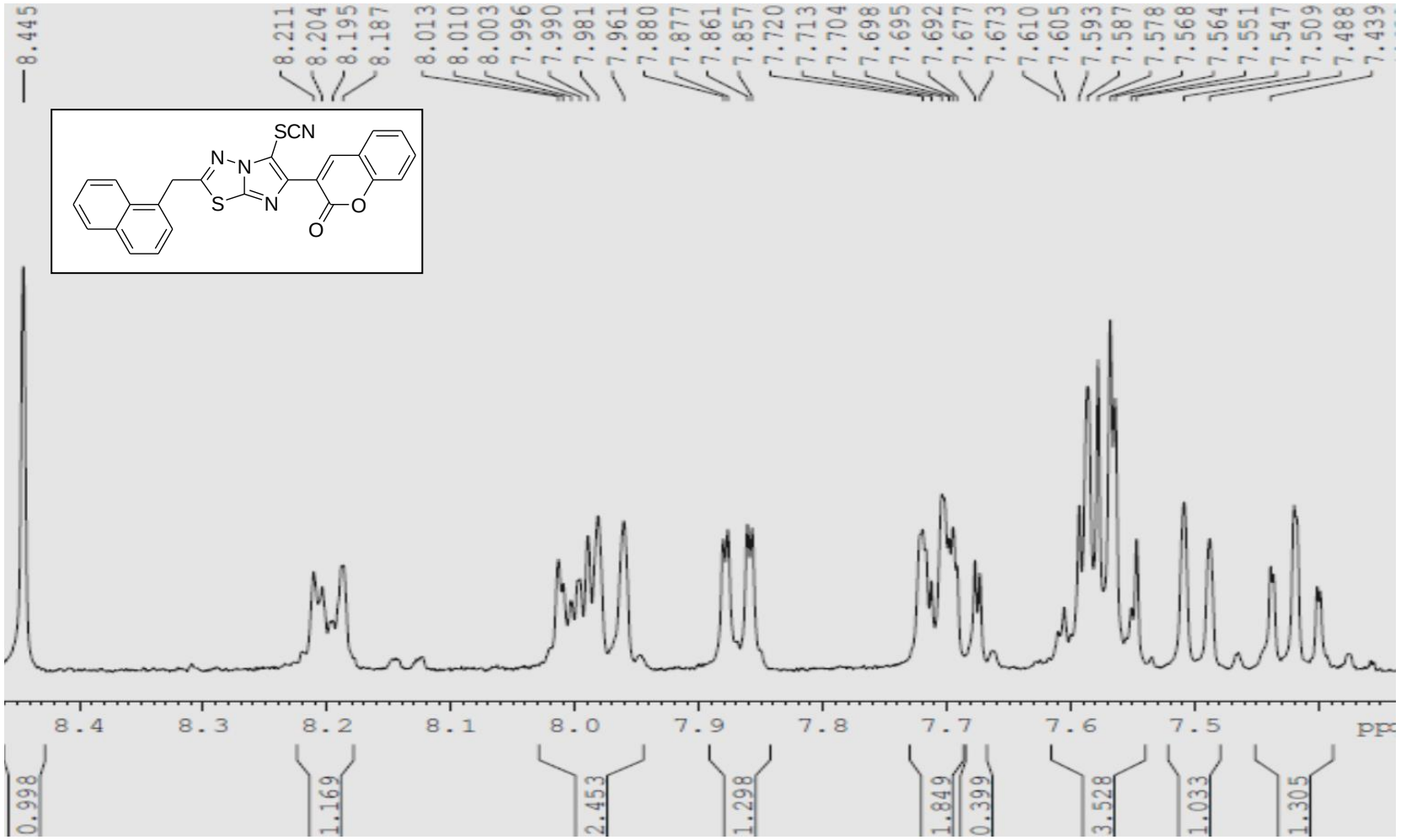

Fig. 4.10: ^{1}HNMR spectrum of CH-50.

Table-4.13: FTIR spectral data of 2,6-disubstitued-imidazothiadiazoles.

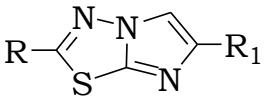

(CH 1-15)

Code	Transmittance peaks (cm^{-1})
CH 2	3068-3010 (-CH, Ar.), 2929-2847 (-CH, Al.), 1596 (-C=N), 1469 (-C=C, Ar.).
CH 8	3100-3067, 2898-2764 (-CH, Al.), 1702 (-C=O), 1563 (-C=N), 1463 (-C=C, Ar.).
CH 9	3066-3037 (-CH, Ar.), 2947-2919 (-CH, Al.), 1607 (-C=N), 1525 (-C=C, Ar.).
CH 10	3093-3027 (-CH, Ar.), 2944 (-CH, Al.), 1592 (-C=N), 1531 (-C=C, Ar.)
CH 11	3120-3065 (-CH, Ar.), 2931 (-CH, Al.), 1585 (-C=N), 1522 (-C=C, Ar.).
CH 14	3125-3019 (-CH, Ar.), 2927-2851(-CH, Al.), 1621 (-C=N), 1545 (-C=C, Ar.).
CH 13	3045-3008 (-CH, Ar.), 2959-2834 (-CH, Al.), 1612 (-C=N), 1543 (-C=C, Ar.).
CH 12	3096-3003 (-CH, Ar.), 2933 (-CH, Al.), 1599 (-C=N), 1504 (-C=C, Ar.).
CH 15	3068-3047 (-CH, Ar.), 2969-2945 (-CH, Al.), **1716 (-C=O),** 1513 (-C=N-), 1472 (-C=C, Ar.).

Table 4.14: FTIR spectral data of 5-bromo-imidazothiadiazoles.

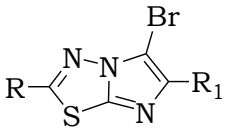

(CH 16-27)

Code	Transmittance peaks (cm^{-1})
CH 16	3058-3008 (-CH, Ar.), 2886-2704 (-CH, Al.), 1586 (-C=N), 1467 (-C=C, Ar.).
CH 17	3060-3038 (-CH, Ar.), 2942-2844 (-CH, Al.), 1567 (>C=N), 1460 (-C=C, Ar.)
CH 18	3058 (-CH, Ar.), 2876-2778 (-CH, Al.), 1565 (-C=N), 1450 (-C=C, Ar.)
CH 19	3065-3044 (-CH, Ar.), 2963-2886 (-CH, Al.), 1569 (-C=N), 1468 (-C=C, Ar.)
CH 20	3057 (-CH, Ar.), 2837-2789 (-CH, Al.), 1581 (-C=N), 1475 (-C=C, Ar.).
CH 21	3058 (-CH, Ar.), 2962-2938 (-CH, Al.), 1599 (-C=N), 1528 (-C=C, Ar.).
CH 22	3065 (-CH, Ar.), 2932-2891 (-CH, Al.), 1605 (-C=N), 1535 (-C=C, Ar.).
CH 23	3063-3010 (-CH, Ar.), 2936 (-CH, Al.), 1520 (-C=N), 1475 (-C=C, Ar.).
CH 25	3076-3001 (-CH, Ar.), 2941 (-CH, Al.), 1515 (-C=N), 1484 (-C=C, Ar.).
CH 24	3127-3010 (-CH, Ar.), 2960-2935 (-CH, Al.), 1611 (-C=N), 1543 (-C=C, Ar.).
CH 26	3107-3005 (-CH, Ar.), 2959-2829 (-CH, Ar.), 1625 (-C=N), 1491 (-C=C, Ar.).
CH 27	3105-3005 (-CH, Ar.), 2954-2831 (-CH, Ar.), 1629 (-C=N), 1521 (-C=C, Ar.).

Table 4.15: FTIR spectral data of 5-formyl-imidazothiadiazoles.

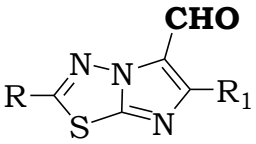

(CH 28-36)

Code	Transmittance peaks (cm^{-1})
CH 28	3053-3054 (-CH, Ar.), 2900-2736 (-CH, Al.), **1669 (-C=O),** 1601 (-C=N-), 1447 (-C=C, Ar.).
CH 30	3091-3015 (-CH, Ar.), 2929-2899 (-CH, Al.), **1675 (-C=O),** 1563 (-C=N), (-C=C, Ar.).
CH 31	3125-3009 (-CH, Ar.), 2899 (-CH, Al.), **1675 (-C=O),** 1599 (-C=N), (-C=C, Ar.).
CH 32	3151-3015 (-CH, Ar.), 2915-2892 (-CH, Al.), **1681 (-C=O),** 1598 (-C=N), 1515 (-C=C, Ar.).
CH 34	3125-3025 (-CH, Ar.), 2975-2891 (-CH, Al.), **1665 (-C=O),** 1609 (-C=N), 1509 (-C=C, Ar.).
CH 33	3057-3005 (-CH, Ar.), 2936-2836 (-CH, Al.), **1661 (-C=O),** 1607 (-C=N), 1524 (-C=C, Ar.).
CH 35	3066-3005 (-CH, Ar.), 2975-2850 (-CH, Al.), **1677 (-C=O),** 1600 (-C=N), (-C=C, Ar.).
CH-36	3106-3009 (-CH, Ar.), 2991-2897 (-CH, Al.), **1667 (-C=O), 1683 (-C=O),** 1591 (-C=N), 1501 (-C=C, Ar.).

Table 4.16: FTIR spectral data of 5-thiocyanato-imidazothiadiazoles.

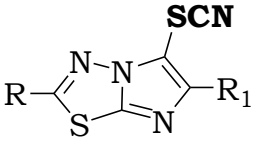

(CH 37-50)

Code	Transmittance peaks (cm-^{1})
CH 37	3063 (-CH, Ar.), 2758 (-CH, Al.), **2163 (-C≡N),** 1598 (-C=N**),** 1470 (-C=C, Ar.)
CH 38	3150-3067 (-CH, ar.), 2950-2768 (-CH, al.), **2168 (-C≡N),** 1601 (>C=N-), 1465 (-C=C, Ar.)
CH 39	3068-3032 (-CH, Ar.), 2856-2788 (-CH, Al.), **2171 (-C≡N),** 1602 (-C=N), 1445 (-C=C, Ar.)
CH 40	3060-3043 (-CH, Ar.), 2863-2776 (-CH, Al.), **2164 (-C≡N),** 1567 (-C=N), 1466 (-C=C, Ar.)
CH 41	3066-3029 (-CH, Ar.), 2889-2798 (-CH, Al.), **2164 (-C≡N),** 1588 (-C=N), 1480 (-C=C, Ar.)
CH 42	3050 (-CH, Ar.), 2880-2770 (-CH, Al.), **2165 (-C≡N),** 1610 (-C=N), 1486 (-C=C, Ar.)
CH 43	3061 (-CH, Ar.), 2960-2759 (-CH, Al.), **2159 (-C≡N), 1692 (-C=O),** 1606 (-C=N-), 1572 (-C=C, Ar.)
CH 44	3091-3048 (-CH, Ar.), 2935-2841 (-CH, Al.), **2156 (-C≡N),** 1598 (-C=N-), 1510 (-C=C, ar.).
CH 45	3101-3055 (-CH, Ar.), 2948-2839 (-CH, Al.), **2158 (-C≡N),** 1601 (-C=N-), 1508 (-C=C-, Ar.).
CH 46	3101-3005 (-CH, Ar.), 2905-2839 (-CH, Al.), **2166 (-C≡N),** 1599 (-C=N-), 1515 (-C=C<, Ar.)
CH 48	3046-3017 (-CH, Ar.), 2923-2868 (-CH, Al.), **2159 (-C≡N),** 1513 (-C=N-).
CH 47	3049-3005 (-CH, Ar.), 2945-2878 (-CH, Al.), **2161 (-C≡N),** 1598, (-C=N-), 1491 (-C=C, Ar.).
CH 49	3091-3048 (-CH, Ar.), 2935-2841 (-CH, Al.), **2156 (-C≡N),** 1598 (-C=N-), 1510 (-C=C, Ar.).
CH 50	3071-3049 (-CH, Ar.), 2977-2927 (-CH, Al.), **2158 (-C≡N), 1702 (-C=O),** 1606 (-C=N), 1483 (-C=C, Ar.)

Table 4.17: ^{1}H-NMR spectral data of 2,6-disubstituted-imidazothiadiazoles.

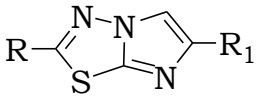

(CH 2-15)

Code	Chemical shift (400 MHz, DMSO-d_6) δ ppm)
CH 2	8.60 (s, 1H, Im-CH), 7.89-7.84 (m, 2H, Ar.), 7.32 (d, 2H, J=8.4, Ar.), 7.24 (t, 2H, J=16.4, Ar.), 6.94 (d, 2H, J=8.8, Ar.), 4.35 (s, 2H, -CH_2), 3.74 (s, 3H, -OCH_3).
CH 8	8.65 (s, 1H, Coum-CH), 8.55 (s, 1H, Im-H), 7.87-7.85 (m, 1H, Ar.), 7.62–7.58 (m, 1H, Ar.), 7.46 (d, 1H, J=8.4, Ar.), 7.39 – 7.35 (m,1H, Ar.), 7.34 (d, 2H, J=8.4, Ar.), 6.95 (d, 2H, J=8.4, Ar.), 4.38 (s, 2H, -CH_2), 3.74 (s, 3H, -OCH_3).
CH 9	8.61(s, 1H, Im-H), 8.14 (d, 1H, J=8.0, Ar.), 7.99-7.93 (m, 2H, Ar.), 7.81-7.79 (m, 2H, Ar.), 7.66 (d, 1H, J=6, Ar.), 7.60-7.52 (m, 3H, Ar.), 7.37 (t, 2H, J=15.2, Ar.), 7.26 (t, 1H, J= 15.0, Ar.), 4.93 (s, 2H, -CH_2).
CH 10	8.67 (s, 1H, Im-H), 8.10 (d, 1H, J=8.0, Ar.), 7.99-7.92 (m, 2H, Ar.), 7.83 (d, 2H, J= 8.4, Ar.), 7.65 (d, 1H, J= 6.4, Ar.), 7.60-7.51 (m, 3H, Ar.), 7.45 (d, 2H, J= 8.4, Ar.), 4.93 (s, 2H, -CH_2).
CH 11	8.67 (s, 1H, Im-H), 8.13 (d, 1H, J=8.0, Ar.), 7.99-7.92 (m, 2H, Ar.), 7.76 (d, 2H, J=8.2, Ar.), 7.65 (d, 1H, J=7.2, Ar.), 7.59-7.51 (m, 5H, Ar.), 4.93 (s, 2H, -CH_2).
CH 14	8.54 (s, 1H, Im-H), 8.13 (d, 1H, J=8.0, Ar.), 7.99-7.92 (m, 2H, Ar.), 7.70 (d, 2H, J=8.4, Ar.), 7.65 (d, 1H, J=8.0, Ar.), 7.89-7.52 (m, 3H, Ar.), 7.19 (d, 2H, J=8.0, Ar.), 4.92 (s, 2H, -CH_2), 2.29 (s, 3H, -CH_3).
CH 13	8.49 (s, 1H, Im-H), 8.12 (d, 1H, J=8.0 Hz), 7.97-7.92 (m, 2H, Ar.), 7.73 (d, 2H, J=8.4, Ar.), 7.63 (d, 1H, J=6.4, Ar.), 7.59-7.51 (m, 3H, Ar.), 6.93 (d, 2H, J=8.4, Ar.), 4.91 (s, 2H, -CH_2), 3.75 (s, 3H, -OCH_3).
CH 12	8.92 (s, 1H, Im-H), 8.25 (d, 2H, J=8.4, Ar.), 8.13 (d, 1H, J=8.0, Ar.), 8.07 (d, 2H, J=8.4, Ar.), 7.99-7.93 (m, 2H, Ar.), 7.66 (d, 1H, J=6.4, Ar.), 7.59-7.52 (m, 3H, Ar.), 4.95 (s, 2H, -CH_2).
CH 15	8.62 (s, 1H, Im-H), 8.55 (s, 1H, Coum-H), 8.13 (d, 1H, 8.0, Ar.), 7.99-7.94 (m, 2H, Ar.), 7.85-7.83 (m, 1H, Ar.), 7.67-7.65 (m, 1H, Ar), 7.61-7.52 (m, 4H, Ar.), 7.45 (d, 1H, J=8.4, Ar.), 7.38 (t, 1H, J=16, Ar.), 4.95 (s, 2H, -CH_2).

Table 4.18: ^{1}H-NMR spectral data of 5-bromo-imidazothiadiazoles.

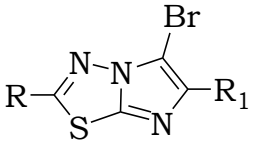

(CH 16-27)

Code	Chemical shift (400 MHz, DMSO-d_6) δ ppm)
CH 16	7.95 (d, 2H, J=7.2, Ar.), 7.70 (d, 1H, J=2.0, Ar.), 7.46 (t, 2H, J=15.2, Ar.), 7.42-7.33 (m, 2H, Ar.), 7.13 (d, 2H, J=8.8, Ar.), 6.95 (d, 1H, J=8.8, Ar.), 4.44 (s, 2H, -CH_2), 3.84 (s, 3H, -OCH_3)
CH 17	7.98– 7.94 (m, 2H, Ar.), 7.33-7.27 (m, 4H, Ar.), 6.94 (d, 2H, J=8.8, Ar.), 4.39 (s, 2H, -CH_2), 3.74 (s, 3H, -OCH_3).
CH 18	7.90 (d, 2H, J=8.4, Ar.), 7.67 (d, 2H, J=8.4, Ar.), 7.34 (d, 2H, J=8.8, Ar.), 6.95 (d, 2H, J=8.8, Ar.), 4.40 (s, 2H, -CH_2), 3.74 (s, 3H, -OCH_3).
CH 19	7.90 (d, 2H, J=8.4, Ar.), 7.67 (d, 2H, J=8.4, Ar.), 7.34 (d, 2H, J=8.4, Ar.), 6.95 (d, 2H, J=8.4, Ar.), 4.40 (s, 2H, -CH_2), 3.74 (s, 3H, -OCH_3).
CH 20	7.86 (d, 2H, J=8, Ar.), 7.36 (t, 4H, J=16.4, Ar.), 6.96 (d, 2H, J=8.4, Ar.), 4.47 (s, 2H, -CH_2, Ar.), 3.75 (s, 3H, -OCH_3).
CH 21	8.14 (d, 1H, J=8.0, Ar.), 7.97-7.90 (m, 4H, Ar.), 7.67 (d, 1H, J=6.4, Ar.), 7.60-7.52 (m, 3H, Ar.), 7.46 (t, 2H, J=15.4, Ar.), 7.36-7.32 (m, 1H, Ar.), 4.97 (s, 2H, -CH_2).
CH 22	8.13 (d, 1H, J=8.0, Ar.), 8.00-7.92 (m, 4H, Ar.), 7.66 (d, 1H, J=7.2, Ar.), 7.61-7.50 (m, 5H, Ar.), 4.98 (s, 2H, -CH_2).
CH 23	8.15 (d, 2H, J=8, Ar.), 8.01-7.99 (m, 1H, Ar.), 7.97 (d, 1H, J=8.8, Ar.), 7.89 (d, 2H, J=8.8, Ar.), 7.67 (d, 3H, J=8.8, Ar.), 7.62-7.53 (m, 3H, Ar.), 4.99 (s, 2H, -CH_2).
CH 25	8.13 (d, 1H, J=8.4, Ar.), 7.98-7.94 (m, 2H, Ar.), 7.81 (d, 2H, J=8.0, Ar.), 7.66-7.52 (m, 4H, Ar.), 7.26 (d, 2H, J=8.0, Ar.), 4.97 (s, 2H, -CH_2), 2.32 (s, 3H, -CH_3).
CH 26	8.33 (d, 2H, J=8.8, Ar.), 8.22 (d, 2H, J=9.2, Ar.), 8.15 (d, 1H, J=8.4, Ar.), 8.00-7.94 (m, 2H, Ar.), 7.67 (d, 1H, J=7.2, Ar.), 7.62-7.53 (m, 3H, Ar.), 5.00 (s, 2H, -CH_2).
CH 27	8.29 (s, 1H, Coum-H), 8.14 (d, 1H, J=8.4, Ar.), 8.00-7.95 (m, 2H, Ar.), 7.83-7.80 (m, 1H, Ar.), 7.68-7.65 (m, 2H, Ar.), 7.63-7.53 (m, 3H, Ar.), 7.46 (d, 1H, J=8.4, Ar.), 7.38-7.34 (m, 1H, Ar.), 4.96 (s, 2H, -CH_2-).

Table 4.19: ^{1}H-NMR spectral data of substituted imidazothiadiazole-5 carbaldehydes.

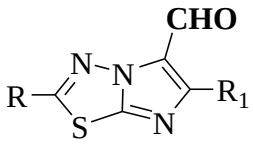

(CH 28-36)

Code	Chemical shift (400 MHz, DMSO-d_6) δ ppm)
CH 28	9.99 (s, 1H, -CHO), 7.95 – 7.93 (m, 2H, Ar.), 7.56 – 7.50 (m, 3H, Ar.), 7.38 (d, 2H, J=8.4, Ar.), 6.99 (d, 2H, J=8.4, Ar.), 4.48 (s, 2H, $-CH_2$), 3.77 (s, 3H, $-OCH_3$).
CH 30	10.05 (s, 1H, -CHO), 8.06 (m, 1H, Ar.), 7.94-7.90 (m, 2H, Ar.), 7.82-7.70 (m, 2H, Ar.), 7.58-7.45 (m, 7H, Ar.), 4.91 (s, 2H, $-CH_2$).
CH 31	10.09 (s, 1H, -CHO), 8.03 (d, 1H, J=8.4, Ar.), 7.96-7.90 (m, 2H, Ar.), 7.83 (d, 2H, J=8.4, Ar.), 7.58-7.51 (m, 4H, Ar.), 7.49 (d, 2H, J=8.8, Ar.), 4.91 (s, 2H, $-CH_2$).
CH 32	10.07 (s, 1H, -CHO), 8.05 (d, 1H, J=8.4, Ar.), 7.93 (m, 2H, Ar.), 7.75 (d, 2H, J=8.4, Ar.), 7.62 (d, 2H, J=8.4, Ar.), 7.58-7.49 (m, 4H, Ar.), 4.90 (s, 2H, $-CH_2$).
CH 33	10.00 (s, 1H, -CHO), 7.94 (d, 2H, J=8.0, Ar.), 7.88-7.84 (m, 1H, Ar.), 7.75 (d, 2H, J=8.4, Ar.), 7.51-7.42 (m, 4H, Ar.), 6.97 (d, 2H, J=8.8, Ar.), 4.85 (s, 2H, $-CH_2$), 3.78 (s, 3H, $-OCH_3$).
CH 34	9.94 (s, 1H, -CHO), 8.15 (d, 1H, J=8.4, Ar.), 8.00-7.94 (m, 2H, Ar.), 7.80 (d, 2H, J=6.8, Ar.), 7.61-7.52 (m, 3H, Ar.), 7.43 (d, 2H, J=8.4, Ar.), 5.02 (s, 2H, $-CH_2$), 2.35 (s, 3H, $-CH_3$).
CH 35	10.07 (s, 1H, -CHO), 8.34 (d, 2H, J=9.2, Ar.), 8.25 (d, 2H, J=9.2, Ar.), 8.15 (d, 1H, J=8.0, Ar.), 8.00-7.95 (m, 2H, Ar.), 7.69 (d, 1H, J=6.4, Ar.), 7.61-7.53 (m, 3H, Ar.), 5.05 (s, 2H, $-CH_2$-).
CH 36	10.01 (s, 1H, -CHO), 8.49 (s, 1H, Coum-H), 8.13 (d, 1H, J=8.0, Ar.), 8.01-7.95 (m, 2H, Ar.), 7.87 (d, 1H, J=8.0, Ar.), 7.71-7.67 (m, 2H, Ar.), 7.62-7.53 (m, 3H, Ar.), 7.48 (d, 1H, J=7.6, Ar.), 7.38 (t, 1H, J=15.4, Ar.), 5.04 (s, 2H, $-CH_2$, Ar.).

Table 4.20: ^{1}H-NMR spectral data of 5-thiocyanato-imidazothiadiazoles.

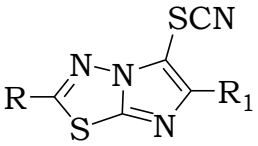

(CH 37-50)

Code	Chemical shift (400 MHz, DMSO-d_6) δ ppm)
CH 37	7.97 – 7.93 (m, 2H, Ar.), 7.54 –7.51 (m, 2H, Ar.), 7.47–7.42 (m, 2H, Ar.), 7.37 (d, 2H, J=8.8, Ar.), 6.96 (d, 2H, J=8.8, Ar.), 4.48 (s, 2H, -CH_2), 3.75 (s, 3H, -OCH_3).
CH 38	8.02–7.94 (m, 2H, Ar.), 7.41–7.28 (m, 4H, Ar.), 6.97–6.93 (m, 2H, Ar.), 4.48 (s, 2H, -CH_2), 3.75 (s, 3H, -OCH_3).
CH 39	7.92 (d, 2H, J=8.4, Ar.), 7.75 (d, 2H, J=8.4, Ar.), 7.37 (d, 2H, J=8.4, Ar.), 6.96 (d, 2H, J=8.4, Ar.), 4.48 (s, 2H, -CH_2), 3.75 (s, 3H, -OCH_3).
CH 40	7.92 (d, 2H, J=8.4, Ar.), 7.75 (d, 2H, J=8.4, Ar.), 7.37 (d, 2H, J=8.8, Ar.), 6.96 (d, 2H, J=8.4, Ar.), 4.48 (s, 2H, -CH_2), 3.75 (s, 3H, -OCH_3).
CH 41	7.92 (2H, d, J=8.8, Ar.), 7.36 (2H, d, J=8.8, Ar.), 7.10 (2H, d, J=8.8, Ar.), 6.96 (2H, d, J=8.8, Ar.), 4.47 (s, 2H, -CH_2), 3.82 (s, 3H, OCH_3), 3.75 (s, 3H, -OCH_3).
CH 42	7.84 (d, 2H, J=8, Ar.), 7.35 (d, 2H, J=8.8, Ar.), 7.27 (d, 2H, J=7.6, Ar.), 6.95 (d, 2H, J=8.4, Ar.), 4.40 (s, 2H, -CH_2), 3.74 (s, 3H, -OCH_3), 2.33 (s, 3H, -CH_3).
CH 43	8.45 (s, 1H, Ar.), 7.88-7.85 (m, 1H, Ar.), 7.71-7.66 (m, 1H, Ar.) 7.50 (d, 1H, J=8.4, Ar.), 7.43-7.39 (m, 1H, Ar.), 7.38 (d, 2H, J=8.4, Ar.), 6.96 (d, 2H, J=8.4, Ar.), 4.50 (s, 2H, -CH_2), 3.75 (s, 3H, -OCH_3).
CH 44	8.19 (d, 1H, J=8, Ar.), 8.00-7.91 (m, 4H, Ar.), 7.70 (d, 1H, J=6.0, Ar.), 7.61-7.50 (m, 5H, Ar.), 7.46-7.42 (m, 1H, Ar.), 5.06 (s, 2H, -CH_2-).
CH 45	8.16 (d, 1H, J=8.0, Ar.), 8.00-7.92 (m, 4H, Ar.), 7.70 (d, 1H, 8.0, Ar.), 7.60-7.53 (m, 5H, Ar.), 5.06 (s, 2H, -CH_2).
CH 46	8.07 (d, 1H, J=8.0, Ar.), 7.95-7.90 (m, 2H, Ar.), 7.83 (d, 2H, J=8.4 Ar.), 7.64-7.49 (m, 6H, Ar.), 4.87 (s, 2H, -CH_2).
CH 48	8.04 (d, 1H, J=8.4, Ar.), 7.95-7.92 (m, 2H, Ar.), 7.83 (d, 2H, J=8.0, Ar.), 7.61-7.50 (m, 4H, Ar.), 7.33 (d, 2H, J=8.0 Ar.), 4.89 (s, 2H, -CH_2), 2.17 (s, 3H, -CH_3).
CH 47	7.97 (d, 1H, J=8.4, Ar.), 7.88-7.80 (m, 4H, Ar.), 7.53-7.42 (m, 4H, Ar.), 6.96 (d, 2H, J=8.8, Ar.), 4.81 (s, 2H, -CH_2), 3.80 (s, 3H, -OCH_3).
CH 50	8.45 (s, 1H, Ar.), 8.21-8.19 (m, 1H, Ar.), 8.01-7.96 (m, 2H, Ar.), 7.88-7.86 (m, 1H, Ar.), 7.72-7.69 (m, 2H, Ar.), 7.59-7.55 (m, 3H, Ar.), 7.51 (d, 1H, J=8.4, Ar.), 7.42 (t, 1H, J=16, Ar.), 5.09 (s, 2H, -CH_2-).

Table 4.21: ^{13}C NMR spectral data of substituted imidazo thiadiazoles.

Code	Chemical shift (400 MHz, DMSO-d_6) δ ppm)
CH 2	165.91, 160.77, 159.13, 145.45, 144.40, 130.84, 128.29, 127.07, 126.99, 116.17, 115.17, 114.78, 110.62, 55.60, 36.58.
CH 8	159.13, 136.37, 131.23, 130.37, 128.25, 127.21, 124.81, 119.87, 116.60, 115.11, 114.77, 55.54, 37.67
CH 16	166.40, 155.34, 134.03, 133.33, 130.40, 129.92, 129.14, 128.36, 126.73, 113.47, 111.24, 56.79, 36.01.
CH 17	167.23, 163.38, 160.94, 159.20, 144.93, 140.64, 130.89, 128.81, 128.73, 116.20, 115.98, 114.83, 92.67, 55.61, 36.63
CH 18	167.49, 159.21, 140.32, 132.57, 132.14, 130.90, 128.57, 128.13, 121.47, 114.84, 55.62, 36.64.
CH 19	167.48, 159.20, 145.13, 140.32, 132.53, 132.13, 130.90, 128.56, 128.13, 121.46, 114.84, 93.24, 55.62, 36.65.
CH 20	168.37, 159.13, 150.18, 148.12, 139.05, 130.90, 129.87, 127.87, 114.88, 110.07, 55.63, 36.56, 21.43.
CH 28	177.70, 168.73, 159.22, 154.56, 151.25, 130.90, 130.10, 129.42, 129.27, 128.22, 123.90, 114.87, 55.63, 36.50.
CH 37	165.85, 159.13, 145.40, 134.42, 130.85, 129.17, 128.32, 127.76, 125.11, 114.79, 110.78, 55.61, 36.59.
CH 38	168.66, 164.12, 161.67, 159.25, 149.51, 148.57, 130.91, 130.18, 130.09, 129.24, 128.16, 116.48, 116.26, 114.89, 111.03, 101.33, 55.63, 36.57.
CH 39	168.86, 159.25, 149.10, 148.67, 132.35, 131.92, 130.92, 129.83, 128.13, 122.87, 114.89, 110.91, 101.86, 55.63, 36.58.
CH 40	168.86, 166.18, 159.25, 159.14, 149.10, 144.14, 132.35, 132.11, 130.92, 130.85, 129.84, 127.09, 114.89, 114.79, 111.25, 110.91, 55.63, 36.58.
CH 41	168.14, 160.30, 159.23, 150.07, 148.06, 130.90, 129.36, 128.23, 125.11, 114.88, 114.76, 110.01, 100.00, 55.80, 55.63, 36.55.
CH 42	166.97, 159.20, 144.75, 141.60, 137.72, 130.88, 130.55, 129.68, 128.20, 126.66, 114.83, 92.33, 55.61, 36.63, 21.37.
CH 43	169.27, 159.38, 159.28, 153.84, 148.58, 144.17, 133.39, 130.93, 129.75, 128.07, 125.57, 120.32, 119.34, 116.75, 114.89, 110.18, 55.64, 36.60.

Table 4.22: HRMS data of substituted imidazothiadiazoles.

Code	Molecular formula & ionization mode.	Cal. Mass	Obs. Mass
CH 2	$[C_{18}H_{15}N_3OS]+$	339.3867	340.0926
CH 8	$[C_{21}H_{15}N_3O_3S]+$	389.4271	390.0899
CH 16	$[C_{18}H_{14}BrN_3OS]+$	400.2923	402.0069
CH 17	$[C_{18}H_{13}BrFN_3OS]+$	418.2827	419.9996
CH 18	$[C_{18}H_{13}BrClN_3OS]+$	434.7373	435.9708
CH 19	$[C_{18}H_{13}Br_2N_3OS]+$	479.1883	479.9204
CH 20	$[C_{19}H_{16}BrN_3OS]+$	414.3188	416.0247
CH 28	$[C_{19}H_{15}N_3O_2S]+$	349.4063	350.0955
CH 37	$[C_{19}H_{14}N_4OS_2]+$	377.0536	379.0675
CH 38	$[C_{19}H_{13}FN_4OS_2]+$	396.4611	397.0591
CH 39	$[C_{19}H_{13}ClN_4OS_2]+$	412.9157	413.0299
CH 40	$[C_{19}H_{13}BrN_4OS_2]-$	457.3667	456.9610
CH 41	$[C_{20}H_{16}N_4O_2S_2]+$	408.4966.	409.0798
CH 42	$[C_{20}H_{16}N_4OS_2]+$	392.4972	393.0864
CH 43	$[C_{22}H_{14}N_4O_3S_2]+$	446.5016.	447.0583

+: Positive mode, -: Negative mode.

Biology:

2-(4-Methoxybenzyl)-6-aryl-imidazo[2,1-b][1,3,4]thiadiazoles

Cytotoxicity:

The cytotoxic (anti-proliferative) property was evaluated against murine and human cancer cell lines. Melphalan and levamisole were used as reference standard. The IC_{50} values (in µM) were summarized in table 4.23.

Table 4.23: Anti-proliferative effects of CH 1-8, 16-20, 28, 29 and 37-43.

Compound	IC_{50}^{*} (µM)		
	CEM	**HeLa**	**L1210**
CH 1 (5a)	> 250	> 250	> 250
CH 2 (5b)	> 250	> 250	> 250
CH 3 (5c)	> 250	> 250	> 250
CH 4 (5d)	> 250	> 250	> 250
CH 5 (5e)	> 250	> 250	> 250
CH 6 (5f)	NT	NT	NT
CH 7 (5g)	> 250	> 250	> 250
CH 8 (5h)	5.0 ± 3.3	70 ± 4	90 ± 24
CH 16 (6a)	> 250	> 250	= 250
CH 17 (6b)	> 250	> 250	= 250
CH 18 (6c)	46 ± 9	> 250	2020 ± 68
CH 19 (6d)	39 ± 5	46 ± 9	> 250
CH-20 (6e)	13 ± 7	18 ± 0	33 ± 10
CH 37 (7a)	8.8 ± 2.4	17 ± 0	42 ± 19
CH 38 (7b)	28 ± 2	23 ± 0	59 ± 29
CH 39 (7c)	61 ± 6	21 ± 5	87 ± 20
CH 40 (7d)	59 ± 14	20 ± 3	100 ± 15
CH-41 (7e)	11 ± 7	16 ± 5	65 ± 41
CH-42 (7f)	84 ± 31	63 ± 13	58 ± 40
CH-43 (7g)	**0.79 ± 0.35**	**0.78 ± 0.13**	**1.6 ± 0.2**
CH-28 (8a)	> 250	96 ± 24	> 250
CH-29 (8b)	**0.94 ± 0.12**	**1.3 ± 0.2**	**1.1 ± 0.2**
Melphalan	1.4±0.4	NT	2.13±0.02
Levamisole	>250	>250	206

[*] The values are the mean ± SEM, (n = 3)

CC_{50} and selective cytotoxicity:

It determines the potential of a compound to selectively kill the cancer cells and sparing the non-cancerous cells. The comparative study was performed on leukemia Jurkat and CEM cells and non-cancerous human fibroblast Hs27 cells. Results obtained were summarized in table 4.24.

Table 4.24: Selectivity index of CH 43 (7g) and CH (8b) towards cancer and non-cancer cells.

Compound	Cell line	CC_{50}	SCI
CH-43 (7g)	CEM	4.73±0.22	6.65
	Jurkat	2.36±0.10	13.33
	Hs27	31.45±0.74	
CH-29 (8b)	CEM	3.62±0.26	0.65
	Jurkat	1.65±0.19	1.43
	Hs27	2.36±0.03	

Data are mean ± standard deviation S.D. (n=3).

Annexin-V-FITC assay, mitochondrial depolarization and caspase 3 activation:

The ability to cause cell death by apoptosis is studied by Annexin-V-FITC assay. Results summarized in fig. 4.11 A-C suggest high degree of phosphatidylserine externalization in CH-43 (7g) treated cells indicating apoptosis. No mitochondrial depolarization was observed in CH-43 (7g) treated cells however, caspase-3 activation was observed by CH-43 (7g) treated cells suggesting blockage of DNA synthesis and cytokinesis.

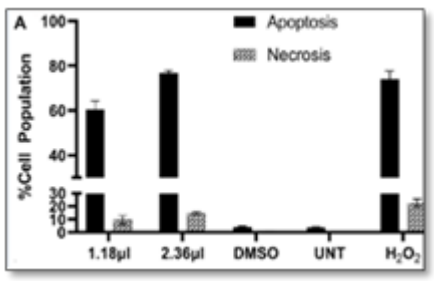

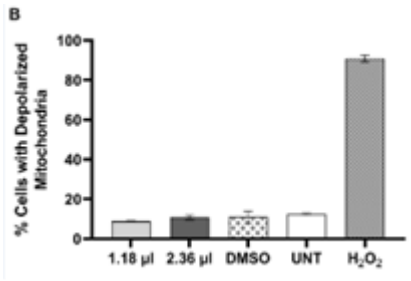

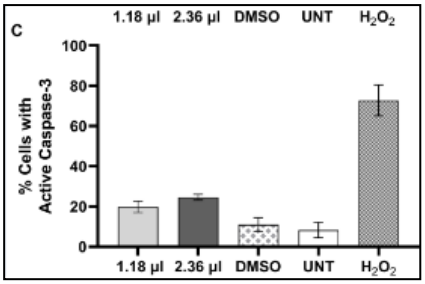

Fig. 4.11: A. Phosphatidylserine externalization observed in CH-43 (7g) treated cells indicating apoptosis. B. No mitochondrial depolarization observed in CH-43 (7g) treated cells. C. Caspase-3 activation by CH-43 (7g) treated cells.

Cell cycle analysis

Blocking of DNA synthesis and cytokinesis was observed in CH-43 (7g) treated cells. Results were summarized in fig 4.12 A-D.

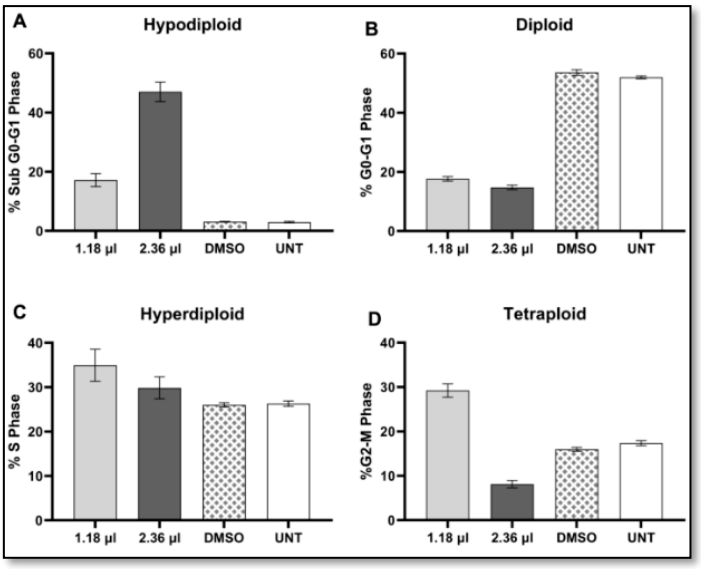

Fig. 4.12: Jurkat cells treated with compound 7g. A. Increase in the sub-G0-G1 phase subpopulation, B. Decrease in G0-G1 phase cell population. C. Increase S phase cell population, D. The increase in the G2-M phase cell population after treatment with CC_{50} of test compounds.

***In-silico* study (Molecular docking):**

Molecular docking performed on TGF β type I receptor kinase (PDB ID: 1RW8) taking potent derivatives based on *in-vitro* cytotoxicity data. The nature and strength of interaction between the receptor and test compounds were summarized in table 4.25 and fig. 4.13a-c.

Table 4.25: Nature and types of interaction between TGF β type I receptor kinase and the test molecule CH-43 (7g) and CH-29 (8b).

Molecule	XPGlide score (kcal/mol)	Molecular interactions towards TGF β type I receptor kinase domain				
		Hydrogen bond	Hydrophobic interactions			Other
CH-43 (7g)	-7.012	S280	A230	K232	L260	--
		Y282	V219	A350	L340	
			I211	--	--	
CH-29 (8b)	-4.864	K232	V219	K232	L278	D290 (Electrostatic)
		S280	A230	L260	L340	
		G212	K213	--	--	
[a] Co-ligand	-8.784	H283	L260	L278	Y249	H283 (Halogen)
		Y282	V219	K232	A350	
		D351	A230	L340	--	
Melphalan[a]	-5.291	I211	A230	K232	V219	L278 (Halogen)
		E284	L340	--	--	
		S280	--	--	--	

[a] Reference molecule used in Glide docking.

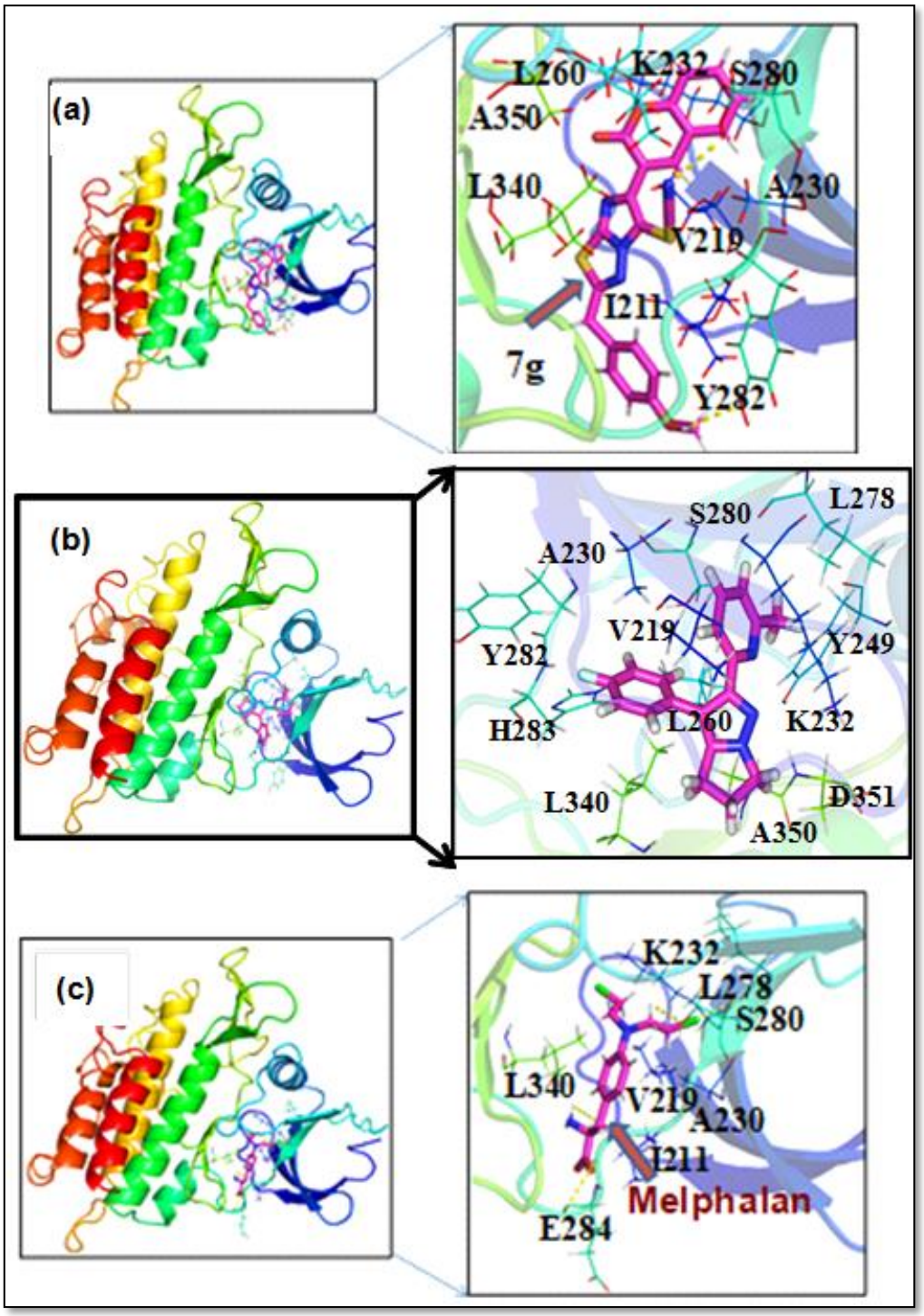

Fig. 4.13: Interactions between TGF beta kinase I and (a) CH-43 /7g (b) Ligand and (c) Melphalan.

5-(Naphthalen-1-yl)- methyl-6-aryl-imidazothiadiazoles:

Cytotoxicity/Anti-proliferative effect:

The synthesized molecules screened against murine and human cancer cell lines. Melphalan and levamisole were used as reference standard. The IC_{50} values (in µM) were summarized in table 4.26.

Table 4.26: Anti-proliferative effects on L1210, CEM and HeLa cells.

Compound	IC_{50}^{*} (µM)		
	L1210	**CEM**	**HeLa**
CH-9 (5a)	116 ± 6	138 ± 13	87 ± 2
CH-10 (5b)	94 ± 49	108 ± 33	78 ± 13
CH-11 (5c)	> 250	111 ± 20	≥ 250
CH-14 (5d)	> 250	> 250	> 250
CH-13 (5e)	131 ± 20	111 ± 7	120 ± 36
CH-12 (5f)	116 ± 15	121 ± 6	117 ± 52
CH-15 (5g)	2.1 ± 0.8**	80 ± 5**	4.0 ± 3.1**
CH-21 (6a)	≥ 250	136 ± 84	> 250
CH-22 (6b)	120 ± 13	82 ± 12	79 ± 14
CH-23 (6c)	94 ± 14	71 ± 0	66 ± 18
CH-25 (6d)	113 ± 21	77 ± 2	81 ± 8
CH-24 (6e)	70 ± 10	51 ± 5	75 ± 2
CH-26 (6f)	71 ± 54	64 ± 17	85 ± 4
CH-27 (6g)	3.4 ± 1.5	54 ± 6	4.5 ± 0.8
CH-30 (7a)	9.7 ± 0.1	7.9 ± 1.6	8.2 ± 0.8
CH-31 (7b)	5.0 ± 0.5	5.4 ± 0.3	4.6 ± 0.4
CH-32 (7c)	4.8 ± 0.3	4.9 ± 0.4	4.4 ± 0.5
CH-34 (7d)	127 ± 4	113 ± 3	86 ± 14
CH-33 (7e)	4.9 ± 0.5	5.0 ± 0.0	7.7 ± 0.2
CH-35 (7f)	107 ± 21	95 ± 11	74 ± 12
CH-36 (7g)	NT	NT	NT
CH-44 (8a)	57 ± 39	44 ± 34	13 ± 8
CH-45 (8b)	66 ± 0	40 ± 21	13 ± 6
CH-46 (8c)	79 ± 31	51 ± 0	27 ± 6

CH-48 (8d)	82 ± 11	42 ± 20	25 ± 5
CH-47 (8e)	62 ± 35	53 ± 1	9.8 ± 1.9
CH-49 (8f)	126 ± 4	103 ± 5	70 ± 5
CH-50 (8g)	16 ± 3	70 ± 10	28 ± 22
Melphalan	2.13±0.02	1.4±0.4	NT
Levamisole	206	>250	>250

***In-silico* study:**

In-silico study were performed on the biologically active molecule from the series. The ADME and Lipinski Ro5 parameters were calculated using FAF-Drug4 web-server. The docking and molecular dynamics simulation study was performed on EGFR; pdbID: 1M17 (residues: 684-951) using Desmond's Schrodinger tool. Results summarized in table 4.27, 4.28 and fig. 4.14-4.18.

Table 4.27: Pharmacological properties of virtual screening and rationally designed compounds.

Compounds	Binding Affinity (kcal/mol)	MW	logP	tPSA	Rotatable Bonds	Flexibility	HBD	HBA	Lipinski Violation	Solubility (mg/L)	Solubility ForecastIndex	Oral Bioavailability VEBER	Fsp^3
CH-9 (5a)	-9.0	341.43	5.72	58.43	3	0.1	0	3	1	1046.22	Reduced Solubility	Good	0.05
CH-10 (5b)	-8.9	375.87	6.34	58.43	3	0.1	0	3	1	629.48	Reduced Solubility	Good	0.05
CH-11 (5c)	-8.8	420.32	6.41	58.43	3	0.1	0	3	1	511.31	Reduced Solubility	Good	0.05
CH-14 (5d)	-9.1	355.46	6.08	58.43	3	0.1	0	3	1	819.85	Reduced Solubility	Good	0.09
CH-13 (5e)	-8.8	371.45	5.69	67.66	4	0.13	0	4	1	1069.18	Reduced Solubility	Good	0.09
CH-12 (5f)	-9.1	386.43	5.54	104.25	4	0.13	0	6	1	1093.8	Reduced Solubility	Good	0.05
CH-15 (5g)	**-10.3**	409.46	5.71	88.64	3	0.09	0	5	1	812.93	Reduced Solubility	Good	0.04
CH-21 (6a)	-9.2	420.32	6.74	58.43	3	0.1	0	3	1	415.33	Reduced Solubility	Good	0.05

CH-22 (6b)	-8.9	454.77	7.37	58.43	3	0.1	0	3	1	244.05	Reduced Solubility	Good	0.05
CH-23 (6c)	-8.6	499.22	7.43	58.43	3	0.1	0	3	1	195.83	Reduced Solubility	Good	0.05
CH-25 (6d)	-9.0	434.35	7.11	58.43	3	0.1	0	3	1	321.02	Reduced Solubility	Good	0.09
CH-24 (6e)	-8.8	450.35	6.71	67.66	4	0.13	0	4	1	418	Reduced Solubility	Good	0.09
CH-26 (6f)	-9.1	465.32	6.57	104.25	4	0.13	0	6	1	422.06	Reduced Solubility	Good	0.05
CH-27 (6g)	-10.3	488.36	6.74	88.64	3	0.09	0	5	1	310.69	Reduced Solubility	Good	0.04
CH-30 (7a)	-9.0	369.44	5.51	75.5	4	0.13	0	4	1	1184.03	Reduced Solubility	Good	0.05
CH-31 (7b)	-8.9	403.88	6.14	75.5	4	0.13	0	4	1	703	Reduced Solubility	Good	0.05
CH-32 (7c)	-8.7	448.34	6.2	75.5	4	0.13	0	4	1	570.42	Reduced Solubility	Good	0.05
CH-34 (7d)	-9.0	383.47	5.88	75.5	4	0.13	0	4	1	916.81	Reduced Solubility	Good	0.09
CH-33 (7e)	-8.8	399.46	5.48	84.73	5	0.16	0	5	1	1198.47	Reduced Solubility	Good	0.09

CH-35 (7f)	-9.2	414.44	5.34	121.32	5	0.15	0	7	1	1217.01	Reduced Solubility	Good	0.05
CH-36 (7g)	-	-	-	-	-	-	-	-	-	-	-	-	-
CH-44 (8a)	-9.1	398.5	6.61	107.52	4	0.13	0	4	1	533.37	Reduced Solubility	Good	0.05
CH-45 (8b)	-9.7	432.95	7.24	107.52	4	0.13	0	4	1	314.71	Reduced Solubility	Good	0.05
CH-46 (8c)	-8.7	477.4	7.3	107.52	4	0.13	0	4	1	253.66	Reduced Solubility	Good	0.05
CH-48 (8d)	-9.4	412.53	6.98	107.52	4	0.13	0	4	1	411.89	Reduced Solubility	Good	0.09
CH-47 (8e)	-9.0	428.53	6.58	116.75	5	0.16	0	5	1	536.91	Reduced Solubility	Good	0.09
CH-49 (8f)	-8.5	443.5	6.44	153.34	5	0.15	0	7	1	543.88	Reduced Solubility	Good	0.05
CH-50 (8g)	-9.7	466.53	6.61	137.73	4	0.11	0	6	1	401.48	Reduced Solubility	Good	0.04
Melphalan	-5.8	305.2	-0.69	71.01	8	0.53	3	4	0	125389.7	Good Solubility	Good	0.46
Levamisole	-6.0	204.29	1.84	40.9	1	0.06	0	2	0	19086.31	Good Solubility	Good	0.36

Co-ligand	-7.2	393.44	3.19	74.73	10	0.36	1	7	0	8316.35	Reduced Solubility	Good	0.27

HBD: hydrogen bond donor; HBA: hydrogen bond acceptor; tPSA: topological polar surface area; LogP: indicator of hydrophobicity.

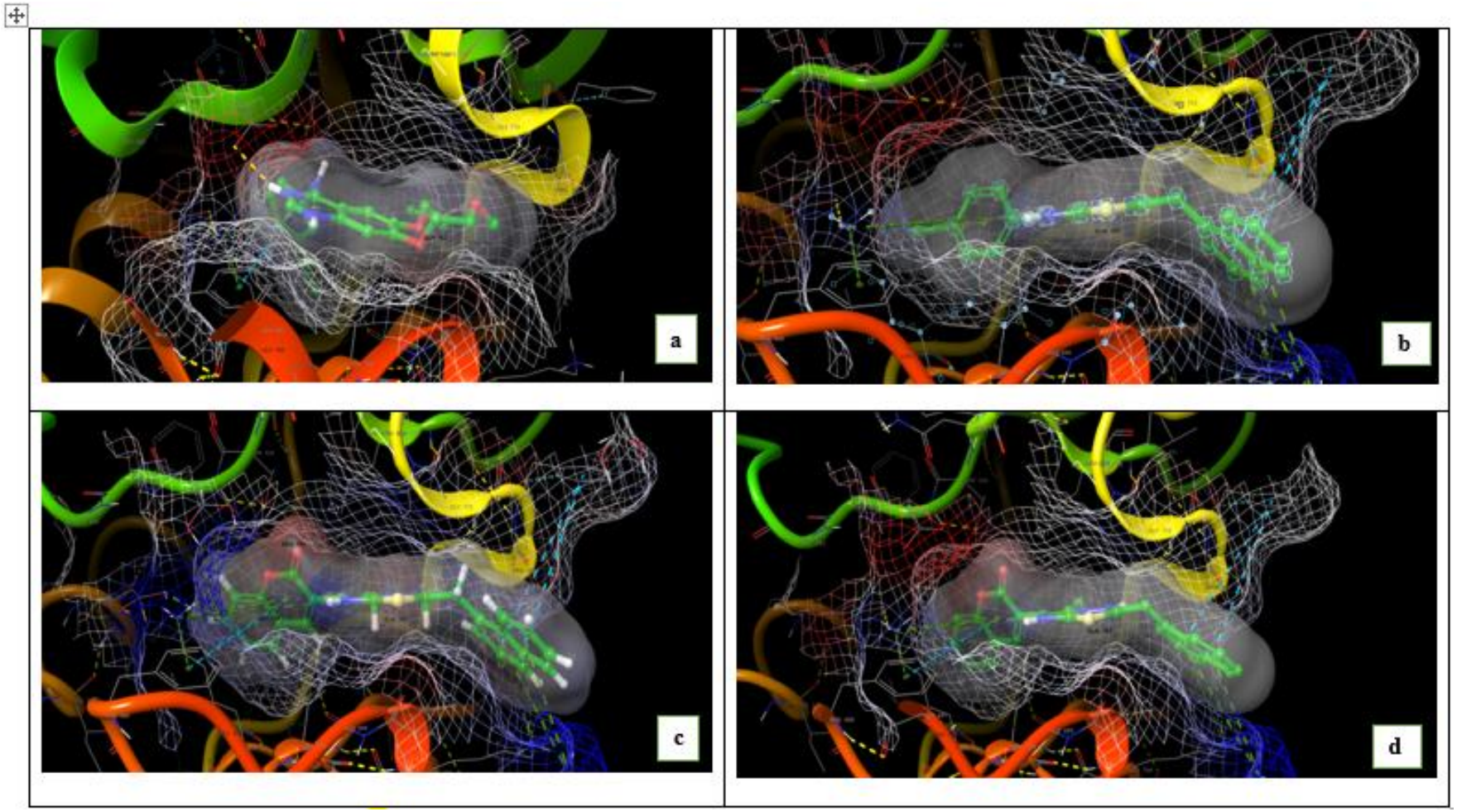

Fig. 4.14: 3D interactions between the receptor 1m17 and co-ligand (a), CH-11/5c (b), CH-15/5g (c), and CH-27/6g (d).

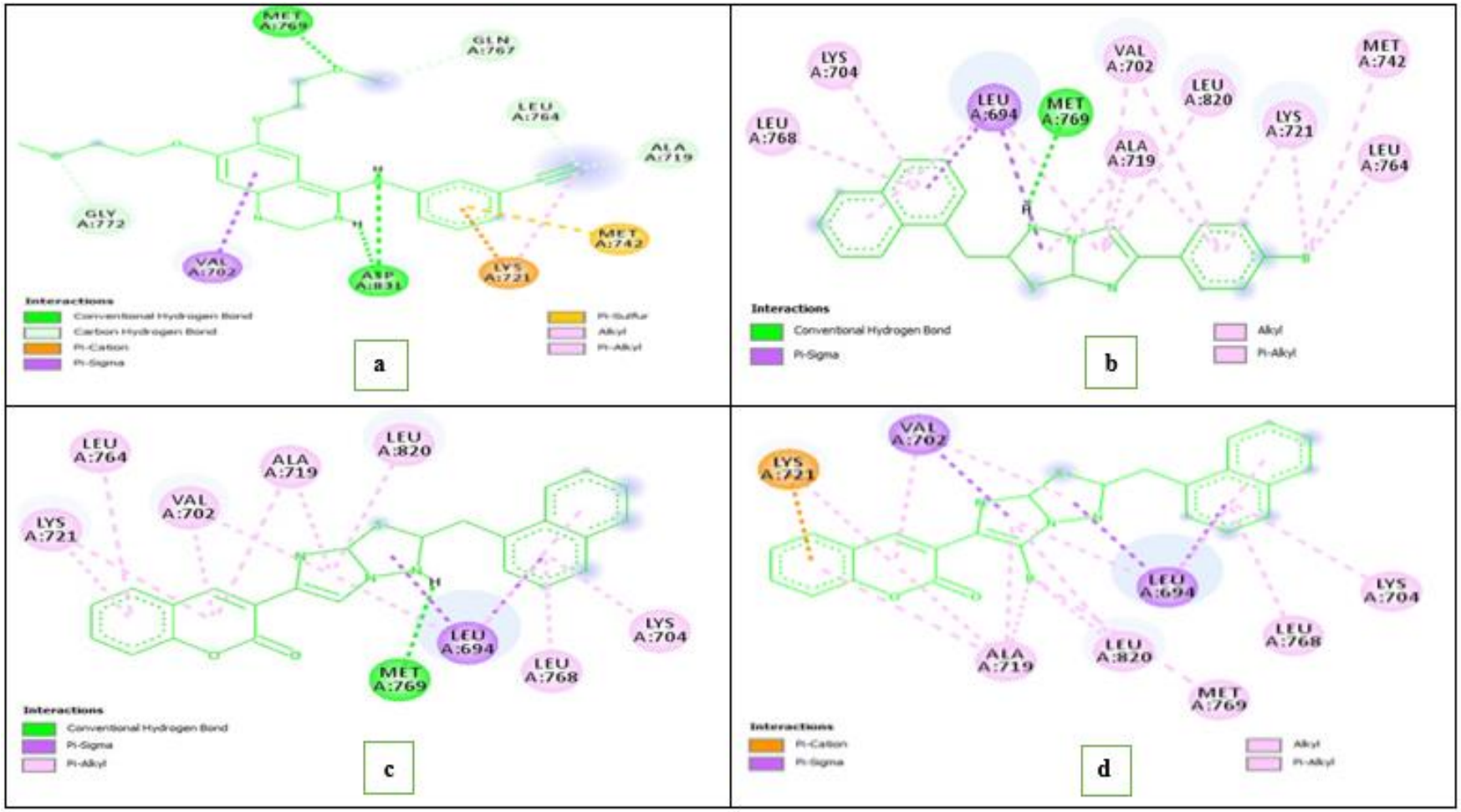

Fig. 4.15: 2D interactions between 1m17 receptor and co-ligand (a), CH-11/5c (b), CH-15/5g (c), and CH-27/6g (d).

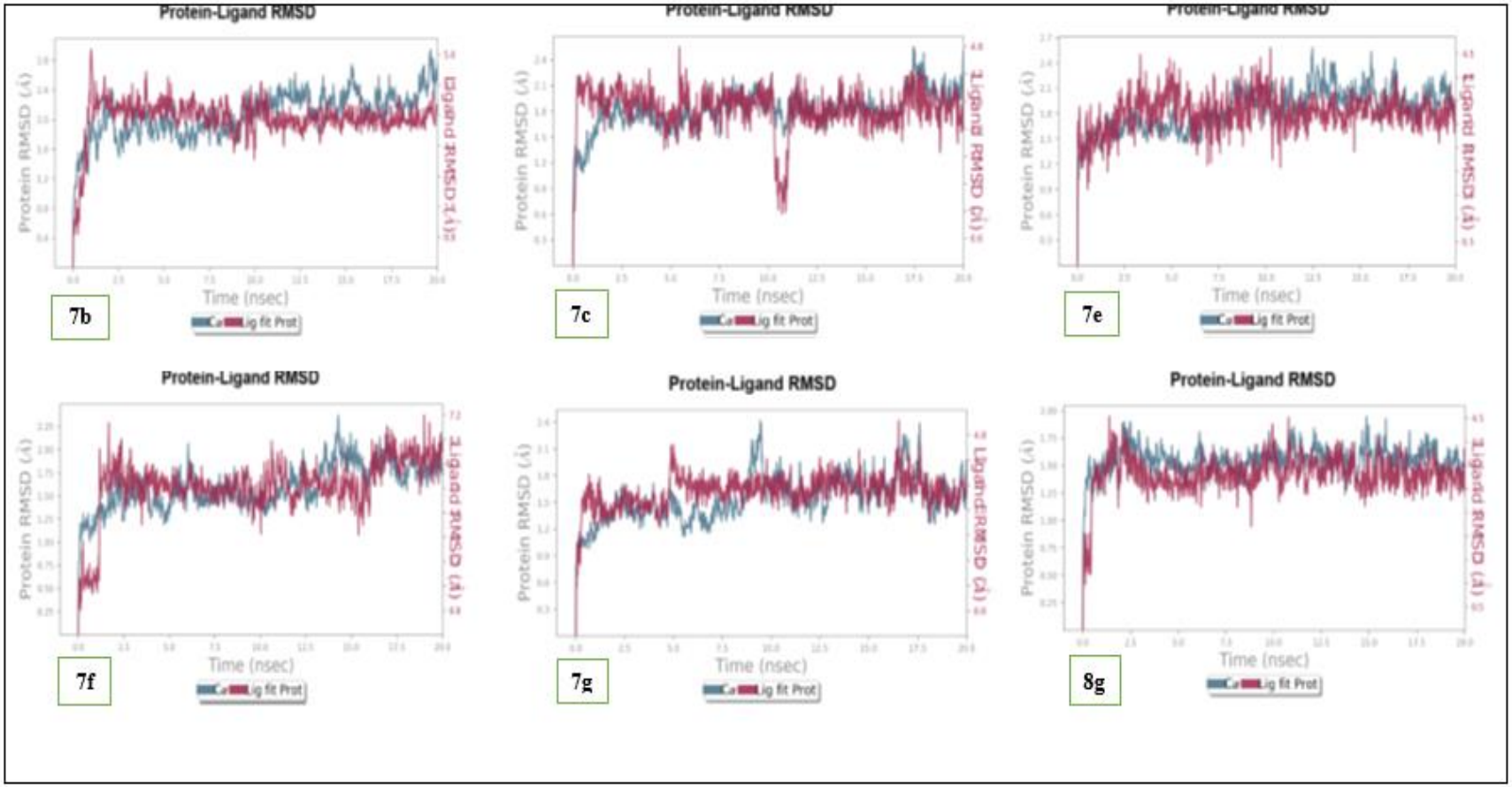

Fig. 4.16: RMSD plot obtained molecular dynamics simulation. Blue represents protein backbone while the ligands are in red for CH 31 (7b), CH 32 (7c), CH 33 (7e), CH 35 (7f), CH 36 (7g) and CH 50 (8g).

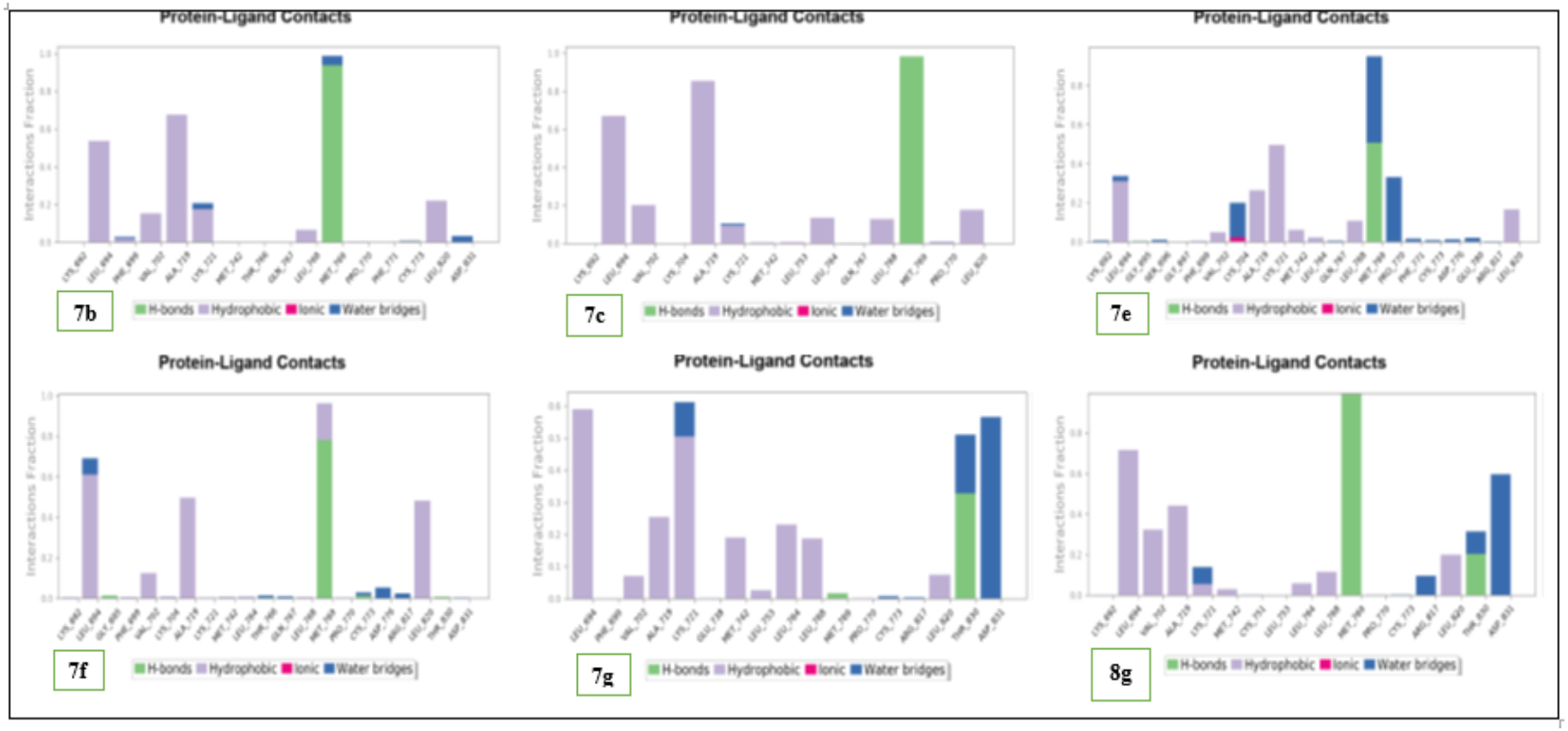

Fig.4.17: Protein ligand contact for the compounds CH 31 (7b), CH 32 (7c), CH 33 (7e), CH 35 (7f), CH 36 (7g) and CH 50 (8g).

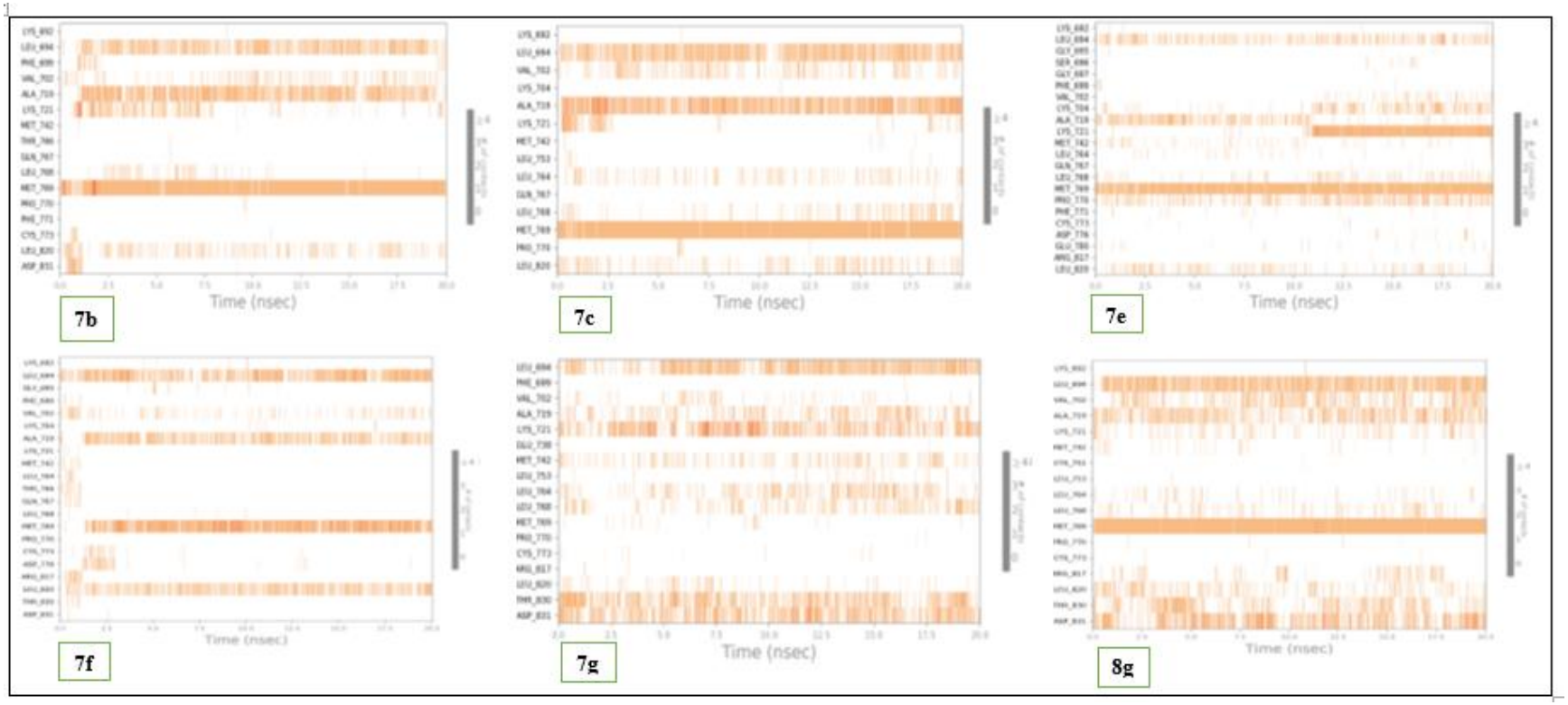

Fig. 4.18: Molecular dynamics simulation time line (in ns) for CH 31 (7b), CH 32 (7c), CH 33 (7e), CH 35 (7f), CH 36 (7g) and CH 50 (8g).

Table 4.28: Nature of interaction with 1m17 EGFR receptor.

Compound			
	Hydrogen bond	**Hydrophobic Interactions**	**Others**
CH-9 (5a)	Met769	Leu694, Ala719, Leu820, Met769	Leu694, Cys773
CH-10 (5b)	Met769	Leu694, Val702, Ala719, Leu820, Met769	Leu694, Cys773
CH-11 (5c)	Met769	Leu694, Ala719, Met742, Leu820	Met769
CH-14 (5d)	--	Leu694, Ala719, Met742, Leu820	Leu694, Met769
CH-13 (5e)	Met769	Leu694, Ala719, Lys721, Met742, Leu820	Leu694, Lys704, Pro770, Glu780
CH-12 (5f)	--	Leu694, Phe699, Val702, Ala719, Met742, Leu820	Gln767, Met769
CH-15 (5g)	Met769	Leu694, Val702, Ala719, Leu820	Leu694
CH-21 (6a)	--	Leu694, Ala719, Lys721, Leu768, Leu820	--
CH-22 (6b)	--	Leu694, Val702, Leu768, Leu820	--
CH-23 (6c)	--	Leu694, Phe699, Val702, Leu820	Leu694, Met769
CH-25 (6d)	Met769	Leu694, Ala719, Met742, Leu820	Met769, Pro770
CH-24 (6e)	--	Leu694, Val702, Leu768	Lys721, Glu738, Asp831
CH-26 (6f)	Lys721	Leu694, Phe699, Val702, Leu820, Lys721	Lys721, Thr766, Gln767, Met769, Asp831
CH-27 (6g)	Met769	Leu694, Val702, Ala719, Phe771, His781, Leu820	Leu694
CH-30 (7a)	Met769	Leu694, Val702, Ala719, Leu820	--
CH-31 (7b)	Met769	Leu694, Val702, Ala719, Lys721, Leu820	Lys721, Met769

CH-32 (7c)	Met769	Leu694, Val702, Ala719, Leu764, Leu768, Leu820	--
CH-34 (7d)	Met769, Lsy721	Leu694, Val702, Ala719, Leu820	Lys721, Met769, Asp831
CH-33 (7e)	Met769	Leu694, Ala719, Lys721, Met742, Leu820	Lys704, Met769, Pro770
CH-35 (7f)	Met769	Val702, Ala719, Met769, Leu820	Leu694
CH-36 (7g)	Thr830	Leu694, Ala719, Lys721, Met742, Leu768	Lys721, Thr830, Asp831
CH-44 (8a)	Met769, Cys773	Leu694, Phe699, Leu820	Cys773, Asp776
CH-45 (8b)	Met769	Leu694, Ala719, Lys721, Met742, Leu820	Cys773, Asp776
CH-46 (8c)	--	Leu694, Lys721, Leu768	Ser696, Met769
CH-48 (8d)	Met769, Cys773	Leu694, Ala719, Lys721, Met742, Leu820	Pro770, Cys773, Asp776
CH-47 (8e)	Met769	Leu694, Ala719, Lys721, Met742	Met769, Lys704, Pro770, Asp776
CH-49 (8f)	Met769	Leu694, Phe699, Leu820	Leu694, Met769, sp776
CH-50 (8g)	Met769, Thr830	Val702, Ala719, Leu768, Leu820	Arg817, Thr830, Asp831

5. DISCUSSION

Chemistry:

A total of, 50 imidazothiadiazole derivatives CH 1-50 were synthesized as per scheme 3.21 – 3.2.3 and procedure 1-6. Physical constant values (M.P) of intermediates 5a & b and, the final derivatives CH 1-50 were determined using Thiel's' apparatus in liquid paraffin (heavy). All values were reported uncorrected. Progress of reactions was confirmed by TLC on pre-coated silica gel plates. The structural confirmation done by FTIR, NMR (^{1}H and ^{13}C) and HRMS data. Table 3.2 - 4.22 represent the physicochemical properties, structure and spectral data while fig. 4.1-4.10 represent the spectra of synthesized molecules. The different α-bromoacetophenones were compared for their M.P with literature.

2-amino-5-aralkyl-1,3,4-thiadiazoles

Aminothiadiazoles 5a & 5b were prepared adopting scheme 3.2.2 and procedure 2. The FTIR transmittance peaks at 3272 in 5b represent -NH_2 while the peaks between 3078 cm^{-1} represent aromatic -CH stretching. The aliphatic -CH stretching observed between 2960-2770 cm^{-1}. Peaks at 1634 and 1498 cm^{-1} represent -C=N, -C=C (Ar.) stretching respectively. In ^{1}H-NMR spectra, peaks in the range of 8.96 -7.48, 6.95 and 4.61 δ ppm represent Ar. -CH, -NH_2 and -CH_2- protons respectively.

2-aralkyl-6-aryl-imidazo-[2,1-*b*][1,3,4]-thiadiazoles

Series of 2,6-disubstituted-imidazothiadiazoles CH 1-15 were prepared following scheme 3.2.3 and procedure 3. The FTIR spectra find peaks in the range of 3125-3008 and 2969-2764 cm^{-1} for aromatic and aliphatic -CH respectively. The imine (-C=N) and -C=C (Ar.) stretching observed between 1621-1563 and 1545-1463 cm^{-1} respectively. Presence of -C=O stretching at 1702 and 1716 cm^{-1} in CH-8 and CH-15 respectively. The ^{1}H-NMR spectra showed peaks between 8.92-8.49, 8.25-6.93, and 4.95-4.35 δ ppm for imidazole -CH, aromatic -CH, and -CH_2 protons respectively. The 2*H*-chromen-2-one proton of CH-8 and CH-15 appeared at 8.65 and 8.55 δ ppm respectively. The -OCH_3 protons appeared between 3.75-3.74 δ ppm for CH-2, 8 and CH-13. The -CH_3 protons appeared at 2.29 δ ppm in CH-14. ^{13}C-NMR spectra of CH-2 and CH-8 had shown peaks between 165-110 and 37-36 δ ppm for aromatic and -CH_2 carbons respectively. The methyl carbons (-O-CH_3) of CH-2 and 8 appeared at 55 δ ppm. The mass spectra of CH-2 and CH-8

had shown molecular ion peaks in positive mode at m/z 340.02 and 390.08 respectively. The FTIR, ^{1}HNMR, ^{13}C-NMR and HRMS data were summarized in table 4.13, 4.17, 4.21 and 4.22 respectively.

2-aralkyl-6-aryl-5-bromo-imidazo-[2,1-*b*][1,3,4]-thiadiazoles

A total of twelve brominated imidazothiadiazole derivatives (CH 16-27) were obtained adopting scheme 3.2.3 and procedure 4. The FTIR spectra showed peaks between 3127- 3001and 2963-2704 cm^{-1} for -CH aromatic and aliphatic stretching respectively. The imine (-C=N) and aromatic -C=C stretching appeared between 1629-1515 and 1543-1460 cm^{-1}, respectively. Molecule CH-27 had shown -C=O stretching peaks at 1670 cm^{-1}. Peaks between 8.33-6.97 and 5.00-4.40 δ ppm in ^{1}H-NMR spectra appeared for aromatic and methylene (-CH_2) protons respectively. The 2*H*-chromen-2-one proton of CH-27 appeared at 8.29 δ ppm. -O-CH_3 protons in CH 16-20 appeared between 3.84-3.74 while the -CH_3 protons of CH-25 appeared at 2.32 δ ppm. The ^{13}C-NMR spectra of CH 16-20 find peaks for aromatic carbons between 168-110 δ ppm. The methylene carbon (-CH_2) appeared between 20-36 δ ppm while the -CH_3 carbons appeared between 56-55 δ ppm. Mass spectra had shown molecular ion peak in positive mode for CH 17-20. Table 4.14, 4.18, 4.21 and 4.22 contain FTIR, ^{1}H-NMR, ^{13}C-NMR and HRMS data respectively.

2-Aralkyl-6-aryl-imidazo-[2,1-b][1,3,4]-thiadiazole-5-carbaldehyde

A total of nine 5-formylated imidazothiadiazoles CH 28-36 were obtained following scheme-3.2.3 and procedure 5. The FTIR spectral data find aromatic -CH stretching in the range of 3151-3009 and aliphatic -CH stretching between, 2991-2736 $cm^{-1.}$ The -C=N- and -C=C (Ar.) stretching appeared between 1609-1563 and 1524-1447 cm^{-1} respectively. The -C=O stretching appeared between 1677-1661 cm^{-1}. The additional -C=O stretching appeared at 1683 cm^{-1} in CH-36 represent chromen-2-one nuclei. In ^{1}H-NMR spectra peaks for -CHO observed between of 10.09-9.94 δ ppm. The aromatic and methylene (-CH_2) protons appeared between 8.34-6.97 and 5.05-4.48 δ ppm respectively. Chromen-2-one protons of CH-36 appeared at 8.49 δ ppm. The -CH_3 protons of CH-34 appeared at 2.35 δ ppm while the -OCH_3 protons of CH-28 and CH-33 appeared at 3.77 and 3.78 δ ppm respectively. ^{13}C-NMR spectra of CH-28 had shown carbonyl carbon (-C=O) at 177 δ ppm while the aromatic carbons appeared between 168-114 δ ppm and the -CH_2 carbon at 36.50 δ ppm. The methyl protons (-O-CH_3) were observed at 55 δ ppm. Mass spectrum of CH-28 had shown

molecular ion peak in positive mode at m/z 350.09 (M.W 349.40). Table 4.15, 4.19, 4.21 and 4.22 contain FTIR, ^{1}H-NMR, ^{13}C-NMR and HRMS data respectively.

2-Aralkyl-6-aryl-5-thiocyanato-imidazo-[2,1-b][1,3,4]-thiadiazole

A total of 14 thiocynated imidazothiadiazole derivatives CH 37-50 prepared as per scheme 3.2.3 and procedure 6 The infra-red spectral data find transmittance peaks for aromatic -CH stretching between 3150-3005 cm^{-1} and the aliphatic -CH stretching exhibited between 2950-2758 cm^{-1}. The -C=N imine and aromatic -C=C stretching between 1610-1513 and 1515-1445 cm^{-1} respectively. The nitrile stretching (-C≡N) peaks appeared between 2117-2156 cm^{-1}. Peaks at 1668 and 1708 cm^{-1} in CH-43 and CH-50 represent the chromen-2-one carbonyl (-C=O) stretching peaks. The ^{1}H-NMR spectra find aromatic protons between 8.45-6.39 δ ppm while the -CH_2 protons appeared between 5.09-4.40 δ ppm. The chromen-2-one proton of CH-43 and 50 appeared at 8.45 δ ppm while, the -OCH_3 protons were observed between 3.80-3.74 δ ppm in CH 37-43 and CH-47. The -CH_3 protons of CH-42 and CH-48 appeared at 2.33 and 2.17 δ ppm. The aromatic carbons appeared between 168-110 δ ppm in ^{13}C-NMR spectra while methylene carbons observed between 36-21 δ ppm. The -CH_3 carbons (-O-CH_3 and CH_3) of CH37-43 and CH 47 and 48 at 55δ ppm. Molecular ion peaks in positive mode were found in mass spectra (HRMS) of synthesized analogues. Table 4.16, 4.20, 4.21 and 4.22 contain FTIR, ^{1}H-NMR, ^{13}C-NMR and HRMS data respectively.

Substitution of -Br (CH 16-27), -CHO (CH 28-36) and -SCN (CH 37-50) at 5th position of imidazothiadiazole ring (CH 1-15) were confirmed by absence of imidazole protons between 8.92-8.49 δ ppm in ^{1}H-NMR spectra of respective derivatives.

Biology:

Synthesized derivatives CH 1-50 were screened for cytotoxic property as per literature after due structural characterization. MOA was established taking the most active molecule from the series. To understand the molecular basis of mechanism, *In-silico* study was performed on receptors downloaded from PDB. Results summarized in table 4.23-4.28 and fig. 4.11-4.18.

2-(4-Methoxybenzyl)-6-aryl-imidazo[2,1-b][1,3,4]thiadiazoles:

Cytotoxic evaluation and MOA

22 derivatives were screened for their anti-proliferative property against L1210, CEM and Hela cell lines. Levamisole and melphalan were taken as reference standard during the study. Results were summarized in table 4.23. Among CH 1-8 (5a-h) series except CH-8 (5h) (IC_{50}: 5.0 µM, against T-lymphocyte), remaining molecules were inactive. Among 5-Br derivatives (6a-e) the, 6d and 6e exhibited moderate cytotoxicity (IC_{50}: 13-46 µM) against all cell lines. Further, the thiocyanation at 5^{th} position of imidazo-thiadiazole ring in CH 37-43 (7a-7g) had shown improved cytotoxicity. The CH-43 (7g) was most potent (IC_{50}: 0.78-1.6 µM) among all. The 5^{th} formylated derivative CH-29 (8b) was twice more potent (IC_{50}: 0.94-1.3 µM) than reference standard. In short, it can be concluded that, the 5^{th} formylated and thiocynated derivatives were potent than others and standard levamisole against all cell lines. The potency of melphalan against all cell lines were observed in the range of 1.4-2.13 µM.

Further, the selective cytotoxicity of CH-43 (7g) and CH-29 (8b) towards leukemic CEM, Jurkat and non-cancerous Hs fibroblast cells were studied and the results were summarized in table 4.24 Compound CH-43 (7g) and CH-29 (8 exhibited cytotoxicity against the Jurkat cells with CC_{50}: 1.65 and 4.73 µM respectively. Against non-cancerous cell HS the cytotoxic effect of CH 43 (7g) was less (CC_{50}: 31.45 µM) exhibiting its high selectivity index, while CH-29 (8b) fou to lack the selectivity against HS27 with CC_{50}: 2.36 µM. Hence, further biological studies such as prediction of MO performed on CH-43 (7g).

The ability to cause cell death by apoptosis was determined by Annexin V-FITC-PI assay. High level phosphatidylserine externalization was observed in CH-43 (7g) treated cells (CC_{50}: 2.36 and CC_{100}: 4.27 µM) seen as hall mark of apoptosis (sign of compromised cell membrane), as depicted in fig. 4.11 A.

No depolarization in mitochondrial membrane potential was observed as evident from the non-aggregation of JC-1 dye. Under normal condition, the JC-1 dye aggregates in mitochondria and gives red fluorescence but, in case of apoptotic cells it fails to aggregates hence, gives the original green fluorescence as measured by flow cytometer, fig. 4.11 B.

Caspase-3 activation observed by CH-43 (7g) (CC_{50}: 2.36 4.27 µM and CC_{100}: 4.724.27 µM) suggesting activation of intrinsic apoptotic pathway, fig. 4.11 C.

To understand the mechanism further, cell cycle analysis performed on CH-43 (7g) treated CC_{50} (2.36 μM) and CC_{100} (4.72 μM) Jukart cells suggesting increase in sub-G0-G1 phase (increased DNA fragmentation) and increase in S and G2/M phase. The high population of cells in G2-M phase reflects blocking of DNA synthesis and cytokinesis, as in fig. 4.12.

***In-Silico* Analysis (Molecular docking)**

Compound CH-43 (7g) and CH-29 (8b) were docked against TGF β receptor kinase I (PDB: 1RW8) using Glide module. The docking score summarized in table 4.24 showed better binding affinity (7.012 kcal/mol) for CH-43 (7g) compared to melphalan and CH-29 (8b). The hydrogen bonding and hydrophobic interactions observed at kinase I binding site as depicted in fig. 4.13a-c The higher binding affinity with kinase I by CH-43 (7g) could correlated with its potent and selective *in-vitro* cytotoxic property. The CH-43 (7g) was involved in hydrophobic interaction with A230, K232, L260, V219, A350, L340 and I121 while H-bonding interaction reported with S280 and Y282 during docking as depicted in fig. 4.13a-c. The receptor interaction details were summarized in table 4.25.

5-(Naphthalen-1-yl)- methyl-6-aryl-imidazo[2,1-b][1,3,4]-thiadiazoles:

Cytotoxic evaluation

The cytotoxicity study of 27 derivatives performed on CEM, HeLa, and L1210 cells. 5g had exhibited equipotent cytotoxicity against L1210 (IC_{50}: 2.1 μM) and HeLa cells (IC_{50}: 4.0 μM) in comparison to melphalan ((IC_{50}: 2.13 μM). In comparison to levamisole (206 to >250 μM) the molecule CH-15 (5g) was much more potent against all cell lines (2.1-4.0 μM). The CH 9-14 (5a-f) found less potent hence, excluded from discussion. Among 5-bromo derivatives, only 6g was active against L1210 (IC_{50}: 3.4 μM) and HeLa cells (IC_{50}: 4.5 μM) revealing importance of 2*H*-chromen over the phenyl ring at the 6th position. Compare to melphalan (IC_{50}: 1.4-2.13 μM), the 5-formylated (-CHO) derivatives were better cytotoxic against all three cell lines (IC50: 4.4-9.7 μM) to melphalan. The thiocyanate derivatives CH 44-50 (8a-g) exhibited moderate cytotoxicity. Compound 8e ($IC5_0$: 9.8 μM) found most potent against HeLa cells.

Based on *in-vitro* cytotoxicity data it could be concluded that presence of -Br at 5^{th} position is not necessary for cytotoxicity property while substitution of -CHO and -SCN group leads to potent cytotoxic agent e.g., CH 30-34 (7a-e)

and CH 44-50 (8 a-g), as mentioned in table 4.26. The cytotoxicity of CH-15 (5g) and CH 27 (6g) (exception from the series) could be attributed to the chromen-2-one substitution.

***In-silico* study**

The MW, absorption percentage, logP, tPSA, and Lipinski's Ro5 violation were calculated and summarized in table 4.27 and 4.28.

Violation of Ro5 was exhibited by all molecules including, co-ligand. The tPSA values were calculated and found within the range (≤140 $Å^2$) for all, except 8f. Further, Fsp^3 vale calculated to predict CYP inhibition. The low Fsp^3 value by tested molecules indicate strong CYP inhibition. Compound CH-15 (5g), CH-27 (6g), CH-30 (7a), CH-31 (7b), CH-32 (7c), CH-33 (7e) and CH-47 (8e) had exhibited better *in vitro* cytotoxicity and improved binding affinity in comparison to co-ligand and reference melphalan and levamisole.

Docking study performed on EGFR (PDB: 1m17) protein using 6,7-bis(2-methoxy-ethoxy)quinazoline-4-yl]-(3-ethynyl phenyl)amine as the co-ligand. Highest docking score was reported for CH-15 (5g) and CH-27 (6g).

To predict the stability of protein-ligand complex at physiological condition, the MD simulation performed. The H-bonding, hydrophobic, ionic and water-bridge interactions observed during simulation study. Except CH-14 (5d), CH-12 (5f), CH 21-23 (6a-c), CH-24 (6e) and CH-46 (8c), remaining molecules had shown strong H-bond interaction with MET769. In addition, the CH-44 (8a) and CH-48 (8d) had shown additional H-bonding with CYS773, CH-34 (7d) with LYS73 and CH-50 (8g) with THR830. Residues LEU694, ALA719, and LEU820 were involved in hydrophobic interactions with test molecules. Ionic and water bridges interactions observed in few interactions. Based on RMSD plot and interaction study it could be concluded that CH-31 (7b), CH-32 (7c), CH-33 (7e), CH-35 (7f), CH-36 (7g), and CH-50 (8g) form most stable enzyme complex. Results were summarized in table 4.27, 4.28 and fig. 4.14-4.18.

6.0 SUMMARY

- Cancer is a class of disease responsible for millions of death globally. In search of an effective anticancer agent, a total of fifty 2,6-disubstituted-imidazo[2,1-b] [1,3,4] thiadiazoles were prepared as levamisole derivative.
- Electrophilic substitution (-CHO and -SCN) at 5^{th} position of imidazothiadiazole ring resulted in biologically active molecule CH-43 (7g).
- The synthesized derivatives were duly characterized and subjected to *in-vitro* cytotoxicity against human and murine cancerous cell lines.
- Selective cytotoxicity study was performed and mechanism of action was established taking potent molecule (CH-43, 7g) in the group. Blockage of DNA synthesis and caspase-3 activation was observed by (CH-43, 7g) treated cells.
- *In-silico* study performed to calculate ADME aparmeters and understand the molecular basis of receptor interaction.

In short, the imidazothiadiazole can be described as ***"A molecule with potential."***

7.0 CONCLUSION

Irrespective of the nature of substitution at 2nd position, the 5th -SCN and (or) -CHO substituted molecules had exhibited cytotoxic property equal to standard melphalan against CEM, L1210 and HeLa cells. All molecules were potent than levamisole. Bromine substitution not desired for cytotoxicity, as most of the compounds were inactive except chromene-2-one bearing derivatives CH 27. The *in-vitro* cytotoxicity data were further supported by docking study of potent molecules on 1RW8 and 1M17 receptors, showing strong binding affinity. The CH-43 found to inhibit cancerous cell growth by inducing apoptosis, Caspase-3 activation, and interfering with DNA synthesis, as evident from the submitted biological studies data.

Based on the results obtained, it could be concluded that 2-aralkyl-6-aryl-imidazo[2,1-*b*] [1,3,4]thiadiazole is a scaffold with potential and can give a lead against cancer e.g., CH-43.

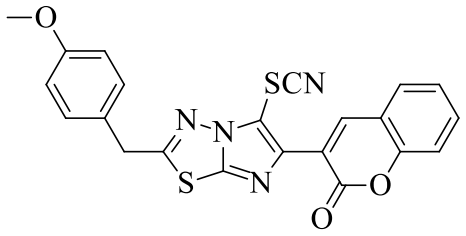

(CH-43)

3-(2-(4-methoxybenzyl)-5-thiocyanatoimidazo[2,1-*b*]
[1,3,4]thiadiazol-6-yl)-2*H*-chromen-2-one

(IC_{50}: 1.60-0.79)

8.0 BIBLIOGRAPHY

1. Rabia Z, Mutahir M. Cancer metastasis-tricks of the trade. Bosn J Basic Med Sci 2017;17:172-82.
2. https://www.who.int/news-room/fact-sheets/detail/cancer [Accessed on 30th July 2021].
3. Kenji K, Makoto MT. Significance and mechanism of lymph node metastasis in cancer progression. Cancer Res 2011;71:1214-8.
4. Knudson AG. Two genetic hits (more or less) to cancer. Nat Rev Cancer 2001;1:157-62.
5. Calabresi P, Chabner BA. Chemotherapy of neoplastic diseases. In: Hardman JG, Limbird LE, Gilman AG, editors. Goodman and Gilman's, the pharmacological basis of therapeutics. 10th ed. New Delhi (ND): Mc Graw-Hill medical publishing division; 2001. p. 1381-8.
6. Weiming S, Qianling S, Huiyun Z, Kexin Y, Yuxia K, Yuping W, et al. Advances in the techniques and methodologies of cancer gene therapy. Discov Med 2019;27:45-55.
7. Justine H, Jean-Luc P. Recent advances in cell penetrating peptide-based anticancer therapies. Molecules 2019;7:927.
8. Martins P, Jesus J, Santos S, Raposo LR, Rodrigues CR, Baptista PV, et al. Heterocyclic anticancer compounds: recent advances and the paradigm shift towards the use of nanomedicine's tool box. Molecules 2015;20:16852-91.
9. Lima LM, Barreiro EJ. Bioisosterism: a useful strategy for molecular modification and drug design. Curr Med Chem 2005;12:23-49.
10. Kapetanovic IM. Computer-aided drug discovery and development (CADDD): in silico-chemico-biological approach. Chem Biol Interact 2008;171:165-76.
11. Yu W, MacKerell AD Jr. Computer-aided drug design methods. Methods Mol Biol. 2017;1520:85-106.
12. Raeymaekers AH, Roevens LF, Janssen PA. The absolute configurations of the optical isomers of the broad spectrum anthelmintic tetramisole. Tetrahedron Lett 1967;8:1467-70.

13. Stevenson HC, Green I, Hamilton JM, Calabro BA, Parkinson DR. Levamisole: known effects on the immune system, clinical results, and future applications to the treatment of cancer. J Clin Oncol 1991;9:2052-66.
14. Kovach JS, Svingen PA, Schaid DJ. Levamisole potentiation of fluorouracil antiproliferative activity mimicked by orthovanadate, an inhibitor of tyrosine phosphatase. J Natl Cancer Inst 1992;84:515-9.
15. Fajgelj S, Stanovnik B, Tisler M. Transformations of N-heteroaryl-formamidines: a novel synthesis of imidazo-[2,1-b]-thiazole and imidazo-[2,1-b][1,3,4]-thiadiazole derivatives. Heterocycles 1986;24:379-86.
16. Torgova SI, Shtykov NM, Abolin AG, Karamysheva LA, Ivashchenko AV, Barnik MI. Liquid-crystal imidazo-[2,1-b][1,3,4]-thiadizoles. Part 3. Synthesis and dielectric-properties of imidazo-[2,1-b][1,3,4]-thiadiazoles containing polar substituents. Zh Org Khim 1988;24:1306-10.
17. Kidwai M, Rastogi S. Green synthesis of substituted imidazo-thiadiazoles using ionic liquid. Indian J Chem B 2006;45:2321-4.
18. Khazi IA, Mahajanshetti CS, Gadad AK, Tarnalli AD, Sultanpur CM. Synthesis, anticonvulsant and analgesic activities of some 6-substituted-imidazo-[2,1-b][1,3,4]-thiadiazole-2-sulphonamides and their 5-Br derivatives. Arzneimittelforschung 1996;10: 949-52.
19. Kidwai M, Rastogi S. Green route to the 2,6-di-substituted imidazo-[2,1-b][1,3,4]-thiadiazoles by the cyclocondensation of α-bromo-acetophenone derivative and 1,3,4-thiadiazoles using ionic liquids. Lett Org Chem 2006;3:149-52.
20. Karki SS, Panjamurthy K, Kumar S, Nambiar M, Ramareddy SA, Chiruvella KK, et al. Synthesis and biological evaluation of novel 2-aralkyl-5-substituted-6-(4-fluorophenyl)-imidazo-[2,1-b][1,3,4]-thiadiazole derivatives as potent anticancer agents. Eur J Med Chem 2011;46:2109-16.
21. Hough TL. Reactions of some 5-substituted-imidazo-[2,1-b][1,3,4-] thiadiazoles. J Heterocycl Chem 1983;20:1003-5.
22. Torgova SI, Shtykov NM, Abolin AG, Karamysheva LA, Ivashchenko AV, Barnik MI. Liquid-crystal imidazo-[2,1-b][1,3,4]-thiadizoles. Part 3. Synthesis and dielectric properties of imidazo-[2,1-b][1,3,4]-thiadiazoles containing polar substituents. Zh Org Khim 1988;24:1306-10.

23. Hegde VS, Kolavi GD, Lamani RS, Khazi IA. Mannich bases and novel benzothiazole derivatives of imidazo-[2,1-b][1,3,4]-thiadia zoles and their biological evaluation. J Sulfur Chem 2006;27:553-69.
24. Iyer D, Vartak SV, Mishra A, Goldsmith G, Kumar S, Srivastava M, et al. Identification of a novel BCL2-specific inhibitor that binds predominantly to the BH1 domain. FEBS J 2016;283:3408-37.
25. Ivashchenko AV, Petrova OS, Titov VV. 5-aryl-azoimidazo-[2,1-b][1,3,4]-thiadiazoles-new dichroic T-dyes For LCD. Mol Cryst Liq Cryst 1987;145:25-9.
26. Matsukawa T, Ban S, Shirakawa Y. Chemotherapeutics. XXXII. Action of several compounds on tubercule bacilli. J Pharm Soc 1953;73:159-63.
27. Barnish IT, Cross PE, Dickinson RP, Gadsby B, Parry MJ, Randall MJ, et al. Cerebro-vasodilatation through selective inhibition of the enzyme carbonic anhydrase. 2. Imidazo-[2,1-b]-thiadiazole and imidazo[2,1-b]-thiazole-sulfonamides. J Med Chem 1980;23:117-21.
28. Askin S, Tahtaci H, Turkes C, Demir Y, Ece A, Ciftci GA, et al. Design, synthesis, characterization, in-vitro and in-silico evaluation of novel imidazo[2,1-b][1,3,4] thiadiazoles as highly potent acetylcholinesterase and non-classical carbonic anhydrase inhibitors. Biorg Chem 2021;113:105009.
29. Reddy AG, Sireesha R, Babu VH, Rao YJP, Susithra E, Rao MBV. Design, synthesis, anti-proliferative and molecular docking studies of quinazolinone-imidazo[2,1-b][1,3,4] thiadiazole hybrid derivatives. Chem Data Collect 2021;31:100014.
30. Nakashima K, Okada SY, Watanabe H, Shimizu Y, Nakamoto Y, Ono M. Synthesis and evaluation of 68Ga-labeled imidazothiadiazole sulfonamide derivatives for PET imaging of carbonic anhydrase-IX. Nucl Med Biol 2021;93:46-53.
31. Cascioferro S, Petri GL, Parrino B, Carbone D, Funel N, Bergonzini C et al. Imidazo[2,1-b][1,3,4]thiadiazoles with antiproliferative activity against primary and gemcitabine-resistant pancreatic cancer cells. Eur J Med Chem 2020;189:112088.

32. Iikuni S, Kitano A, Watanabe H, Shimizu Y, Ono M. Synthesis and evaluation of novel technetium-99m-hydroxamamide complex based on imidazothiadiazole sulfonamide targeting carbonic anhydrase-IX for tumor imaging. Bioorg & Med Chem Lett 2020;30:127596.
33. Vartak SV, Iyer D, Santhoshkumar TR, Sharma S, Mishra A, Goldsmith G, et al. Novel BCL2 inhibitor, disarib induces apoptosis by disruption of BCL2-BAK interaction. Biochem Pharmacol 2017;131:16-28.
34. Kumar R, Bua S, Ram S, Prete SD, Capasso C, Supuran CT, et al. Benzenesulfonamide bearing imidazothiadiazole and thiazolo-triazole scaffolds as potent tumor associated human carbonic anhydrase IX and XII inhibitors. Bioorg Med Chem 2017;25:1286-93.
35. Iyer D, Vartak SV, Mishra A, Goldsmith G, Kumar S, Srivastava M, et al. Identification of a novel BCL2-specific inhibitor that binds predominantly to the BH1 domain. FEBS J 2016;283:3408-37.
36. Katiyar A, Metikurki B, Prafulla S, Kumar S, Kushwaha S, Schols D, et al. Synthesis and pharmacological activity of imidazo-[2,1-b][1,3,4]-thiadiazole derivatives. Acta Pol Pharm-Drug Research 2016; 73:937-47.
37. Romagnoli R, Baraldi PG, Prencipe F, Balzarini J, Liekens S, Estevez F. Design, synthesis and antiproliferative activity of novel heterobivalent hybrids based on imidazo-[2,1-b] [1,3,4]-thiadiazole and imidazo-[2,1-b][1,3]-thiazole scaffolds. Eur J Med Chem 2015;101:205-17.
38. Kamal A, Dastagiri D, Ramaiah MJ, Reddy JS, Bharathi EV, Srinivas C, et al. Synthesis of imidazo-thiazole chalcone derivatives as anticancer and apoptosis inducing agents. Chem Med Chem 2010;5:1937-47.
39. Kamal A, Rao NMP, Das P, Swapna P, Polepalli S, Nimbarte VKD, et al. Synthesis and biological evaluation of imidazo-[2,1-b][1,3,4]thiadiazole-linked oxindoles as potent tubulin polymerization inhibitors. Chem Med Chem 2014;9:1463-75.
40. Tegginamath G, Kamble RR, Taj T, Kattimani PP, Meti GY. Synthesis of novel imidazo [2,1-b][1,3,4]thiadiazoles appended to sydnone as anticancer agents. Med Chem Res 2013;22:4367-5.
41. Gohil CKJ, Noolvi MN. Synthesis of new diaryl derivatives comprising imidazo-thiadiazole moiety as potential anticancer agents. Int J Pharm Chem Anal 2015;2:84-96.

42. Hegde M, Karki SS, Thomas E, Kumar S, Panjamurthy K, Ranganatha SR, et al. Novel levamisole derivative induces extrinsic pathway of apoptosis in cancer cells and inhibits tumor progression in mice. PLoS One 2012;7:e43632.
43. Noolvi MN, Patel HM, Kamboj S, Kaur A, Mann V. 2,6-di-substituted imidazo[2,1-b][1,3,4]thiadiazoles:Search for anticancer agents. Eur J Med Chem 2012;56:56-69.
44. Taher AT, Georgey HH, El-Subbagh HI. Novel 1,3,4-heterodiazole analogues:synthesis and in-vitro antitumor activity. Eur J Chem 2012;47:445-51.
45. Noolvi MN, Patel HM, Singh N, Gadad AK, Cameotra SS, Badiger A. Synthesis and anticancer evaluation of novel 2-cyclopropyl imidazo-[2,1-b][1,3,4]-thiadiazole derivatives. Eur J Chem 2011;46:4411-8.
46. Terzioglu N, Gursoy A. Synthesis and anticancer evaluation of some new hydrazone derivatives of 2,6-dimethyl-imidazo-[2,1-b][1,3,4]-thiadiazole-5-carbohydrazide. Eur J Med Chem 2003;38:781-6.
47. Hamama WS, Ibrahim ME, Raoof HA, Zoorob HH. Synthesis and antimicrobial evaluation of some novel 5-phenyl-5H-thiazolo[4,3-b][1,3,4]thiadiazole systems. J Heterocycl Chem 2017;54:2360-6.
48. Ramprasad J, Nayak N, Dalimba UK, Yogeeswari P, Sriram D, Peethambar SK, et al. Synthesis and biological evaluation of new imidazo-[2,1-b][1,3,4]-thiadiazole-benzimidazole derivatives. Eur J Med Chem 2015;95:49-63.
49. Arif M, Turgut K, Yakup S. Recent studies of nitrogen containing heterocyclic compounds as novel antiviral agents: A review. Bioorg Chem 2021;114:105076.
50. Arora RK, Kaur N, Bansal Y, Bansal G. Novel coumarin-benzimidazole derivativesas antioxidants and safer anti-inflammatory agents. Acta Pharm Sin B 2014;4:368-75.
51. Aicher TD, Balkan B, Bell PA, Brand LJ, Cheon SH, Deems RO, et al. Substituted tetrahydropyrrolo[2,1-b]oxazol5(6H)-ones and tetrahydropyrrolo[2,1-b]thiazol-5(6H)-ones as hypoglycemic agents, J Med Chem 1998;41:4556-66.
52. Srivastava M, Nambiar M, Sharma S, Karki SS, Goldsmith G, Hegde M, et al. An inhibitor of nonhomologous end-joining abrogates double-strand break repair and impedes cancer progression. Cell 2012;151:147-87.

53. Lema C, Varela-Ramirez A, Aguilera RJ. Differential nuclear staining assay for high throughput screening to identify cytotoxic compounds. Curr Cell Biochem 2011;1:1-14.
54. Tait SWG, Green DR. Mitochondria and cell death: outer membrane permeabilization and beyond. Nat Rev Mol Cell Biol 2010;11:621-32.
55. Kumar S, Metikurki B, Bhaduria VS, Schols ED, Tokuda H, Karki SS. Synthesis of imidazo[2,1-b][1,3,4]thiadiazole derivatives as possible biologically active agents. Acta Pol Pharm 2016;73:913-29.
56. Alley MC, Scudiero DA, Monks PA, Hursey ML, Czerwinski MJ, Fine DL et al. Feasibility of drug screening with panels of human tumor cell lines using a microculture tetrazolium assay. Cancer Res 1988;48:589-601.
57. Chiruvellaa KK, Karia V, Choudhary B, Nambiara M, Ghanta RG, Raghavan SC. Methyl angolensate, a natural tetranortriterpenoid induces intrinsic apoptotic pathway in leukemic cells. FEBS Lett 2008;582:4066-76.
58. Nagata S. Apoptotic DNA fragmentation. Exp Cell Res 2000;256:12-18.
59. Shahabuddin MS, Nambiar M, Choudhary B, Advirao GM, Raghavan SC. A novel DNA intercalator, butylamino-pyrimido[4′,5′:4,5]selenolo(2,3-b)quinoline, induces cell cycle arrest and apoptosis in leukemic cells. Invest New Drugs 2010;28:35-48.
60. Robles-Escajeda E, Das U, Ortega NM, Parra K, Francia G, Dimmock JR et al. A novel curcumin-like dienone induces apoptosis in triple negative breast cancer cells. Cell Oncol 2016;39:265-77.
61. Sawyer JS, Beight DS, Britt KS, Anderson BD, Campbell RM, Goodson Jr T et al. Synthesis and activity of new aryl and heteroaryl substituted 5,6 dihydro-4H-pyrrolo[1,2-b]pyrazole inhibitors of the transforming growth factor-β type I receptor kinase domain. Bioorg Med Chem Lett 2004;14:3581-4.
62. Wishart DS, Knox C, Guo AC, Cheng D, Shrivastava S, Tzur D et al. Drug Bank: a knowledgebase for drugs, drug actions and drug targets. Nucleic Acids Res 2008;36:901-6.
63. Friesner RA, Banks JL, Murphy RB, Halgren TA, Klicic JJ, Mainz DT et al. Glide: a new approach for rapid, accurate docking and scoring. 1. Method and assessment of docking accuracy. J Med Chem 2004;47:1739-49.

64. Friesner RA, Banks JL, Murphy RB, Halgren TA, Klicic JJ, Mainz DT et al. Extra precision glide: docking and scoring incorporating a model of hydrophobic enclosure for protein-ligand complexes. J Med Chem 2006;49:6177-96.
65. Jorgensen WL, Chandrasekhar J, Madura JD, Impey RW, Klein ML. Comparison of simple potential functions for simulating liquid water. J Chem Phys 1983:79:926-35.
66. Becke AD. Density-functional thermochemistry. III. The role of exact exchange. The J Chem Phys 1993;98:5648-52.
67. Lee C, Yang W, Parr RG. Development of the Colle-Salvetti correlation-energy formula into a functional of the electron density. Phys Rev B Condens Matter1988;37:785-9.
68. Trott O, Olson AJ. AutoDock Vina: improving the speed and accuracy of docking with a new scoring function, efficient optimization, and multithreading. J Comput Chem 2010;31:455-61.
69. Lagorce D, Sperandio O, Galons H, Miteva MA, Villoutreix BO. FAF-Drugs2:free ADME/tox filtering tool to assist drug discovery and chemical biology projects. BMC Bioin 2008;9:396.
70. https://www.schrodinger.com/desmond (Accessed 10th December 2020).
71. Lipinski CA, Lombardo F, Dominy BW, Feeney PJ. Experimental and computational approaches to estimate solubility and permeability in drug discovery and development settings. Adv Drug Del Rev 1997;23:3-25.
72. Veber DF, Johnson SR, Cheng HY, Smith BR, Ward KW, Kopple KD. Molecular properties that influence the oral bioavailability of drug candidates. J Med Chem 2002;45:2615-23.
73. Hirata K, Kotoku M, Seki N, Maeba T, Maeda K, Hirashima S, et al. SAR exploration guided by LE and Fsp3: discovery of a selective and orally efficacious RORγ inhibitor. ACS Med Chem Lett 2016;7:23-7.
74. Lovering F, Bikker J, Humblet C. Escape from flatland: increasing saturation as an approach to improving clinical success. J Med Chem 2009;52:6752-6.
75. Dagli M, Er M, Karakurt T, Onaran A, Alici H, Tahtaci H. Synthesis, characterization, antimicrobial evaluation, and computational investigation of substituted imidazo[2,1-b][1,3,4]thiadiazole derivative. ChemistrySelect 2020;5: 11753-63.

9.0 ANNEXURE

- **List of publication**

1. Choodamani B, Kumar S, Gupta AK, Schols D, Tahtaci H, Karakurt T, Kotha S, Swapna B, Setty R, and Karki SS. Synthesis, molecular docking, and preliminary cytotoxicity study of some novel 2-(naphthalen-1-yl)-methylimidazo[2,1-b] [1,3,4]thiadiazoles. J Mol Struct 2021;1234:130174. **[I.F: 3.196].**

2. Chudamani B, Hernandez KGC, Kumar S, Tony AM, Bustamante AYS, Aguilera RJ, Schols D, Mohan CG, and Karki SS. Synthesis, molecular docking and preliminary antileukemic activity of 4-methoxybenzyl derivatives bearing an imidazo[2,1-b][1,3,4]thiadiazoles. Chem Biodivers 2021;18:e2000800. **[I.F: 2.408]**